SIMPLIFIED NUMERICAL BASED METHOD FOR CALCULATION OF DC GROUND ELECTRODE RESISTANCE IN MULTI-LAYERED EARTH

by

Chong Kiat Ng

A Thesis

Submitted to the Faculty of Graduate Studies
in partial fulfillment of the requirements for the degree of

Master of Science

The Department of Electrical and Computer Engineering

The University of Manitoba
Winnipeg, Manitoba, Canada

THE UNIVERSITY OF MANITOBA

FACULTY OF GRADUATE STUDIES

*****

COPYRIGHT PERMISSION PAGE

SIMPLIFIED NUMERICAL BASED METHOD FOR CALCULATION OF DC GROUND ELECTRODE RESISTANCE IN MULTI-LAYERED EARTH

BY

CHONG KIAT NG

A Thesis/Practicum submitted to the Faculty of Graduate Studies of The University of Manitoba in partial fulfillment of the requirements of the degree of

MASTER OF SCIENCE

Acknowledgements

The author wishes to express his sincere and profound gratitude to his dissertation supervisor Dr. M. R. Raghuveer for his valuable support, encouragement, advice and excellent lectures throughout this project. Funding from Manitoba HVDC Research Centre and NSERC Canada is gratefully acknowledged.

A special thank goes to Mr. John Kendall for all the technical support and assistance that he has provided, Dr. Ian Ferguson for providing useful geophysical information and others who have provided support and advice during this project.

The author, finally, wishes to express his special gratitude to his parents and brothers in Malaysia for their loves and encouragement during the course of the study.

Abstract

The main focus of this thesis is to develop an efficient method for handling DC grounding problems involving earth non-homogeneity. A numerical technique has been employed using a commercial *Finite Element Method* (FEM) package called *ANSYS 5.5*. Due to the large scale of the problem domain a technique known as *'substructuring'* has been used.

Classical analytical solutions were utilized to establish the accuracy of the numerical solutions. It is shown that an error of no worse than 10% in the estimation of the ground resistance can be guaranteed with only a few exceptions, which are pointed out in the thesis.

A technique for reducing a problem involving two-layered earth to a homogeneous earth is proposed. This procedure can be extended to cover for cases involving multi-layered earth. The effects of inclined earth layers have been considered and suggestions for handling such situations are proposed.

Contents

List of Figures

List of Tables

Nomenclature

Some of the most frequently occurring abbreviators and symbols used in the thesis are tabulated below:

∇ ---------- $\mathbf{x}\,\partial/\partial x + \mathbf{y}\,\partial/\partial y + \mathbf{z}\,\partial/\partial z$

V ---------- Electric Potential

$\boldsymbol{E}$ ---------- Electric Potential Gradient

$\boldsymbol{H}$ ---------- Magnetic Field Intensity

$\boldsymbol{J}$ ---------- Current Density

FEM ---------- Finite Element Method

BC ---------- Boundary condition

σ ---------- Electric Conductivity

ρ_k ---------- Resistivity of k^{th} layer

ρ_1 ---------- Resistivity of top layer

ρ_2 ---------- Resistivity of bottom layer

ρ_{eqv_n} ---------- Normalized equivalent resistivity

ρ_{eqv} ---------- Equivalent resistivity

ρ_{eqv_nx} ---------- Normalized equivalent resistivity after x^{th} approximation

ρ_{eqv_x} ---------- Equivalent resistivity after x^{th} approximation

L_x ---------- Effective rod length for the x^{th} approximation

R_{exact} ---------- Exact ground resistance evaluated by using analytical solution

R'_{exact} ---------- Apparent exact ground resistance evaluated by using FEM

R_{exact_p} ---------- Projected exact resistance based on a FEM simulation

R_{est} ---------- Estimated ground resistance

R_N ---------- Normalization factor for normalizing the equivalent resistivity curves

Chapter 1

Introduction

In view of the paramount importance of the safety and performance of HVDC converter stations, the grounding system must be carefully and adequately designed. The common types of DC converter station configurations are monopolar, homopolar and bipolar. Monopolar and homopolar systems normally use the earth as a return and therefore the earth electrode carries the continuous full rated current for a monopolar system and double the continuous rated current for a homopolar system. The electrode must also be designed to carry a short-time overload current. The direction of the return current flows is fixed.

In bipolar systems, normally, only a small differential current flows through the earth return. This differential current, also called out-of-balance current, is due to the differences in reactances, characteristics of the 2 poles, etc. The magnitude of this differential current is small as compared to the rated current and its direction is not predictable. In the event of a fault on one of the poles, the bipolar system can be switched over to a monopolar mode, which is capable of sustaining half its rated power. In such an event, the full rated current will flow through the earth return. This scenario must be accounted for when designing a HVDC bipolar system.

Many factors and criteria are involved in the design of a HVDC earth electrode. However, the most significant governing factor is undoubtedly, the soil resistivity (ρ), which is measured in ohm-meter (Ω-m).

1.1 Soil Resistivity

Soil resistivity is affected by a wide range of factors [64 Tagg] such as:

(a) Type of soil
(b) Temperature
(c) Moisture content
(d) Chemical composition
(e) Closeness of packing and pressure

The measurement of resistivity is a complicated task and normally carried out by geologists or geological engineers. A modern method of measuring the resistivity is called the ***Magnetotelluric Method (TM)***, which is used for very large scale surveying such as across the entire province of Manitoba. A discussion on this type of large scale soundings can be found in [97 Ian]. For smaller scale surveying, encompassing an area of approximately 5 km^2, methods such as the *Wenner*, *Schlumberger* and *Dipole-Dipole* array can be employed. Detailed discussions on these methods can be found in [90 Ward], [90 McNeill]. All these methods are based on soundings, which involve the measurement of electromagnetic quantities, such as the electric field, $\boldsymbol{E}$ and magnetic field intensity, $\boldsymbol{H}$. The reliability of these methods depends heavily on the degree of expertise of the operator who performs the measurement. Large errors usually result if the tests are not performed carefully.

The measured resistivity is an estimation pertaining to the prevailing conditions at the instant of measurement because the resistivity in a given locality will vary over time. The reasons for the variation may be due to natural causes or due to human intervention. Natural causes include seasonal variations of temperature, formation of perma frost, changes in the availability of ground water etc. Human intervention causes are pollution, chemical treatment of soil and installation of large underground structure.

Along with other pertinent geological data such as porosity, mineral content, moisture etc, information on resistivity is gathered and stored in data banks. Data banks maintained by universities and government agencies are good sources to obtain this information.

1.2 Earth Electrode

There are many possible configurations for designing a earth electrode. Some of the simplest configurations are the single driven vertical rod, a single horizontal straight wire and horizontal disc. Slightly more complicated arrangements consist of wires connected in star formation, wires in the form of a square loop and a group of driven rods. Approximate analytical solutions exist for these relatively simple arrangements in a homogeneous earth i.e., ground with only a single value of resistivity [36 Dwight], [64 Tagg]. Some work has been done to take into account the effects of earth non-homogeneity [48 Sunde], [64 Tagg], [82 Ciric].

However, the analytical analysis is complicated and is possible only with some very simple and well-defined configurations. The calculation of earth resistance was first tackled by H.B. Dwight, in his paper titled *'Calculation of Resistance to Ground'*, [36 Dwight] and by Erling Sunde, who authored a text titled *'Earth Conduction Effects in Transmission Systems'*, [48 Sunde]. More recently, G.F. Tagg has authored the text, *'Earth Resistances'*, [64 Tagg] which contains a collection of information and references representing the efforts of earlier researchers, including Sunde and Dwight. Other than those mentioned above, [71 Kimbark] and [90 Rao] also present good discussions on various aspects of the problems associated with earth electrode design. It may be mentioned that the information in [36 Dwight] and [48 Sunde] are still used extensively today.

The analysis of practical grounding systems involving multiple-rod, non-homogeneous earth etc, can not be carried out by conventional analytical methods. With the evolution of the digital computer, numerical methods such as *the Finite Element Method* (FEM) and *Boundary Element Method* (BEM) have been used to solve such problems.

1.3 Design Criteria

The design of a ground electrode has to consider adequacy of performance, reliability, ease of maintenance and environmental effects. Often, the desired ground resistance cannot be achieved by having only one ground rod. Under this situation, an electrode made up of multiple-rod is needed. Vertical driven rods arranged in different configurations offer the most practical designs. Such a scheme facilitates maintenance work and is relatively easier to install. A group of vertical ground rods can be serviced by taking a few rods out of service at a time, and yet maintaining a satisfactory performance of the entire ground electrode system [88 Prabhakara]. Another very favorable advantage is that the vertical rods are relatively immune to seasonal variations of temperature, especially when dealing with perma frost.

1.3.1 Adequacy of Performance

This is the desired performance characteristic as prescribed by a client. It normally involves parameters such as the maximum acceptable earth resistance, the electric field, $\boldsymbol{E}$, and the current density, $\boldsymbol{J}$, at the earth electrode and in its immediate vicinity, the estimated service life and the ability to handle abnormal conditions. One important factor here is the heating effect. Soil in the immediate vicinity of the electrode is subjected to heating due to current flows, resulting in evaporation of moisture and hence the resistance and temperature rise progressively [46 Sunde], which must be accounted for to prevent catastrophic consequences.

1.3.2 Reliability

The final design must be reliable with minimum maintenance throughout its service life. The ability of the electrode system to perform adequately under an incomplete configuration is a desired feature. This feature enables sectionalizing and servicing the electrode system section by section while maintaining a satisfactory overall performance.

1.3.3 Environmental Effects

It is inevitable that the installation of a huge ground electrode system will cause some environmental effects. The ultimate task here is to strike for a balance between an engineering design and preserving nature.

1.4 Theoretical Considerations

This research project focuses on dealing with vertical driven type of ground electrodes in non-homogeneous earth. The analytical tool used throughout the research is a commercial FEM package called *ANSYS 5.5*. The following is a quick and simplified review of basic theoretical considerations.

1.4.1 Laplace's Equation in Conducting Medium

For steady direct current, we have the following differential relation:

$$\nabla \cdot \bar{J} = 0 \qquad (1-1)$$

Ohm's Law at a point is:

$$\bar{J} = \sigma \bar{E} \qquad (1-2)$$

The electric field $\boldsymbol{E}$, can be obtained as the negative gradient of the electric potential:

$$\overline{E} = -\nabla V \qquad (1-3)$$

From Eqs. (1-1), (1-2) and (1-3), we obtain

$$\sigma \nabla \cdot \overline{E} = 0 \qquad (1-4)$$

$$\sigma \nabla \cdot (\nabla V) = 0 \qquad (1-5)$$

Finally, we arrive at the Laplace's equation

$$\nabla^2 V = 0 \qquad (1-6)$$

This derivation shows that problems involving the distribution of steady direct currents in conducting mediums are analogous to static field problems in insulating mediums. If a solution to Laplace's equation which satisfies all the boundary conditions as prescribed by the problem of interest can be found, we then have the solutions for the potential and current distribution in the conducting medium [92 Kraus].

1.4.2 Boundary Conditions

In order to handle the large domain that is involved in solving grounding problems using the FEM, truncation of the domain is necessary to ensure a manageable problem size. The domain dictates the finite element model and hence the total number of nodes and the degrees of freedom, which have a direct effect on the accuracy of the solution.

Depending on the structure of the problem, there may exist planes of symmetry, which can be used to reduce the problem size dramatically. Under some special conditions, such as a single vertical rod in homogeneous earth, the problem geometry becomes axisymmetric.

If the boundary of truncation is sufficiently far from the electrodes, both Dirichlet (specification of potential on boundaries, also known as the Jury conditions) or Neumann (specification of normal component of a field quantity on the boundaries such as $\partial\phi/\partial n$ or $\partial \boldsymbol{J}/\partial n$) conditions may be applied at the boundary of truncation. These two different boundary conditions will change the flux distribution (current flow) at the boundary of truncation but will have an insignificant effect on the overall solution. In fact, if the domain is sufficiently large, there will be virtually no effect on the overall solution at all.

1.5 Chronological Order of Outline of Methods Available for Solving Earth Resistance Problems

Before the evolution of the digital computer, methods used for dealing with earth electrode problems were the average-potential method, successive imaging method etc. These classical methods are often mathematically very challenging and possible only with well-defined and simple geometries. The final product of these analyses are closed-form mathematical expressions, which are regarded as the classical solutions or analytical solutions or exact solutions in this thesis.

Approximations and assumptions are necessary in order to derive an analytical solution. The validity of these approximations and assumptions such as the assumption of a uniform charge distribution and uniform current density, have been shown to be inappropriate under certain situations [71 Trinh]. However, if used with care, these classical solutions yield very accurate theoretical results.

The evolution of the high speed digital computer has made numerical techniques a feasible way of dealing with earth electrode problems. The so called *'Matrix method'* is found to be particularly suitable for solving ground electrode problems. Essentially, this is a numerical approach of solving Laplace's equation and it is a boundary value problem.

Included under the general name of *'Matrix method'*, are the *Finite Element Method* (FEM), the *Boundary Element Method* (BEM) and the *Stencil Method* etc. These methods reduce differential or integral equations to a system of algebraic equations that are solvable. The main computational effort for the computer lies in the inversion of the resultant matrix. The construction of the matrix is time consuming but does not normally involve demanding calculations.

1.6 Scope of Present Work

Chapter 1 delivers background information for this research project. Classical and analytical solutions to simple electrode geometries in homogeneous earth are reviewed in chapter 2. Chapter 3 discusses the implementation of the *Finite Element Method* using *ANSYS 5.5*. This chapter also includes a discussion on the accuracy of the numerical results. Chapter 4 represents the crux of the thesis. Vertical driven rod electrodes are considered in homogeneous and multi-layered earth using a *Finite Element Method* based numerical approach. Suggestions are made for fast and efficient calculation of earth resistance in the practical cases. Chapter 5 examines the effect of neglecting the non-horizontality of earth layers on the calculation of ground resistance. Chapter 6 summarized the main contributions of this project.

Chapter 2

Classical and Analytical Solutions

This chapter discusses some classical and analytical solutions. These analytical solutions have been used by engineers and are known to provide good results, provided that the assumptions inherent in them are met by the problem under investigation. These classical solutions form the basis of comparison for the FEM solutions in this thesis, which are discussed in later chapters.

2.1 Vertical Rod Grounding in Homogeneous Earth

For a vertical ground rod in homogeneous earth as shown in Fig. 2.1, the analytical solution is [36 Dwight], [64 Tagg]:

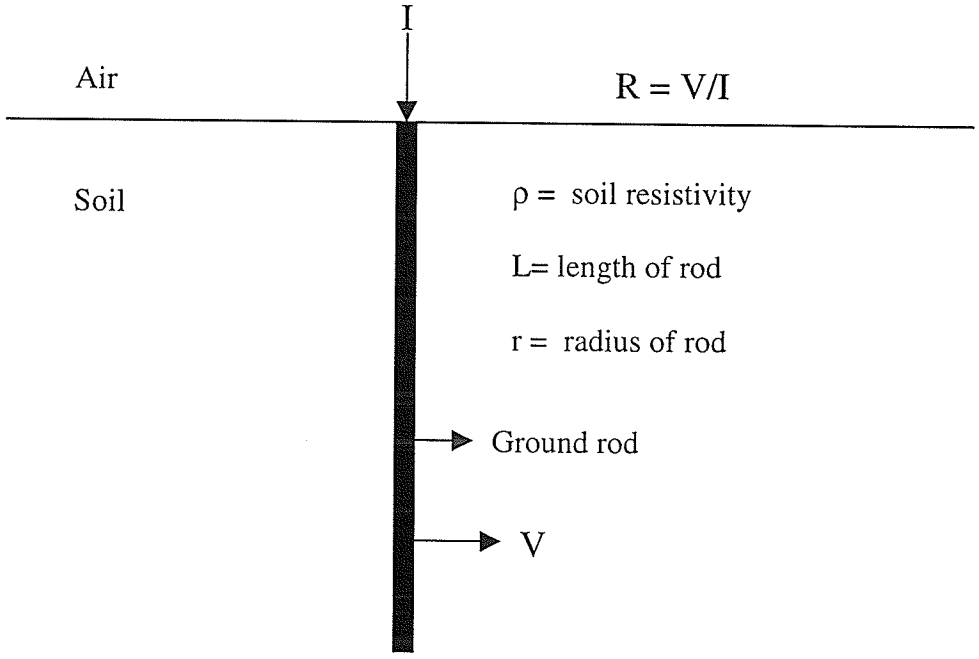

Figure 2.1 Vertical rod grounding in homogeneous earth

$$R = \frac{\rho}{2\pi L}\left(\ln\frac{4L}{r} - 1\right) \qquad (2-1)$$

The most important assumption here is that the length of the rod must be much greater than its radius ie, L >> r.

Close examination of Eq. (2-1) reveals that the radius of the rod does not play a very significant role in terms of determining its ground resistance. However, the radius does affect the heat dissipation capability of the rod, which becomes important once the electrode design becomes more complicated and the current level involved is high.

The length of the rod is the prime design variable that affects the ground resistance. The length of the rod has been found to be inversely proportional to the ground resistance but not in linear fashion. In general, the longer the rod, the lower the ground resistance. The soil resistivity is nonetheless, the most important factor that affects the ground resistance. This is a geological parameter that one has little control over. It becomes a matter of strategic site selection.

Eq. (2-1) is an analytical equation obtained by assuming a uniform charge distribution and truncation of an infinite series. It does not give any information about the field distribution but introduces error of only a few percent[36 Dwight].

2.1.1 Minimum Attainable Resistance

If 2 identical vertical rods are connected in parallel, the question is whether one can use Eq. (2-1) to evaluate the ground resistance with only one rod present and halve this value to arrive at the overall ground resistance of the system. Unfortunately, the answer is no! In order to do this, the 2 rods have to be separated by a very large distance so that the currents flow from one rod does not affect the flow from the other rod. For a given land area, there is a minimum attainable ground resistance regardless of the number of ground rods installed [36 Dwight], [64 Tagg].

2.2 Vertical Rod Grounding in Two-Layered Earth

The analytical solution for a vertical rod grounding in two-layered earth as depicted in Fig. 2.2 can be found in [64 Tagg]. However, those analytical solutions are complicated and difficult to use.

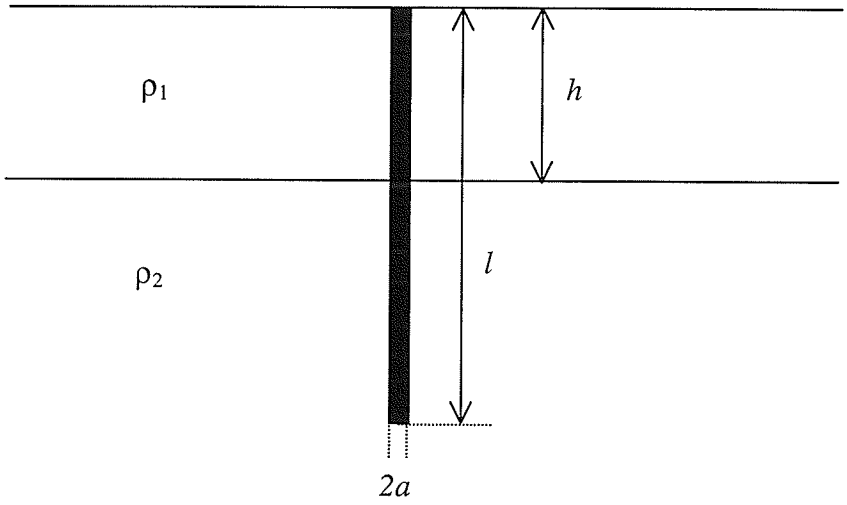

Figure 2.2 Single vertical rod grounding in two-layered earth

From [64 Tagg], the analytical solution is :

$$R_{exact} = \frac{\rho_1}{2\pi l} \cdot \frac{(1+k)}{\left\{(1-k)+2k\frac{h}{l}\right\}} \left[\ln\frac{2l}{a} + \sum_{n=1}^{n=\infty} k^n \ln\frac{(2nh+l)}{\{(2n-2)h+l\}} \right]$$

$$R_{exact} = F[R_1 + R_a] \qquad (2-2)$$

where

$$k = \frac{\rho_2 - \rho_1}{\rho_2 + \rho_1} \qquad \text{and} \qquad F = \sum_{n=1}^{\infty} \frac{k^n}{2} \ln\frac{\{nh/l+1\}}{\{nh/l-1\}}$$

Here, a is the radius and l is the length of the rod, h is the thickness of the top layer. The penetration factor, F is defined by a series of curves in [64 Tagg], R_1 is the ground resistance of the rod in homogeneous earth of resistivity ρ_1, R_a is the additional resistance due to the second layer and k is the reflection coefficient.

2.3 Multiple-Rod Grounding in Homogeneous Earth

Often, the desired ground resistance cannot be achieved by using only one rod and therefore grounding with multiple rods becomes necessary. These rods can be arranged in line, triangle, hollow square, solid square or circle formation etc[64 Tagg].

2.3.1 Equivalent Hemisphere

It is possible to replace a vertical rod with an equivalent hemisphere which yields the same ground resistance. This replacement simplifies the analysis of problems involving grounding with multiple rods but has no significant practical usage other than to calculate the theoretical ground resistance.

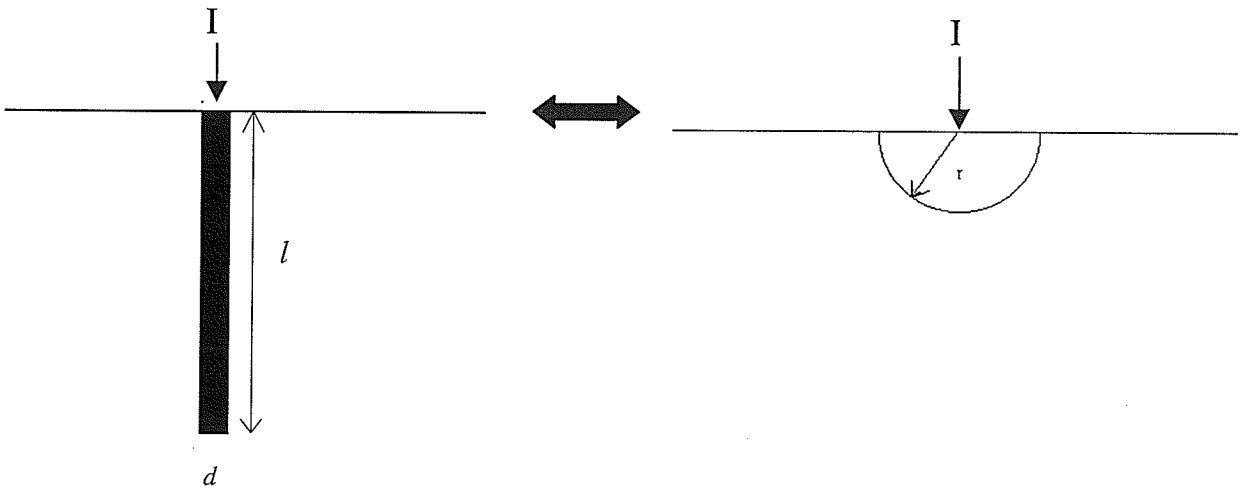

Figure 2.3 Replacement of a vertical rod with an equivalent hemisphere

The formula used for the replacement is[64Tagg]:

$$r = \frac{l}{\ln\frac{8l}{d} - 1} \qquad (2-3)$$

Here, r is the radius of the equivalent hemisphere, l and d are the length and diameter of the vertical rod. With the ability to replace vertical rods with equivalent hemispheres, one may proceed to the case of grounding with multiple rods.

2.3.2 Circle (Ring) Configuration

In order to arrive at a formula that can be used to estimate the resistance of the multiple-rod electrode scheme of Fig. 2.4, the individual rods are replaced by equivalent hemispheres. It is implied here that all the rods are identical and the spacing between rods is constant i.e., the geometry is symmetrical. With this replacement, Eq. (2-4) is obtained [64Tagg]:

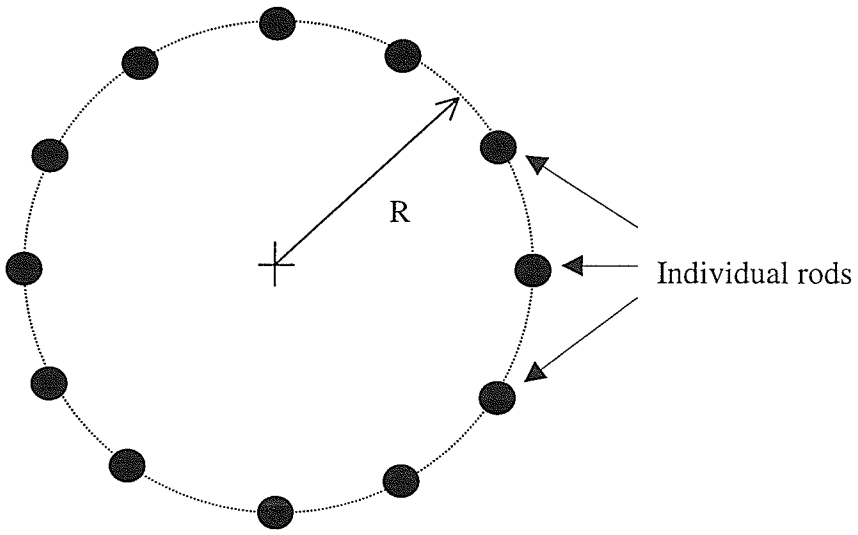

Figure 2.4 Plan view of multiple-rod grounding arranged in a ring, the individual rods extend into the page

To apply Eq. (2-4), one needs knowledge of the ground resistance obtained with the individual rods that are to be used to form the multiple-rod electrode scheme in the selected site. This value can easily be obtained from Eq. (2-1).

$$\frac{R_{Electrode}}{R_{Rod}} = \frac{1 + 0.5\alpha + \alpha \sum_{S=1}^{S=\frac{n}{2}-1} \csc \frac{S\pi}{n}}{n} \qquad (2-4)$$

$R_{Electrode}$ = Ground resistance of the multiple-rod electrode scheme

R_{Rod} = Ground resistance obtained with one individual isolated rod

n = total number of individual rods used

r = radius of the equivalent hemisphere which replaces the rod

R= radius of the circle formed by the rods

$\alpha = r/R$

Since Eq. (2-4) was obtained by replacing the rods by hemispheres, it is assumed that the spacing between the rods must be equal or larger than twice the radius of the equivalent hemisphere. Before using Eq. (2-4), one should always check the geometry of the multiple-rod electrode scheme by using Eq. (2-3) to make sure that this assumption is valid. Problems arise when the rods used are very long in length and are arranged close to one another in the circle. In this case, Eq. (2-4) will produce a completely misleading result!

Eq. (2-4) actually yields a fairly conservative approximation. The true ground resistance may be 5~25% lower that its estimation. Analytical solutions similar to Eq. (2-4) for different multiple-rod electrode schemes do exist. Solutions for arrangements consisting of rods arranged in a straight line, triangle, hollow square and solid square formation can be found in [64 Tagg].

2.3.3 Compact Ring Configuration

A compact ring configuration is one made up of long vertical rods, spaced close to each other and arranged in a circle. In other words, the arrangement is identical to the layout as depicted in Fig. 2.4 but the spacing between rods is much smaller. This implies that Eq. (2-4) cannot be used here. The following equation gives the resistance of such an electrode scheme including all mutual resistances [48 Sunde]:

$$R_n = \frac{1}{n}\left[R_1(a) + \sum_{m=1}^{n-1} R_1\left(D \sin \frac{m \cdot n}{n} \right) \right] \qquad (2-5)$$

where:

$$R_1(x) = \frac{\rho}{2\pi l}\left(\ln\left[\frac{2l}{x}\left(1 + \sqrt{1 + \left(\frac{x}{2l} \right)^2} \right) \right] + \frac{x}{2l} - \sqrt{1 + \left(\frac{x}{2l} \right)^2} \right) \qquad (2-6)$$

ρ = soil resistivity (Ω-m)

l = length of individual rod (m)

D = diameter of the ring (m)

n = total number of rods

a = radius of individual rod or the spacing between rods from rod's centre to rod's centre (m)

Since Eq. (2-5) is obtained by using average potential method, one can expect an accurate theoretical prediction by it. Its accuracy depends heavily on how close the geometry and geophysical scenario in question match up with the assumptions.

2.4 Spheroidal Electrode in Two-Layered Earth

Fig. 2.5 shows a model with a perfectly conducting spheroidal electrode in a two-layered earth. The interface between the two earth layers defines a hyperboloid of revolution, confocal to the spheroid.

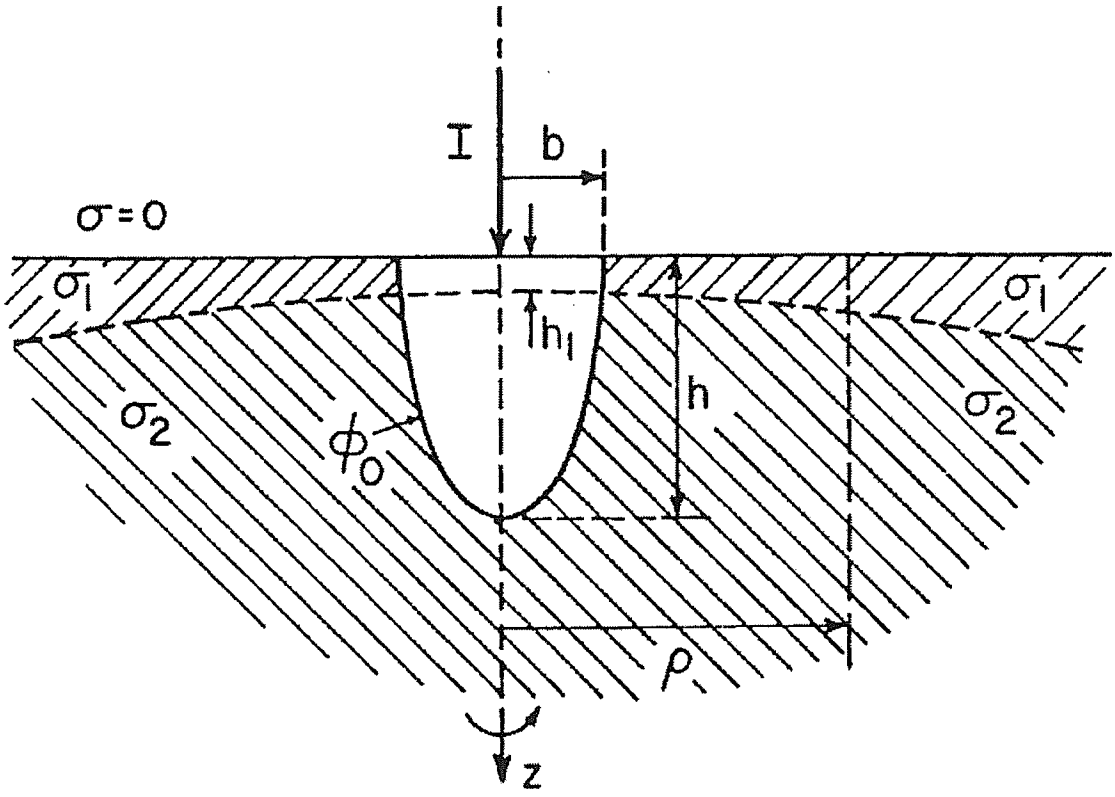

Figure 2.5 Spheroidal electrode in two-layered earth

The analytical solution for such a system has been derived as follow [88 Ciric]:

$$\Phi_0 = \frac{I}{4\pi b \sigma_1 F} \ln \frac{\left[1 + \frac{1}{\left(\frac{h}{b}\right)^2 - 1}\right]^{\frac{1}{2}} + 1}{\left[1 + \frac{1}{\left(\frac{h}{b}\right)^2 - 1}\right]^{\frac{1}{2}} - 1} \qquad (2-7)$$

where

$$F = \left[\left(h/b\right)^2 - 1\right]^{\frac{1}{2}} \cdot \frac{\sigma_2}{\sigma_1} + \frac{h_1}{b}\left(1 - \frac{\sigma_2}{\sigma_1}\right) \qquad (2-8)$$

The potential and radial potential gradient distributions at the ground surface, for $\rho/b \geq 1$ are:

$$\Phi = \frac{I}{4\pi b \sigma_1 F} \ln \frac{\left[1 + \frac{\left(\rho/b\right)^2}{\left(h/b\right)^2 - 1}\right]^{\frac{1}{2}} + 1}{\left[1 + \frac{\left(\rho/b\right)^2}{\left(h/b\right)^2 - 1}\right]^{\frac{1}{2}} - 1} \qquad (2-9)$$

$$E = \frac{I}{2\pi b^2 \sigma_1 F} \frac{1}{\left(\frac{\rho}{b}\right) \cdot \left[1 + \frac{\left(\rho/b\right)^2}{\left(h/b\right)^2 - 1}\right]^{\frac{1}{2}}} \qquad (2-10)$$

The potential and vertical potential gradient distributions along the axis of symmetry i.e., the z-axis(beneath the electrode) are:

$$\Phi = \frac{I}{4\pi b\sigma_1 F} \ln \frac{\left(z/b\right) + \left[\left(h/b\right)^2 - 1\right]^{\frac{1}{2}}}{\left(z/b\right) - \left[\left(h/b\right)^2 - 1\right]^{\frac{1}{2}}} \qquad (2-11)$$

$$E = \frac{I}{2\pi b^2 \sigma_1 F} \frac{\left[\left(h/b\right)^2 - 1\right]^{\frac{1}{2}}}{\left(z/b\right)^2 - \left[\left(h/b\right)^2 - 1\right]} \qquad (2-12)$$

2.5 Toroidal Electrode in Homogeneous Earth

Fig. 2.6 shows a perfectly conducting toroidal electrode, in the form of half a doughnut. The earth is assumed to be of infinite extent and homogeneous. The relationship between the current injected in to the electrode and electrode potential, potential and potential gradient distributions at the ground surface and along the symmetry axis (beneath the electrode) in forms of equations similar to Eqs. (2-7) ~ (2-12) have been derived [88 Ciric]. However, the resulting equations in this system are more complicated than those in section 2.4. Here, toroidal coordinates and toroidal functions (half-order Legendre functions) of the first and second kind are involved. The resultant equations in this section and section 2.4 are obtained by use of an analytical method, hence one can expect good accuracy provided the prevailing conditions match up with the assumptions.

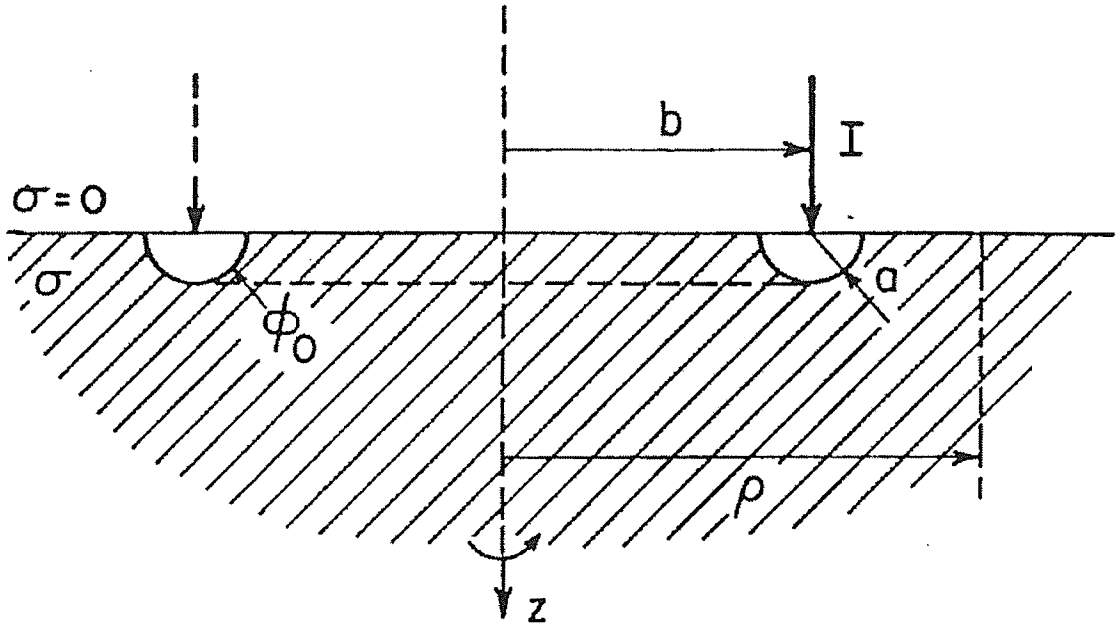

Figure 2.6 Toroidal electrode in homogeneous earth

2.6 Use of Analytical Solutions in This Thesis

The expressions in this chapter except for section 2.5 have been used in chapter 3 in order to establish the accuracy of the *Finite Element Method* based numerical solutions.

Chapter 3

Methodology and Accuracy Assessment

This chapter discusses the methodology employed in this work and establish the accuracy of the numerical method used. In order to do the latter, configurations with known analytical solutions were used and compared against numerical solutions. The configurations considered are: single vertical rod in homogeneous and multi-layered earth, spherical electrode grounding in homogeneous earth and multiple-rod grounding with vertical rod electrodes in homogeneous earth. The analysis tool used is a *Finite Element Method*, FEM package called *ANSYS 5.5 (University high option)*.

3.1 Methodology

The method employed is the *Finite Element Method*, FEM. The electrode and earth system is modeled and a known current, I_0 injected into the electrode. The electrode potential, V_0 and resistance, R are then evaluated. For multiple-rod grounding, each rod is injected with a current and the individual rod ground resistance is evaluated. The overall electrode ground resistance is the equivalent ground resistance of these individual rods that are connected in parallel. Many texts are available to provide good discussions on the FEM, for example [91 Szabo] and [96 Silvester].

In terms of accuracy, there are two main factors that are involved. The first is the domain of earth being modeled and secondly the total number of nodes used. When employing FEM to evaluate the ground resistance of an earth electrode, one has to decide on how much of the surrounding soil will be modeled. In theory, an infinite domain will be needed to include all the resistance. This translates into an infinite amount of nodes in

the FEM model! Regarding the limit of allowable total number of nodes, the FEM package employed *(ANSYS 5.5, University high option)* has a limit of 32,000 nodes.

3.2 Single Vertical Rod Grounding in Homogeneous Earth

This system is depicted in Fig. 2.1 and the exact ground resistance, R_{exact} can be evaluated by using Eq. (2-1). Here, the earth is assumed to be homogeneous. This is an axisymmetric system and therefore a 2D model is sufficient. The axisymmetric model is shown in Fig. 3.1.

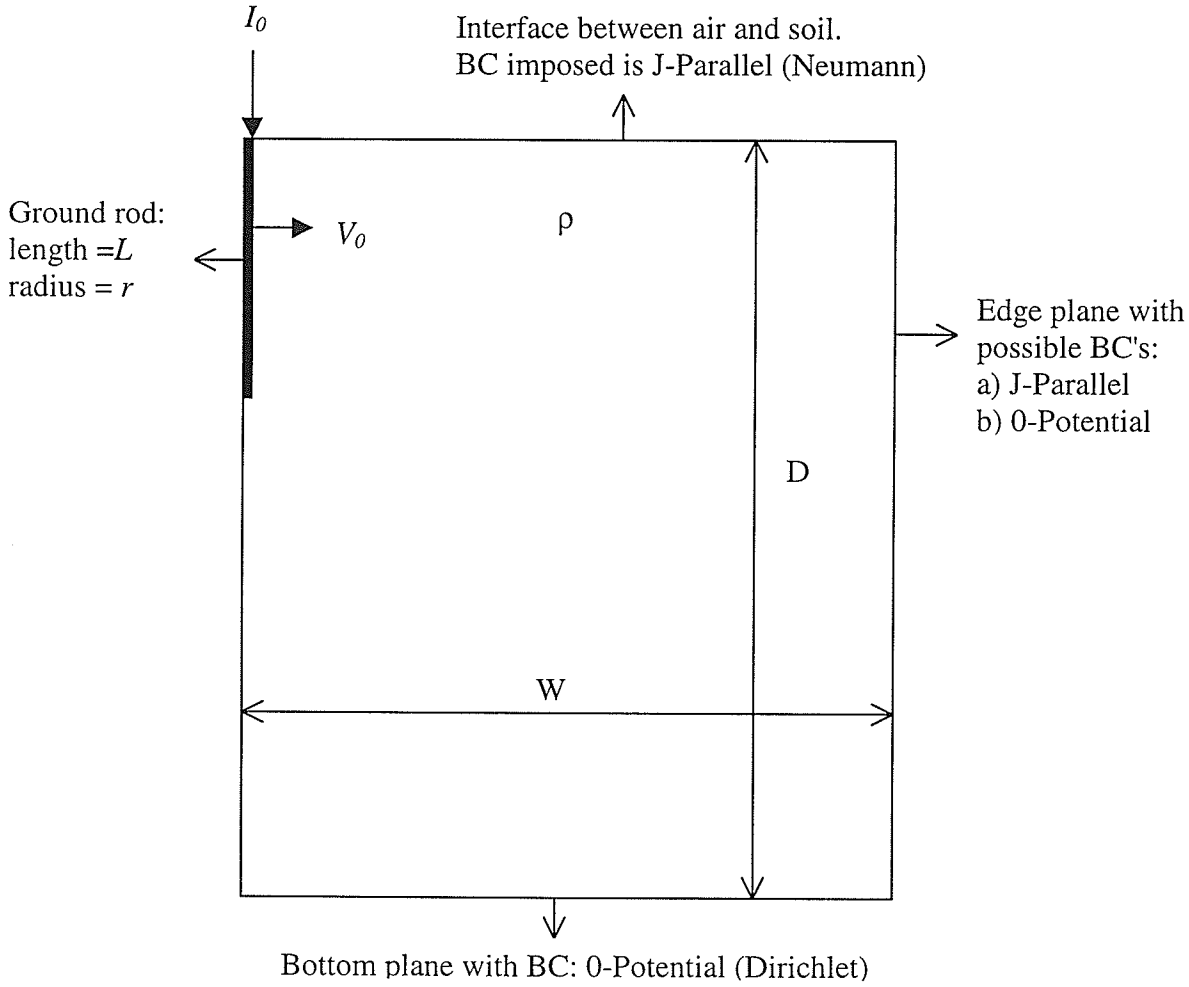

Figure 3.1 Axisymmetric model of grounding with single vertical rod

The edge and bottom planes are the boundaries of truncation. There are two possible boundary conditions for the edge plane, which are either the "J-Parallel" or the "0-Potential" condition. The "J-Parallel" condition refers to the situation where the current density, **J** vector is in parallel with the edge plane. This is essentially a Neumann type boundary condition. The bottom plane is constrained at "0-Potential", which is a Dirichlet type boundary condition. Table 3.1 shows the effects of domain of earth modeled and boundary conditions (BC) imposed on the accuracy of the estimated ground resistance, R_{est}.

Case	W / L	D / L	Nodes	BC's Imposed on Edge Plane	R_{est} (Ω)	Error (%)
A	1	3	1,280	J-Parallel	4.638	-49
				0-Potential	2.500	19
B	2	4	1,391	J-Parallel	3.296	-6
				0-Potential	2.640	15
C	3	5	1,584	J-Parallel	3.001	3
				0-Potential	2.663	14
D	4	6	2,028	J-Parallel	2.915	6
				0-Potential	2.701	12
E	5	7	3,679	J-Parallel	2.937	5
				0-Potential	2.785	10
F	6	8	4,851	J-Parallel	2.924	6
				0-Potential	2.808	10
G	7	9	6,706	J-Parallel	2.937	5
				0-Potential	2.844	8

Table 3.1 Effects of boundaries of truncation and imposed boundary conditions on the accuracy of the estimated ground resistance using an axisymmetric model.
L = 30 m, r =0.127 m and ρ =100 Ω-m
Note: R_{exact} = 3.1041Ω

The results in Table 3.1 are valid for the case where the length of rod, L is 30 m, its radius, r is 0.127 m and the soil resistivity, ρ is 100 Ω-m. W and D are dimensions as depicted in Fig. 3.1 expressed in terms of multiples of the rod length, L. BC's refers to the boundary conditions imposed on the edge plane. R_{est} is the estimated resistance using FEM (ANSYS 5.5). The errors are calculated with respect to the exact ground resistance, R_{exact} obtained by using Eq. (2.1), which yields 3.1041Ω.

It is observed that the difference in errors due to prescription of different types of boundary conditions along the edge plane diminishes as the domain involved grows larger. This reinforces the discussion in section 1.4.2. For case G, the errors due to imposition of "J-Parallel" and "0-Potential" conditions are 5% and 8%, the difference is only 3%. If the domain is further enlarged, this difference in error will get smaller. In theory, if the domain becomes infinitely large, there will be no difference in the estimation obtained by imposing either the "J-Parallel" or "0-Potential" condition.

Other significant sources of error are the total number of nodes used and the node density distribution of the total number of nodes employed to model the system. If the total number of nodes is increased, it results in an increase in memory requirements, computational resources and time. The node density distribution refers to the distribution of nodes. Regions closer to the electrode, especially around sharp points, should have a higher node density whereas regions further away from the electrode may have a lower density of nodes.

From an engineering point of view, case E is the optimum model for modeling a single ground rod embedded in homogeneous earth. It uses 3,679 nodes and by imposing the "O-Potential" condition, an estimation with an error of 10% is obtained. Case G with 13,758 nodes provides an estimation of ground resistance with an error of 8% by imposing of the "O-Potential" condition. This 2% of improvement in accuracy comes at the expense of approximately a two-fold increase in the total number of nodes employed, which is not justified!

3.3 Boundary Conditions Re-examined

It has been discussed in section 1.4.2 that if the domain of soil modeled is sufficiently large enough, imposition of the "J-Parallel" or the "0-Potential" boundary condition on the edge planes will yield very similar results. From Table 3.1, one observes that R_{est} produced by the imposition of "J-Parallel" condition on the edge planes is always larger than the R_{est} produced by the imposition of "0-Potential" condition on the edge planes.

Clearly, the reason behind this is that the soil domain modeled is not large enough! In theory, the domain will have to be extended to infinity to arrive at a same R_{est} regardless of the boundary condition imposed on the edge plane. A more descriptive explanation can be achieved by examining Figs. 3.2 and 3.3., which show sketches of flux lines for the axisymmetric case of a single vertical rod grounding in a homogeneous earth system. Both figures show flux lines along a plane of symmetry.

Fig. 3.2 shows flux lines due to imposition of the "J-Parallel" condition on the edge planes. By imposing this condition, the currents are forced to flow downward upon reaching the edge planes. The net effect is that the cross-section available for currents flow is reduced and therefore a larger R_{est} is obtained.

Fig. 3.3 shows flux lines due to imposition of the "0-Potential" condition on the edge planes. This boundary condition allows the flux lines to terminate at the edge planes, which increases the cross-section available for currents flow and therefore explains a smaller R_{est}.

Due to limited resources, modeling a sufficiently large enough domain is neither possible nor practical. For practical FEM models such as those considered in cases E, F and G in Table 3.1, imposition of the "0-Potential" boundary condition actually produces a more natural and reliable currents flow pattern that makes more sense.

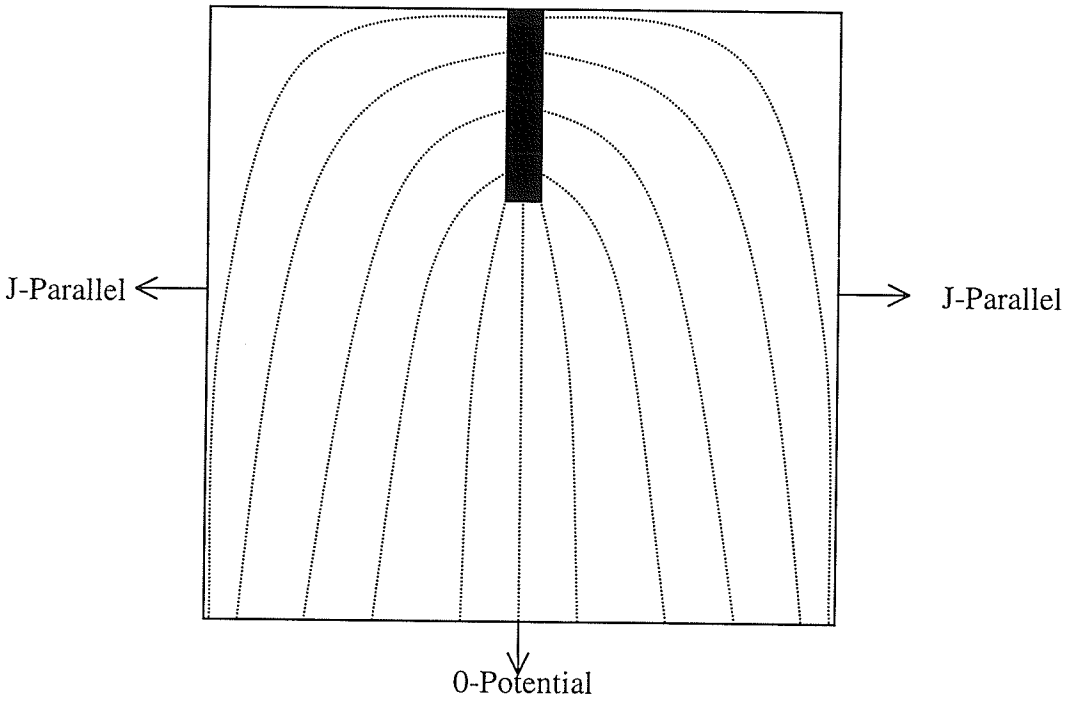

Figure 3.2 Sketch of flux lines due to imposition of "J-Parallel" condition at the edge plane and "O-Potential" condition at the bottom plane

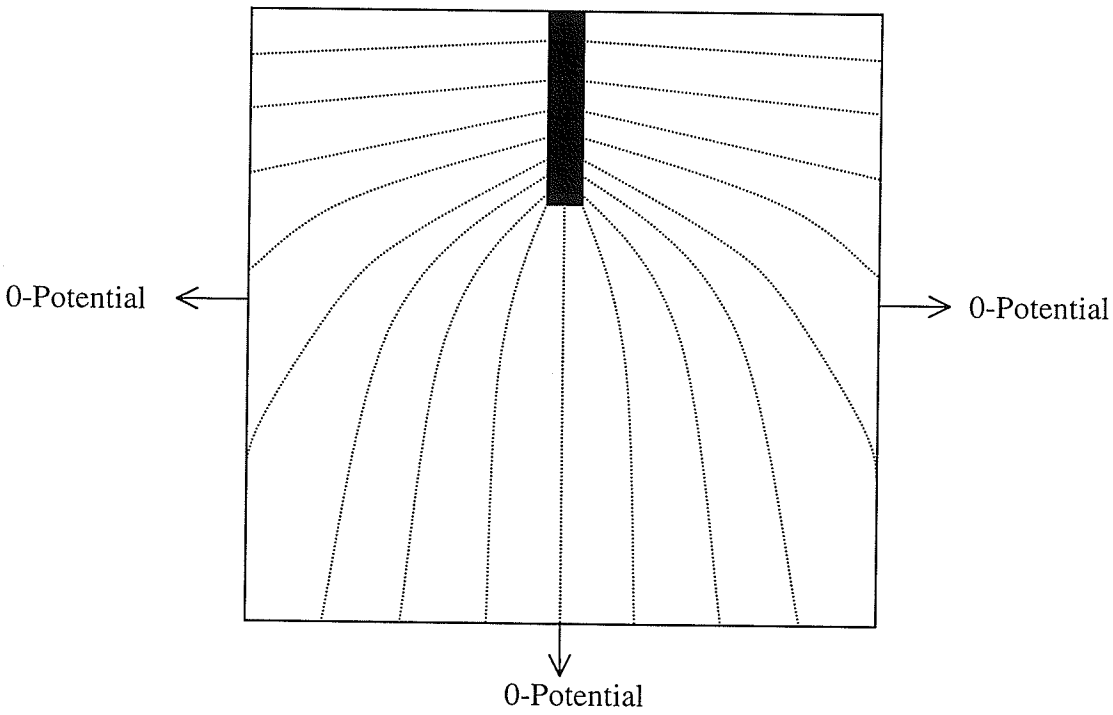

Figure 3.3 Sketch of flux lines due to imposition of "O-Potential" condition at the edge plane and at the bottom plane

3.4 Single Vertical Rod Grounding in Multi-Layered Earth

The assumption of a homogeneous earth simplifies the problem to a great extent. However, this is far from realistic. A more realistic model for the earth is to assume a multi-layered structure with different thicknesses, D_k and resistivities, ρ_k where k indicates the k^{th} layer. This model is shown as Fig. 3.4. Notice that all of the indicated layers run parallel to the earth surface. The effects of inclination of layers will be addressed in a later chapter.

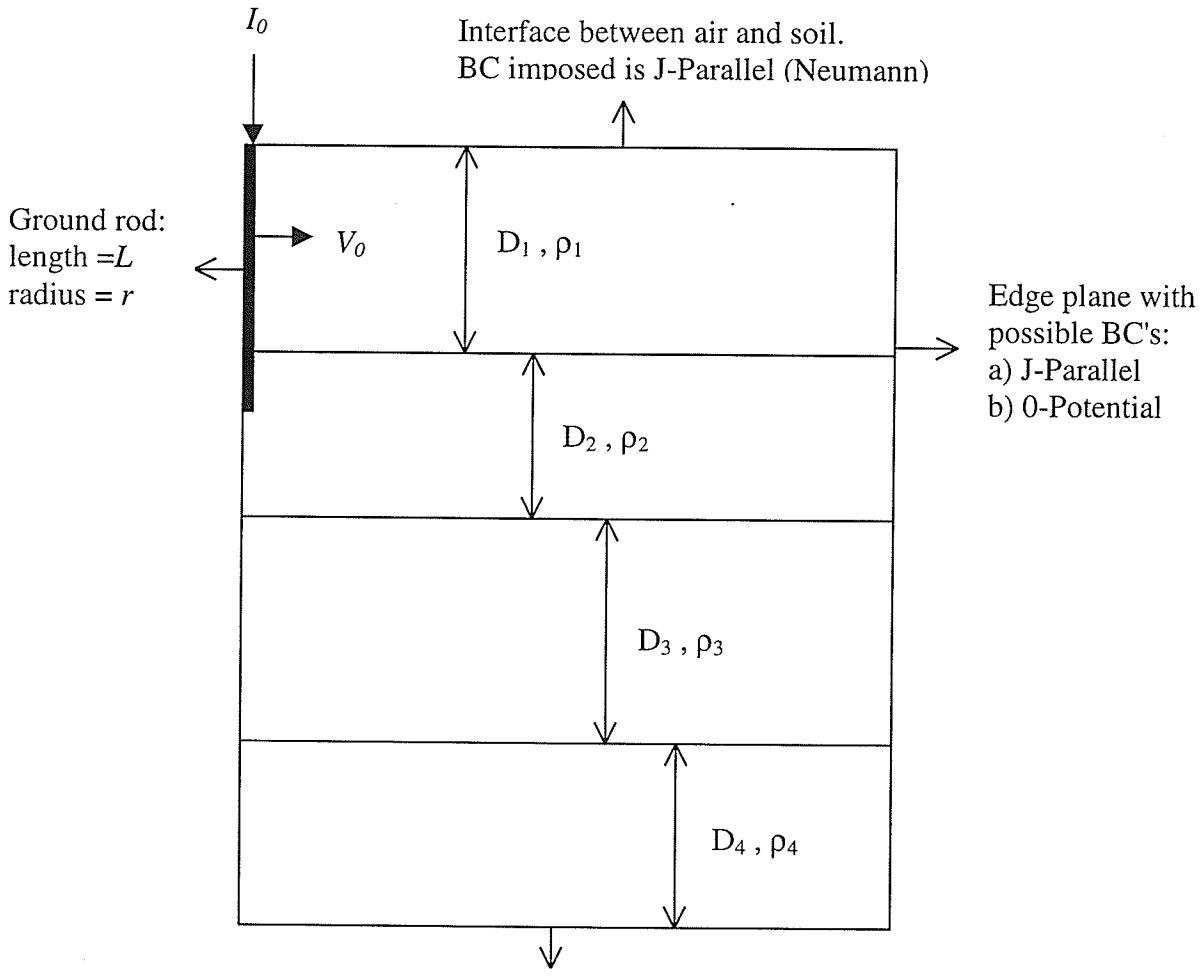

Figure 3.4 Axisymmetric model of single vertical rod grounding in multi-layered earth

An analytical solution similar to Eq. (2-1) is not available for the configuration of Fig.3.4. However, there is a good way to assess the adequacy of the FEM model and the mesh. One can model, mesh the multi-layered structure and then set all the resistivities, ρ_k's equal to one value say, ρ_1. The structure now becomes identical to the one depicted in Fig. 3.1, Eq. (2-1) can now be employed to check the adequacy of the model. If an estimation within 10% error is obtained, one can conclude that the model and mesh is adequate therefore can be used with the multi-layered problem. In the next step, the resistivities, ρ_k's are changed to their corresponding values and a reliable estimation of ground resistance, R_{est} for the case of a single vertical ground rod in multi-layered earth structure is obtained while maintaining the same mesh.

If the error of the model and mesh is known(based on the single rod in homogeneous earth case), the estimated ground resistance, R_{est} for the case of a single vertical ground rod in multi-layered earth can be corrected to obtain the projected exact ground resistance, R_{exact_p} as follows:

$$Error = \frac{R_{exact} - R_{est}}{R_{exact}}$$

$$R_{exact}[1 - Error] = R_{est}$$

$$R_{exact} = \frac{R_{est}}{[1 - Error]}$$

If R_{est} is the estimated ground resistance of a single vertical rod embedded in multi-layered earth obtained with a model and mesh where the error is known, then the projected exact ground resistance, R_{exact_p} of such an arrangement is:

$$R_{exact\_p} = \frac{R_{est}}{[1 - Error]} \qquad (3-1)$$

3.4.1 Verification of The Suggested Method for Accuracy Assessment With Regards to The Estimation of R_{est} in Multi-layered Earth

The following discussion will show that the method for assessing the accuracy of R_{est} in multi-layered earth as proposed in section 3.4 is adequate, based on a single vertical rod grounding in two-layered earth as depicted in Fig 2.2. Suppose that the length of rod, l is 3.048m, the radius of rod, r is 0.03m and h is $0.5l$ (refer to Fig 2.2), ρ_1 and ρ_2 are 100 and 5 Ω-m, which gives a reflection coefficient, k of approximately -0.9.

From Eqs. (2-1), (2-2) and the curves in [64 Tagg] pages 171, 172 and 173, one obtains F=0.1, R_1 = 26.1462Ω and R_a = -2.25Ω therefore,

$$R_{exact} = 0.1\ [26.1462\text{-}2.25]$$
$$= 2.3896\ \Omega$$

The same arrangement is modeled in *ANSYS 5.5*. First, ρ_1 and ρ_2 are set to 100 Ω-m simulating a homogeneous earth. The estimated ground resistance of the rod in this simulated homogeneous earth by using *ANSYS 5.5* is, R_{est} = 23.975 Ω and by analytical solution, which is Eq. (2-1), R_{exact} = 26.1462 Ω, therefore the model and mesh error is:

$$Error = \frac{26.1462 - 23.975}{26.1462}$$

$$\approx 0.083$$

Now using the same model and mesh, ρ_2 is set to 5 Ω-m to simulate the two-layered earth. The estimated gound resistance of the rod by *ANSYS 5.5* is, R_{est} = 2.094 Ω. Using Eq. (3-1), the projected exact ground resistance is,

$$R_{exact\_p} = \frac{2.094}{[1-0.083]}$$

$$= 2.2835\ \Omega$$

The difference between this projected exact ground resistance, R_{exact_p} and the exact ground resistance, R_{exact} is only 4.4%. This shows that the suggested method for assessing the accuracy of the estimated ground resistance, R_{est} and the technique for arriving at the projected exact ground resistance, R_{exact_p} involving a single vertical rod embedded in multi-layered earth are applicable.

3.5 Multiple-Rod Grounding in Homogeneous Earth

Fig. 3.5 shows the plan view of a multiple-rod electrode scheme arranged in a ring formation. The radius of the circle formed by the individual rods is R; the rods extend into the page. Due to the prevailing symmetry, modeling only half of the structure as depicted in Fig. 2.4 is sufficient. Fig. 3.6 is a 3D oblique drawing, which shows more detail of the FEM model employed.

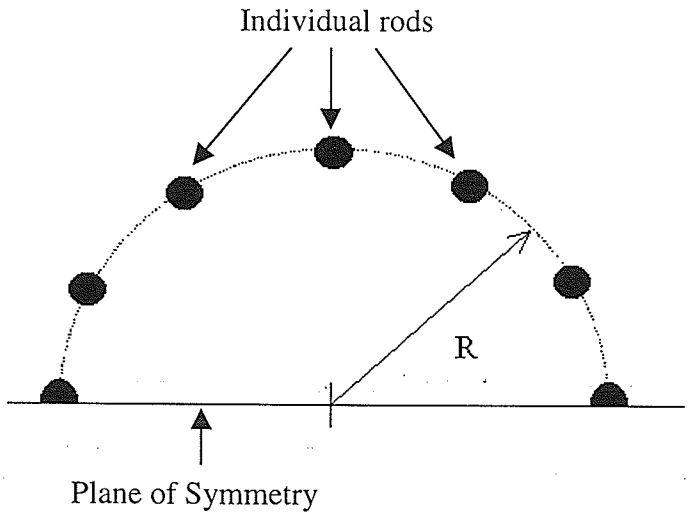

Figure 3.5 Plan view of model for multiple-rod grounding in a ring type electrode structure

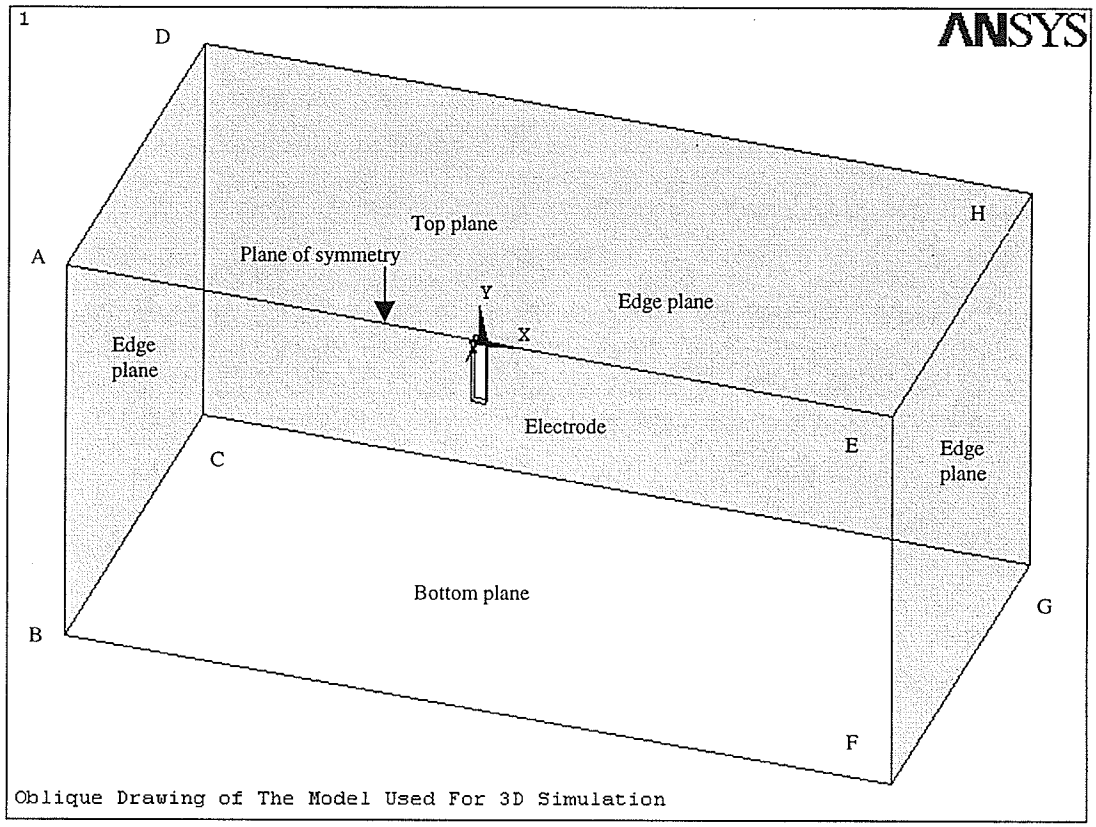

Figure 3.6 3D oblique drawing of the model used for FEM simulation

In Fig. 3.6, the three edge truncation planes(A-B-C-D, C-G-H-D and E-F-G-H)are shaded in gray whereas the top(A-E-H-D) and bottom(B-F-G-C) truncation planes are in white. However, because of the overlapping, one sees the top plane(A-E-H-D) as gray instead of white. According to the indicated coordinate system, the three edge planes are perpendicular to the X, negative X and negative Z axes. The locations of these edge planes are determined by the lateral truncation distances. In this case, they are the distances along the X-axis, negative X-axis and negative Z-axis, which ought to be at least 6 times the rod length, *L*. The top plane is actually the X-Z plane and the bottom plane runs parallel to it. The location of the bottom plane is determined by the vertical truncation distance, which is the distance along the negative Y-axis. This distance should also be at least 6 times *L*. The plane of symmetry is the X-Y plane. The multiple-rod electrode is depicted as a simplified, long block structure.

3.5.1 Complications of 3D Modeling

The model depicted in Fig. 3.5 requires 3D modeling, which introduces extra complications. One obvious complication is the increased number of nodes required. Due to the enormous number of nodes required in a 3D modeling, a technique called *'substructuring'* may be used. This is achieved in *ANSYS 5.5* by condensing a group of finite elements into an element represented as a matrix called *'superelement'*. This *'superelement'* can then be used as an element in the model. The elements within the *'superelement'* are assumed to be linear. This is a key assumption but does not necessarily restrict the application of the technique. Essentially, it is a matrix reduction method by using some forms of approximations. This technique allows one to tackle a bigger problem with limited computer resources and reduces computational time. Some very sketchy information on *'substructuring'* can be found in [99 ANSYS]. A very simple but illustrative example which brings out the essence of the *'substructuring'* technique is included in Appendix B. The author of this work spent a substantial amount of time to understand and implement the *'substructuring'* technique. The *'substructuring'* technique has been employed in all 3D modeling in this study.

3.5.2 Domain and Boundary Conditions

The required model domain and boundary conditions to achieve a reliable result in a 3D situation are similar to those discussed in sections 3.2 and 3.3. In section 3.2, it is recommended that the lateral(along earth surface) distance to be included in the modeling be at least 5 times the length of the ground rod, L and the vertical distance(depth in to earth) be at least 7 times L.

However, for a 3D modeling situation using the *'substructuring'* technique, results have shown that a better and more reliable estimation is possible with the lateral and vertical distances equal to each other, provided the chosen truncation distance is at least 6

times L. For a multiple-rod ring type electrode, this distance is measured from the center of the circle formed by the individual rods and L is the length of the individual rods .

Table 3.2 shows the effects of imposing different boundary conditions and extent of domain modeled on the estimation of ground resistance. The estimated ground resistance, R_{est} is compared with value from Eq. (2-4). It is worth mentioning here that Eq. (2-4) is a very conservative formula, which tends to yield results 5~25% larger than the true value [64 Tagg].

Case	Lateral (Multiple of L)	Vertical (Multiple of L)	BC's Imposed on Edge Planes	R_{est} (Ω)	Error (%)
A	6	6	J-Parallel	6.6450	14
			0-Potential	6.1170	21
B	6	8	J-Parallel	7.2050	7
			0-Potential	6.1650	20
C	12	12	J-Parallel	6.8400	12
			0-Potential	6.5800	15
D	12	16	J-Parallel	7.1200	8
			0-Potential	6.4100	17

Table 3.2 Grounding with multiple rods in homogeneous earth.
Effects of boundaries of truncation and imposed boundary conditions on the accuracy of the estimated ground resistance with 3D modeling.
Note: R_{exact} is 7.7500Ω

The results in Table 3.2 apply to a ring type electrode system with 10 vertical rods, installed in a homogeneous earth with resistivity, ρ of 100 Ω-m. The radius of the circle formed by the individual rods is 3.048m. Each rod is 2.44m in length and with radius of 0.0127m. Using Eq. (2-4), R_{exact} is 7.7500Ω.

Although, Eq. (2-4) tends to overstate the true ground resistance of the electrode, its prediction is still being assumed as exact and used as the basis for comparison. The error calculated in Table 3.2 is the percentage error between R_{exact} and R_{est}. The prescribed boundary conditions are similar to those in section 3.2 where the bottom truncation plane is held at "0-Potential" and the edge truncation planes can have either "J-Parallel" or "0-Potential" condition.

Case C in Table 3.2, shows that imposition of either the "J-Parallel" or "0-Potential" conditions results in values of R_{est} which differ by only 3%. This implies a reliable estimation. Notice case A where the lateral and vertical truncation distances are equal to only 6 times L. If the "J-Parallel" boundary condition is imposed, the value of R_{est} is close to case C. Cases B and D both show that having unequal truncation distances on the lateral and vertical directions create discrepancy in the estimation of R_{est}.

3.6 Spheroidal Electrode

In sections 3.2 to 3.5, the accuracy and reliability of the estimated value of ground resistance, R_{est}, have been assessed. The solutions of potential distribution, V and potential gradient distribution, $\boldsymbol{E}$ thus current density, $\boldsymbol{J}$ should be discussed. In order to achieve this, a spheroidal electrode such as the one depicted in Fig. 2.5, with complete analytical solution, is selected to form the basis for assessment.

The analytical solution of such a ground electrode is provided in section 2.4. The solution in section 2.4 involves a two-layered earth, however, for simplicity, a homogeneous earth model is used instead. Essentially, the earth conductivity σ_1 and σ_2 are assumed to be equal. Eqs. (2-7), (2-8), (2-9), (2-10), (2-11) and (2-12) are used to assess the accuracy of the FEM solution.

3.6.1 Estimated Spheroidal Electrode Earth Resistance

A spheroidal eletrode with semi-minor axis and semi-major axis equal to 0.25m and 2.00m is simulated. The earth is assumed to be homogeneous with resistivity of 100 Ω-m. Using a 3D model and imposing "0-Potential" condition on all the edge planes and on the bottom plane, a good estimation of R_{est} can be obtained. From Eqs. (2-7) and (2-8), R_{exact} is 22.2065 Ω. The solution from FEM yields a R_{est} of 20.2945 Ω. The error is about 9%. A better estimation can be achieved by increasing the size of the domain modeled.

3.6.2 Solution of Potential and Potential Gradient Distribution

The potential and potential gradient profiles are plotted in Figs. 3.7, 3.8, 3.9 and 3.10 Figs. 3.7 and 3.8 are profiles along the earth surface i.e., lateral direction whereas, Figs. 3.9 and 3.10 are profiles along the axis of symmetry beneath the electrode. These plots are generated by assuming that the total current injected into the electrode is 1 A. The solid line is the exact solution and the dashed line is the solution from the FEM simulation. Notice that the potential profiles contain significant error, which worsens as the distance from the electrode increases. This error is primarily due to insufficient total number of nodes used i.e., improper meshing of the model.

As mentioned, the FEM package employed has a maximum capacity of 32,000 nodes. In this case, this capacity is just not enough to produce a good solution for the potential distribution, V. On the other hand, the potential gradient distribution, $\boldsymbol{E}$ turns out to be an accurate approximation. The trend of the exact and FEM solutions of the potential distribution are similar except that the exact solution is shifted upward. When taking the gradient of the potential distribution to obtain the potential gradient distribution, the effect of this offset is eliminated and therefore, the solution of $\boldsymbol{E}$ is accurate. As a consequence, the solution for $\boldsymbol{J}$ is good as well.

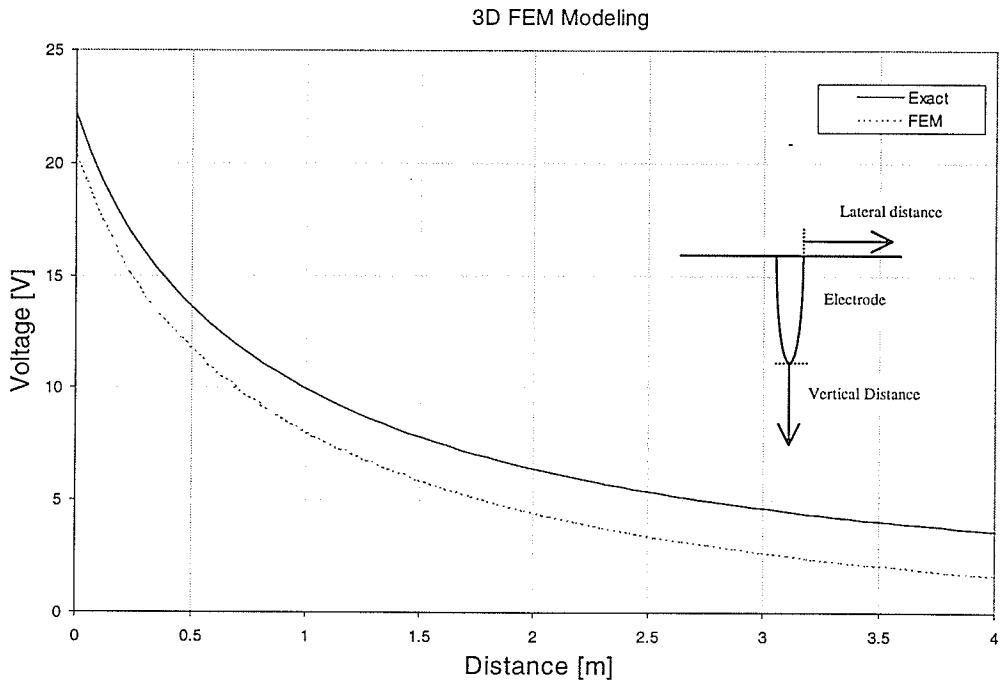

Figure 3.7 Lateral potential distribution profile along ground surface for a spheroidal electrode embedded in a homogeneous earth (Fig. 2.5)

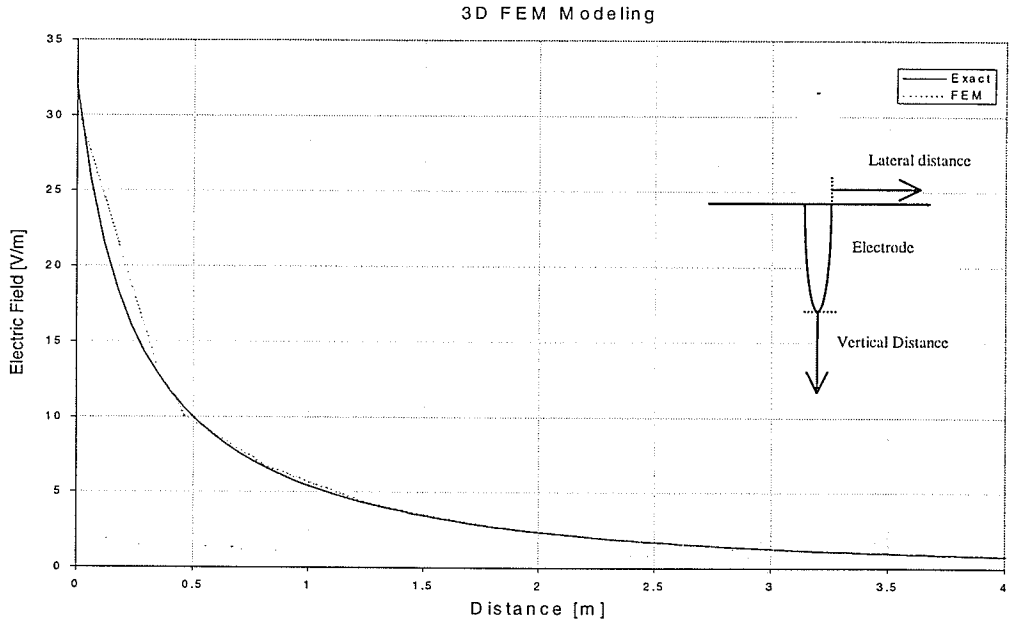

Figure 3.8 Lateral potential gradient distribution profile along ground surface for a spheroidal electrode embedded in a homogeneous earth (Fig. 2.5)

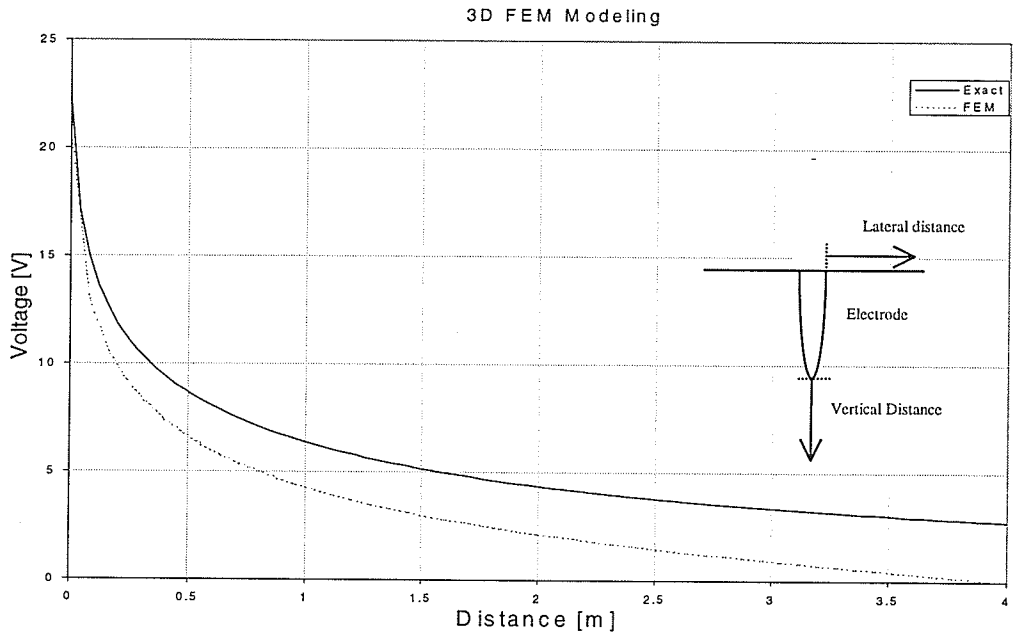

Figure 3.9 Vertical potential distribution profile along the axis of symmetry for a spheroidal electrode embedded in a homogeneous earth (Fig. 2.5)

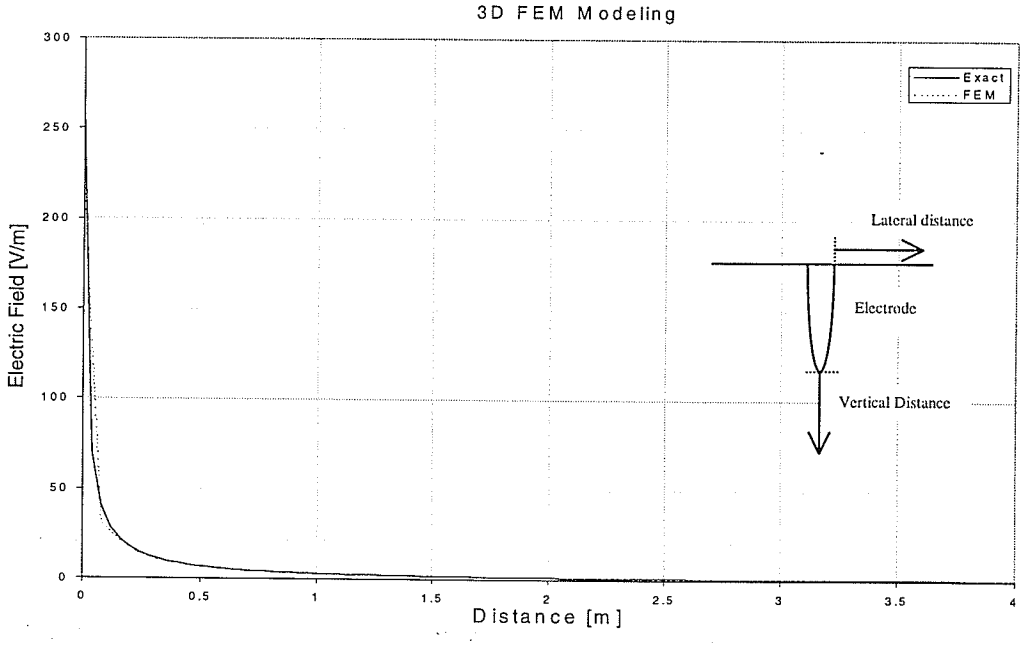

Figure 3.10 Vertical potential gradient distribution profile along the axis of symmetry for a spheroidal electrode embedded in a homogeneous earth (Fig. 2.5)

However, one should not take the solution of $\boldsymbol{E}$ for granted. The primary solution is actually the potential distribution, the potential gradient is a derived solution. If the primary solution is not accurate, it is advisable to proceed with extra caution when interpreting the derived solution.

It is worth mentioning here that the spheroidal electrode problem can be solved by using an axisymmetric model. When an axisymmetric model is used, the selected FEM package with all its limitation, still has the capability to yield very good solutions for all the quantities of interest, including the potential distribution.

3.7 Chapter Summary

This chapter is devoted to discussions on the methodology and the methods used to establish the accuracy of the numerical solutions. The required extent of domain to be modeled in order to produce a reliable solution has been suggested and the accuracy of solutions assessed. It is interesting to note that a good estimation of R_{est} does not necessarily imply a good solution for the potential distribution. Increasing the total number of nodes used in the model is a remedy for arriving at a more reliable solution of the potential distribution.

In the course of performing the FEM simulations, all the models and meshes used were assessed for accuracy and adequacy. An important inference from the results presented in this chapter is that the estimated value of the ground resistance, R_{est}, presented in this thesis will be in error by no more than 10% except for analysis associated with Eq. (2-4).

Chapter 4

Ground Resistance of Vertically Embedded Electrodes in Multi-Layered Earth

In chapter 3, it was pointed out that consideration of a multi-layered earth with different resistivities, ρ_k is more realistic. Given the resistivities and the locations of layers, the challenge is how best the problem can be handled. Most of the analytical solutions are only valid for the case of a homogeneous earth. The solutions are not useful when confronted with a multi-layered earth. An engineering remedy for overcoming such an obstacle is to assume an apparent single valued resistivity. Based on the available geological data, an apparent resistivity can be chosen with certain confidence. In practice, the assumed apparent resistivity tends to be conservative, so that it provides a safety factor in the design of a ground electrode. In addition to this safety factor, there are always over designs involved in an engineering endeavor resulting in excessive usage of materials and wastage of resources. Therefore it is important to arrive at a reasonably accurate value of apparent resistivity for the design. This problem is addressed in this chapter.

Initially a two-layered earth is considered; later, techniques to handle multi-layered earth are suggested. The earth layers are assumed to be parallel to the earth surface as indicated in Fig 3.4. It is obvious that by replacing the different resistivities, ρ_k with an equivalent resistivity, ρ_{eqv} the problem is vastly simplified, which facilitates computation efforts. This equivalent resistivity, ρ_{eqv} also makes it possible for one to resort to the classical analytical solutions to find the ground resistance.

4.1 Single Vertical Rod Grounding in Two-Layered Earth

A vertical ground rod embedded in a two-layered earth is depicted in Fig. 4.1. Although the earth is non-homogeneous, this is still an axisymmetric system. The thickness of the top layer is D and ρ_1, ρ_2 are the resistivities of the two layers. In order to facilitate analysis and discussion, the thickness of the top layer, D is expressed as a percent of the rod length, L. When $D = 0.5L$, it implies that the top layer extends from the surface of earth to a distance of $L/2$, the second layer begins at this point and extends infinitely downward.

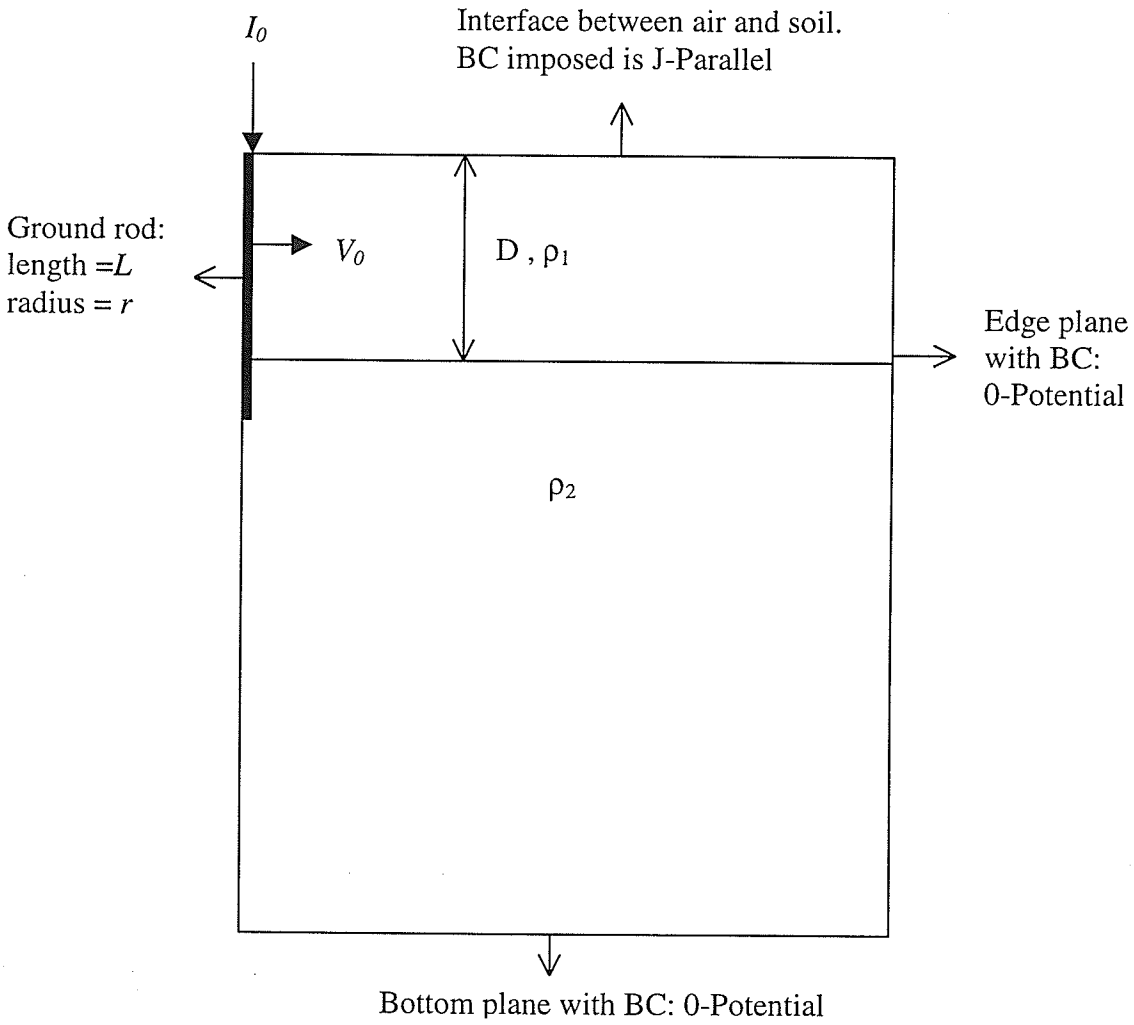

Figure 4.1 Axisymmetric model of single vertical rod grounding in two-layered earth

4.1.1 Trend of Variation

Suppose that the ground electrode is a vertical rod with length, L=20m and radius, r=0.1778m. If the top layer resistivity, ρ_1 is 100 Ω-m and the bottom layer resistivity, ρ_2 is 200 Ω-m, the ratio of ρ_1/ρ_2=1/2. Conversely, if ρ_1 is 200 Ω-m and ρ_2 is 100 Ω-m, this ratio becomes 2. These are two distinct cases that portray two types of very different resistance variations. In order to investigate these variations, the two cases were solved using the FEM technique with boundary conditions as shown in Fig. 4.1. Figs. 4.2 and 4.3 show the results which were obtained by varying the thickness of the top layer, D. The x-axis represents the variable thickness of the top layer as a percent of L and the y-axis is the estimated ground resistance, R_{est}. As mentioned in chapter 3, all these values contain errors no worse than 10%.

Figs. 4.4 and 4.5 are curves with ρ_1/ρ_2 ratio of 1/2 and 2 as in Figs. 4.2 and 4.3. The difference between Figs. 4.2 and 4.4 is that ρ_1 for Fig. 4.2 is 100 Ω-m whereas ρ_1 for Fig. 4.4 is 500 Ω-m. Similarly, ρ_1 for Fig. 4.3 is 200 Ω-m whereas ρ_1 for Fig. 4.5 is 1000 Ω-m. It is obvious that the trend of variations are similar in Figs. 4.2 and 4.4 and in Figs. 4.3 and 4.5. Figs. 4.2 and 4.4 both show a decreasing trend of R_{est}. This is because in both figures, ρ_1 is smaller than ρ_2. As D increases, a larger portion of the electrode is embedded in the lower resistivity soil, and hence R_{est} decreases. This is always true because the ground resistance is proportional to resistivity. On the other hand, Figs. 4.3 and 4.5 both show an increasing trend of R_{est} because in both these figures, ρ_1 is greater than ρ_2.

A quick and simple check concerning the correctness of these curves is possible by examining the points where D is at 0% and 400% of L. If D is 0%, it implies a homogeneous earth with resistivity equal to ρ_2. According to Fig. 4.2, R_{est} is 7.54 Ω, and by Eq. (2-1), R_{exact} is 8.13 Ω. When D is 400% of L, R_{est} is 3.77 Ω, and by Eq. (2-1) R_{exact} is 4.07 Ω. In this case, the effective resistivity approximates to ρ_1. This shows that these curves obey the general expected trend of variation.

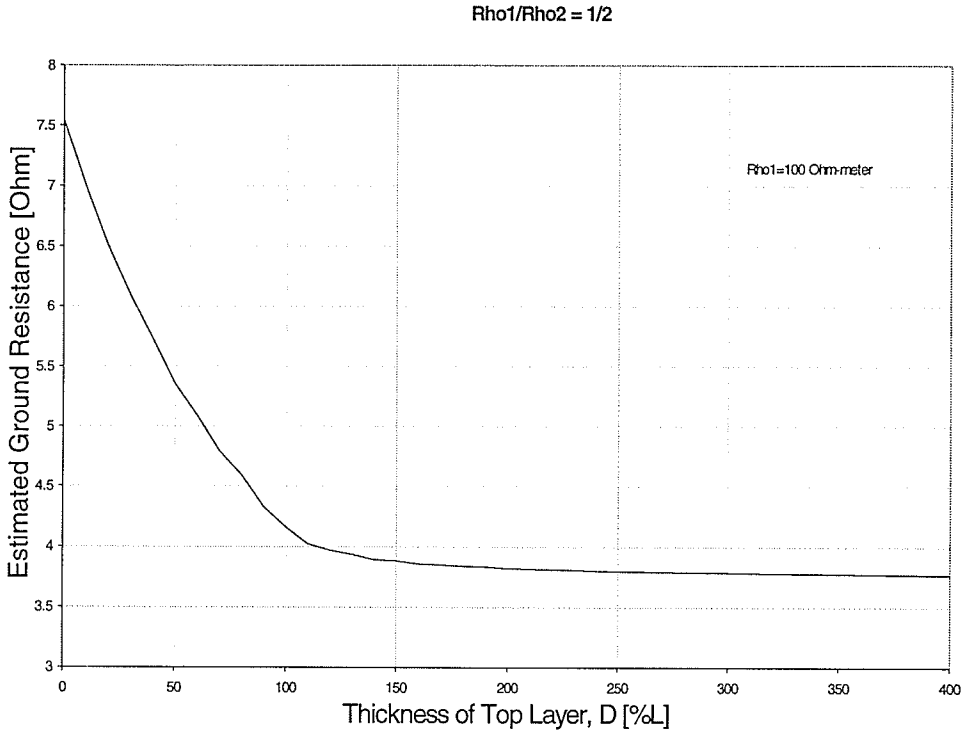

Figure 4.2 Ground resistance variation due to a vertical ground rod in two-layered earth with ρ_1=100 Ω-m $< \rho_2$ and L=20m

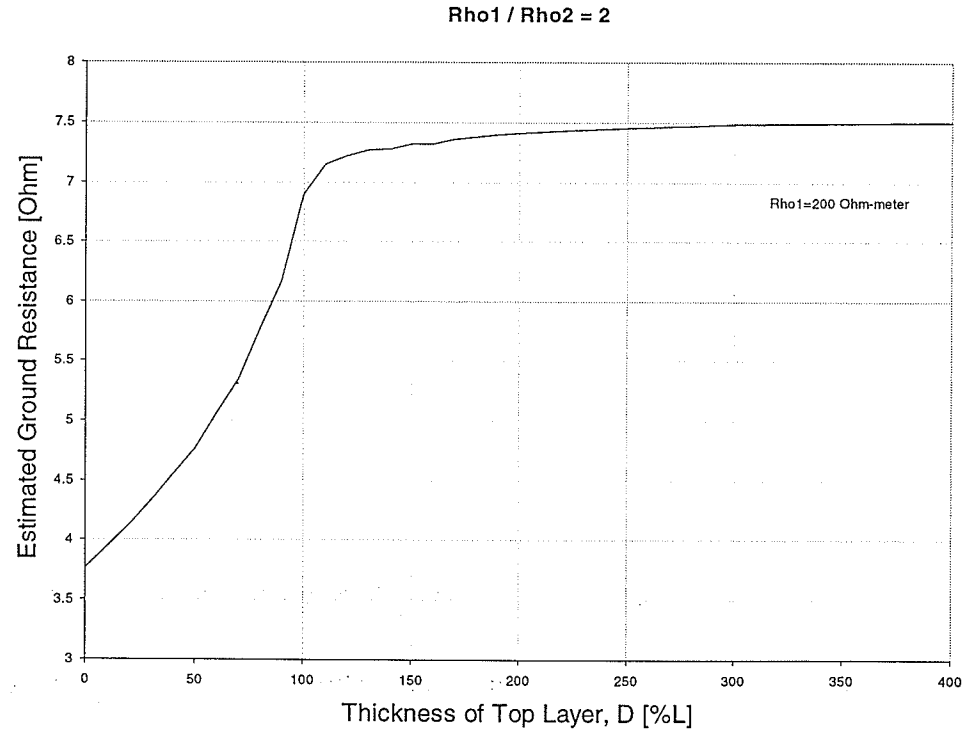

Figure 4.3 Ground resistance variation due to a vertical ground rod in two-layered earth with ρ_1=200 Ω-m $> \rho_2$ and L=20m

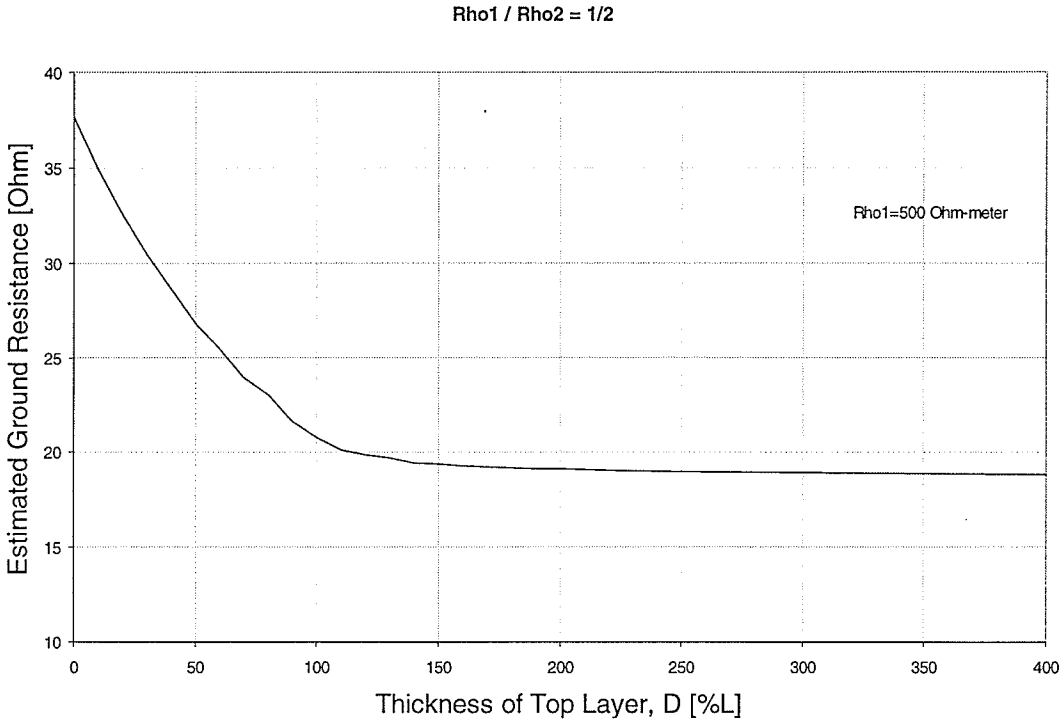

Figure 4.4 Ground resistance variation due to a vertical ground rod in two-layered earth with ρ_1=500 Ω-m < ρ_2 and L=20m

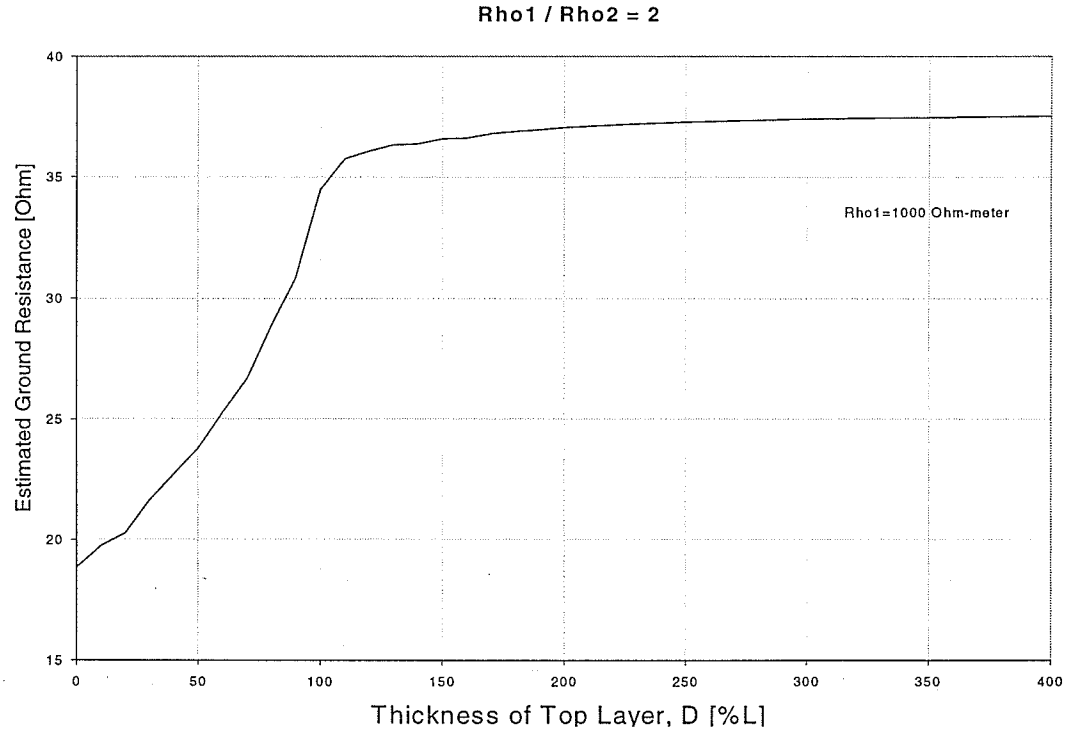

Figure 4.5 Ground resistance variation due to a vertical ground rod in two-layered earth with ρ_1= 1000 Ω-m > ρ_2 and L=20m

4.2 Effect of Depth of Layers

Figs. 4.2 through 4.5 share a common interesting trait, which is that once D exceeds 200% of L, the variation plateaus off. This is an important fact which leads to the first conclusion of this chapter i.e., if the second layer is located at a distance of more than 200% of L below the earth surface, its existence can be safely disregarded. One may simply replace the two-layered earth with a homogeneous earth with an equivalent resistivity, ρ_{eqv} equal to the resistivity of the top layer, ρ_1.

This finding can be generalized to the multi-layered case depicted in Fig. 3.4. Suppose that there is a ground rod of length, L and radius r and the earth contains k layers with k resistivities, ρ_k. Let x be a number greater than 1 and smaller than k. If the x^{th} layer is located at a distance beyond $2L$ from the surface of earth, this layer and all the subsequent layers i.e., from the x^{th} until k^{th} layers, can be replaced by an equivalent resistivity, ρ_{eqv} which is equal to the resistivity of the $(x-1)^{th}$ layer, that is $\rho_{(x-1)}$. This approximation will incur an error no worse than 5%.

Consider an example with a ground rod of 20m in length and radius of 0.1778m. The earth is assumed to have four layers with resistivities ρ_1, ρ_2, ρ_3 and ρ_4. D_1, D_2, and D_3 correspond to the thickness of the 1st, 2nd and 3rd layer. Theoretically, the 4th layer extends infinitely downward hence D_4 approaches infinity. However, in order to simulate this system, a finite domain is needed therefore a finite value of D_4 is used.

Tables 4.1 and 4.2 show the results obtained by employing the approximation discussed in this section. Beware that the R'_{exact} is not R_{exact}! R'_{exact} is the apparent exact ground resistance obtained by simulating the exact system (Using ANSYS 5.5) involving all four earth layers. This is not the exact ground resistance, R_{exact} since there is an error of no worse than 10% that is involved in its estimation.

Although, R'_{exact} isn't the exact ground resistance, it is still being used as the basis for comparison. R_{est} is the estimated ground resistance obtained after layers located at a distance more than $2L$ are replaced by an appropriate ρ_{eqv} as explained in the above paragraph.

Case	ρ_1 (Ω-m)	ρ_2(Ω-m)	ρ_3(Ω-m)	ρ_4(Ω-m)	R'_{exact}(Ω)	R_{est} (Ω)	Error(%)
1	300	100	1000	10	5.50	5.27	4.2
2	300	100	10	1000	5.11	5.27	3.1
3	100	300	1000	10	6.42	6.26	2.5
4	100	300	10	1000	6.05	6.26	3.5

Table 4.1 Illustration of errors incurred in the estimations of ground resistance by using technique of section 4.2. L = 20m, D_1, D_2 and D_3 are equal to 10, 30 and 50m

For the cases illustrated in Table 4.1, D_1 plus D_2 is 40m, which is $2L$, this implies that the 3rd and 4th layers can be replaced by a ρ_{eqv} equal to ρ_2. In other words, the 2nd layer is extended to infinity and replaces the 3rd and 4th layers. This approximation reduces the four-layered earth to a two-layered earth problem.

Case	ρ_1 (Ω-m)	ρ_2(Ω-m)	ρ_3(Ω-m)	ρ_4(Ω-m)	R'_{exact}(Ω)	R_{est} (Ω)	Error(%)
1	300	100	1000	10	7.99	8.29	3.7
2	300	100	10	1000	1.14	1.09	4.4
3	100	300	1000	10	8.03	8.30	3.4
4	100	300	10	1000	1.15	1.10	4.3

Table 4.2 Illustration of errors incurred in the estimations of ground resistance by using technique of section 4.2. L = 20m, D_1, D_2 and D_3 are equal to 8, 8 and 24m

For the cases illustrated in Table 4.2, D_1 plus D_2 is 16m, which is less than $2L$. The effect of the 3rd layer cannot be ignored. Adding D_3 to D_1 plus D_2 yields 40m, which allows one to extend the 3rd layer infinitely to replace the 4th layer. The four-layered earth has now been replaced by a three-layered earth.

Based on the values of R_{est}, R'_{exact} and the error, it is evident that this method of approximation produces acceptable results. Together with a reasonably good FEM mesh, this approximation is likely to yield an estimation error less than or around 10%.

4.3 Finding an Equivalent Resistivity for The Two-Layered Earth

This section is devoted to a discussion on deriving the normalized equivalent resistivity curves. The equivalent resistivity curves can be used to tackle problems involving parallel, multi-layered earth by replacing the different resistivities, ρ_n with an equivalent resistivity, ρ_{eqv}. The application of these curves will be demonstrated through examples.

4.3.1 Derivation of The Normalized Equivalent Resistivity Curves

Figs. 4.2 through 4.5 show the variations of the estimated ground resistance, R_{est} as a function of the thickness of the top layer, D. Using Eq. (2-1) and Figs. 4.2 through 4.5, the normalized equivalent resistivity curves can be obtained. For a single vertical rod in homogeneous earth, the ground resistance is:

$$R = \frac{\rho}{2\pi L}\left(\ln\frac{4L}{r} - 1\right) \qquad (2-1)$$

From Eq. (2-1), if L and r are known, it can be written as:

$$R = \rho \cdot \mathrm{A} \qquad (4-1)$$

where

$$\mathrm{A} = \frac{1}{2\pi L}\left(\ln\frac{4L}{r} - 1\right)$$

If the two-layered earth with resistivities ρ_1 and ρ_2 can be replaced by a homogeneous earth of equivalent resistivity, ρ_{eqv} then:

$$R = \rho_{eqv} \cdot \mathrm{A} \qquad (4-2)$$

The resistance value, R in Eq. (4-2) can be obtained from curves such as Figs. 4.2 through 4.5, depending on the value of ρ_1, ρ_2 and D. In other words, R depends on the prevailing earth and electrode conditions. Suppose R_N is the resistance of the ground rod obtained with homogeneous earth of resistivity equal to the top layer resistivity, ρ_1, then:

$$R_N = \rho_1 \cdot \mathrm{A} \qquad (4-3)$$

We now normalize R by choosing R_N as the base. R_N is a constant that depends on L, r and ρ_1. Dividing Eq. (4-2) by Eq. (4-3), we arrive at

$$\frac{R}{R_N} = \frac{\rho_{eqv}}{\rho_1} \qquad (4-4)$$

4.4 Contributions and Significance of The Normalized Equivalent Resistivity Curves

Equation (4-4) has an important implication. It implies that if Figs. 4.2 through 4.5 are normalized with the appropriate R_N, it makes it possible to read the appropriate ρ_{eqv}/ρ_1 ratio corresponding to a certain D using the normalized curves. Multiplying this ratio by ρ_1, one obtained the ρ_{eqv}, which reduces the two-layered earth to a homogeneous one.

Another very important fact which emerges after normalization of Figs. 4.2 through 4.5 is that, the normalized plots of Figs. 4.2 and 4.4 overlap each other as depicted in Fig. 4.6. The same is true for the normalized plots of Figs. 4.3 and 4.5 as shown in Fig. 4.7. This finding bring us to the conclusion that, the ratio ρ_1/ρ_2 and D are the most significant factors in determining the trend of variation of ground resistance due to a vertical ground rod in a two-layered earth, not the absolute value of ρ_1 and ρ_2.

Figs. 4.6 and 4.7 are the normalized equivalent resistivity curves for ρ_1/ρ_2 ratio of 1/2 and 2. Appendix C contains individual normalized equivalent resistivity curves for ρ_1/ρ_2 ratios of 1/2, 1/3, 1/4, 1/5, 1/6, 1/8, 1/10, 1/12, 1/14, 2, 3, 4, 5, 6, 8, 10, 12 and 14. There is also one graph that contains all the normalized equivalent resistivity curves for ρ_1/ρ_2 ratios of 1/2, 1/3, 1/4, 1/5, 1/6, 1/8, 1/10, 1/12 and 1/14. Similarly, there is one graph that contains all the normalized equivalent resistivity curves for ρ_1/ρ_2 ratios of 2, 3, 4, 5, 6, 8, 10, 12 and 14.

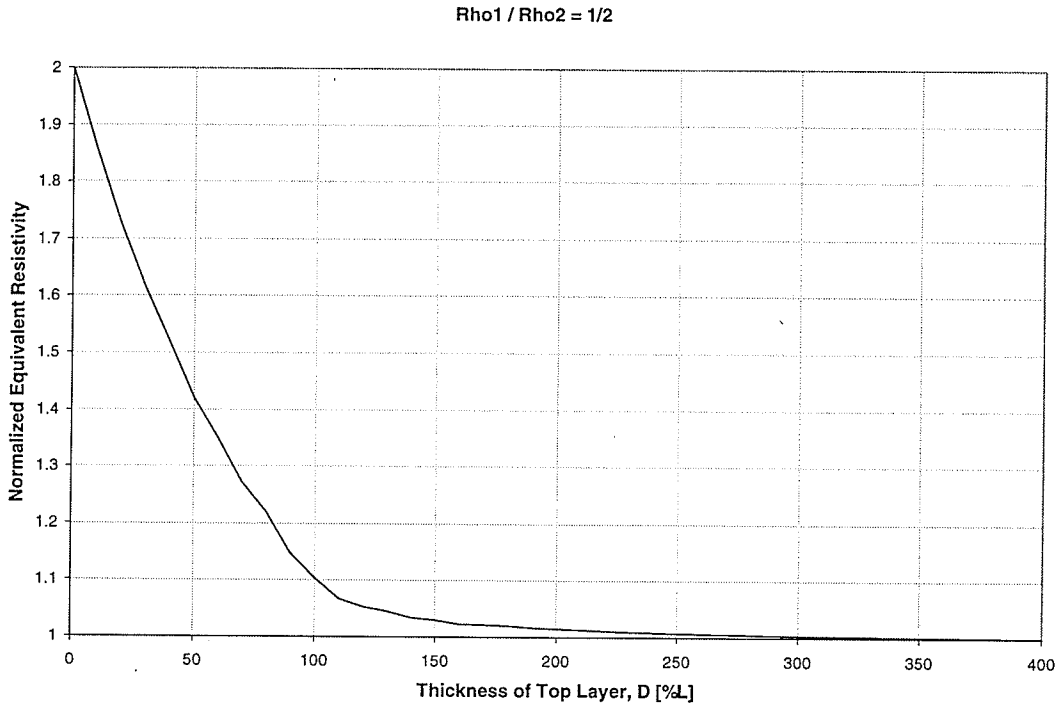

Figure 4.6 Normalized equivalent resistivity curve with $\rho_1/\rho_2 = 1/2$

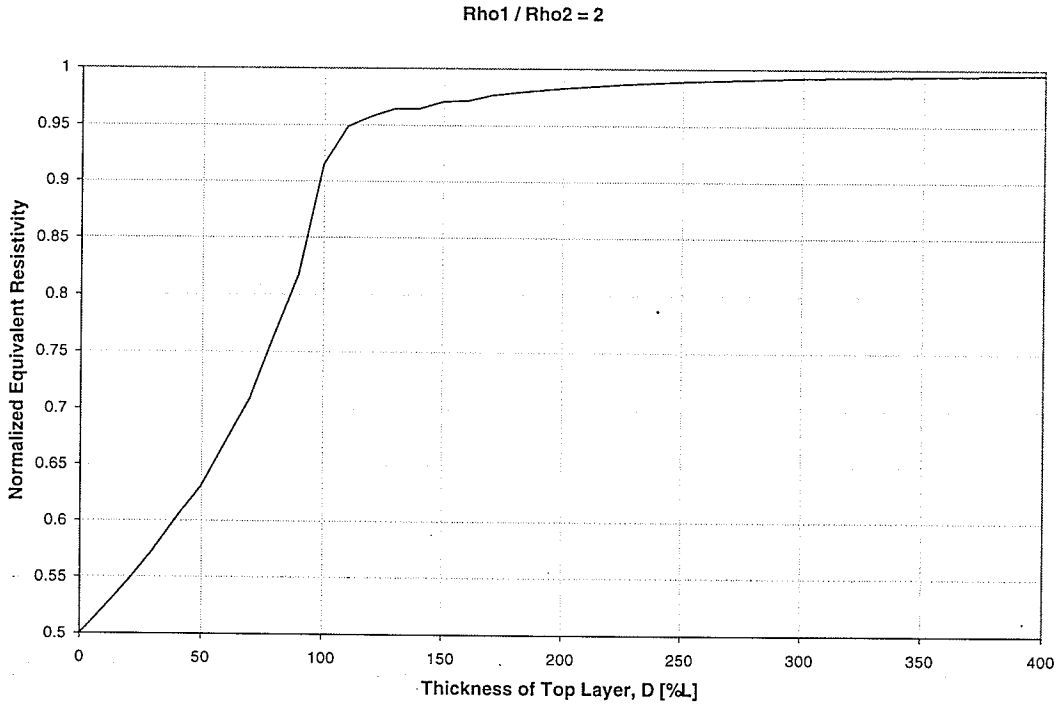

Figure 4.7 Normalized equivalent resistivity curve with $\rho_1/\rho_2 = 2$

Although, these normalized equivalent resistivity curves are generated by using a ground rod with L of 20m and r of 0.1778m, they can be used to deal with problems involving a two-layered earth, regardless of the actual ground rod length and radius, provided that $L >> r$. The influence of r over ρ_{eqv} is insignificant provided that the condition of $L >> r$ is fulfilled, which is essentially true for all practical vertical type ground rods. In order to use these curves to obtain a ρ_{eqv}, one needs to know the values of L/D, ρ_1 and ρ_2. Once, ρ_{eqv} is obtained, one can then use the analytical solutions derived for ground resistance problems involving a homogeneous earth to come up with a ground resistance estimation for the electrode in two-layered earth.

The normalization factor, R_N is worth a closer look. This factor is evaluated by using FEM, not by using Eq. (2-1). This has been done to maintain consistency in the process of deriving the normalized equivalent resistivity curves. Recall that all the values for R_{est} contain error no worse than 10%. That is, Fig. 4.2-4.5 all contain errors no worse than 10%. If one uses Eq. (2-1) to obtain R_N, the normalized resistivity curves will not reach a maximum or minimum value of 1.

Therefore, to maintain consistency, R_N should be obtained by using FEM and must be checked by using Eq. (2-1) to ensure an error of no worse than 10%. Furthermore, when simulating the ground rod in a two-layered earth system to cover the entire range of D from 0% to 400% of L, one must always check the adequacy of the model and mesh. This is done by setting ρ_1 and ρ_2 both equal to an arbitrary ρ, producing a homogeneous earth. The evaluated R_{est} is then compared with R_{exact} by Eq. (2-1). The error should be no worse than 10% throughout the entire range of D. These errors should be very close to the error of R_N. This simple procedure ensures an adequate model and mesh hence a reliable R_{est} and promotes consistency.

4.5 Applications of Normalized Equivalent Resistivity Curves

This section focuses primarily on the application of the normalized equivalent resistivity curves provided in Appendix C through consideration of 3 examples. The first two examples illustrate application of the proposed technique to a single ground rod in two-layered earth. This is followed by consideration of ring type multiple-rod electrode scheme in a two-layered earth. Before proceeding to the examples, the general steps involved in the suggested technique are listed below.

(I) For a single vertical rod grounding in a two-layered earth:

Step 1 : Find *D/L* as a percentage.

Step 2 : Find ρ_1/ρ_2 and from the appropriate normalized equivalent resistivity curve, obtain the normalized equivalent resistivity.

Step 3 : Multiply the normalized equivalent resistivity by the resistivity of the top layer, ρ_1 to obtain the equivalent resistivity.

Step 4 : Either use the equivalent resistivity to solve the problem by using FEM or Eq. (2-1).

(II) For multiple-rod grounding in a two-layered earth:

Step 1 : Assume that there is only one vertical rod installed in the selected site.

Step 2 : Find *D/L* as a percentage.

Step 3 : Find ρ_1/ρ_2 and from the appropriate normalized equivalent resistivity curve, obtain the normalized equivalent resistivity.

Step 4 : Multiply the normalized equivalent resistivity by the resistivity of the top layer, ρ_1 to obtain the equivalent resistivity.

Step 5 : Either use the equivalent resistivity to solve the problem by using FEM or Eqs. (2-4) or (2-5).

4.5.1 Applications of Normalized Equivalent Resistivity Curves for The Case of Single Rod Grounding in Two-Layered Earth

Fig. 4.8 shows the electrode-ground system with L and r equal to 100 and 0.1270m respectively. As discussed, the FEM model is axisymmetric. The first step is to check the adequacy of the FEM model and mesh. Assuming both ρ_1 and ρ_2 both to be 300 Ω-m, by Eq. (2-1), R_{exact} is 3.37 Ω. From FEM simulation, R_{est} is 3.10 Ω. The error between R_{exact} and R_{est} is about 8%, hence the FEM model is considered to be adequate.

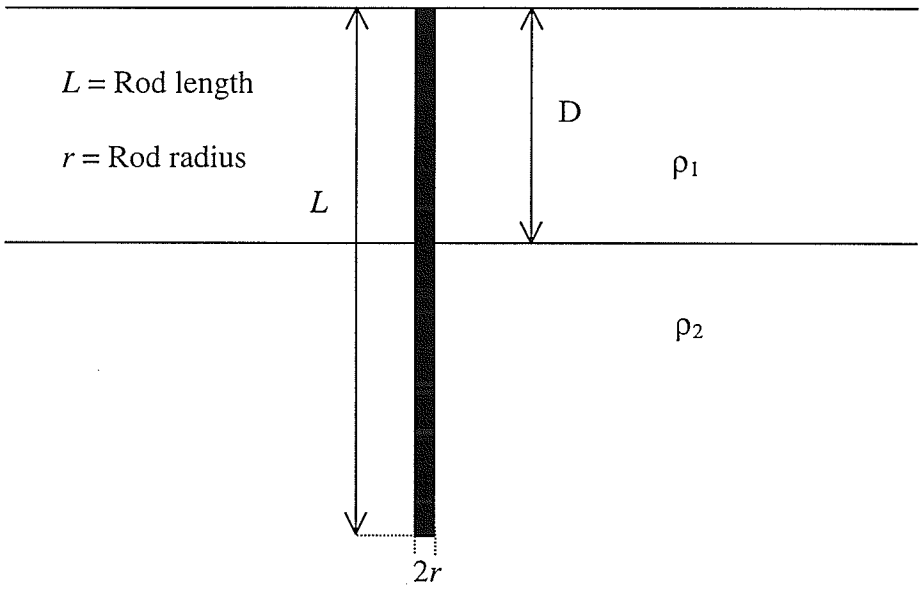

Figure 4.8 Single rod in a two-layered earth

Example 1

Suppose, L = 100m; r = 0.1270m; D = 50% of L; ρ_1 = 300 Ω-m; ρ_2 = 600 Ω-m. By FEM, R'_{exact} is 4.46 Ω. Since the FEM simulation provides solution with an average error of 8%, a projection of the true earth resistance, R_{exact_p} is 4.46/0.92, which is 4.85 Ω.

Step 1:

The thickness of the top layer, $D = 0.5L$

Step 2:

The ρ_1/ρ_2 ratio is 1/2, from Fig. 4.6, the normalized equivalent resistivity curve for ρ_1/ρ_2 = 1/2, when $D = 0.5L$, the corresponding normalized equivalent resistivity, ρ_{eqv_n} = 1.42.

Step 3:

Since, ρ_1 = 300 Ω-m

$$\rho_{eqv} = \rho_{eqv\_n} \times \rho_1$$
$$= 1.42 \times 300$$
$$= 426\ \Omega\text{-m}$$

Step 4: Here we choose to use Eq. (2-1)

From Eq. (2-1),

$$R_{est} = \frac{426}{2\pi(100)}\left(\ln\frac{4(100)}{0.127} - 1\right)$$
$$= 4.7833\ \Omega$$
$$\approx 4.7800\ \Omega$$

This value is close to the projected exact ground resistance R_{exact_p} value of 4.85 Ω.

Example 2

Suppose, L = 10m; r = 0.1270m; D = 50% of L; ρ_1 = 600 Ω-m; ρ_2 = 300 Ω-m. R'_{exact} is 26.85 Ω and with an average error of 8%. Then, the projected R_{exact_p} = 29.19 Ω .

Step 1:

The thickness of the top layer, $D = 0.5L$

Step 2:

The ρ_1/ρ_2 ratio is 2, from Fig. 4.7, ρ_{eqv_n} = 1.42.

Step 3:

$$\begin{aligned}\rho_{eqv} &= \rho_{eqv\_n} \times \rho_1 \\ &= 0.635 \times 600 \\ &= 381\ \Omega\text{-m}\end{aligned}$$

Step 4: Here we choose to use Eq. (2-1)

From Eq. (2-1),

$$\begin{aligned}R_{est} &= \frac{381}{2\pi(10)}\left(\ln\frac{4(10)}{0.127} - 1\right) \\ &= 28.8179\ \Omega \\ &\approx 28.82\ \Omega\end{aligned}$$

Comparing R_{exact_p} to R_{est} in examples 1 and 2, it can be seen that this method of arriving at a value for ρ_{eqv} is indeed a good approximation. The L and r values in examples 1 and 2 are not the same as the L and r used to generate the normalized equivalent resistivity curves, which use L=20 and r=0.1778m. This shows that the normalized equivalent resistivity curves can be used for any L and r as long as $L >> r$.

Table 4.3 and 4.4 illustrate various results showing the applicability of the proposed method. In Tables 4.3 and 4.4 R_{est} is obtained by using the equivalent resistivity in Eq. (2-1). R_{est} should be compared with R_{exact_p}.

Case	ρ_1/ρ_2	D [%L]	ρ_{eqv} (Ω-m)	R'_{exact} (Ω)	R_{exact_p} (Ω)	R_{est} (Ω)
1	1/2	20	172	1.77	1.92	1.93
2	1/3	30	205	2.05	2.23	2.30
3	1/4	40	205	2.05	2.23	2.30
4	1/5	50	190	2.08	2.23	2.13
5	1/6	60	175	1.76	1.92	1.97

Table 4.3 Comparison of R_{est}, R'_{exact} and R_{exact_p} for the case of two-layered earth using the approach of section 4.4 with $\rho_1 = 100$ Ω-m $< \rho_2$, L=100m and r=0.127m.

Case	ρ_1/ρ_2	D [%L]	ρ_{eqv} (Ω-m)	R'_{exact} (Ω)	R_{exact_p} (Ω)	R_{est} (Ω)
1	2	20	109	7.77	8.44	8.24
2	3	30	123	8.54	9.28	9.30
3	4	40	136	9.49	10.31	10.29
4	5	50	150	10.71	11.64	11.35
5	6	60	180	12.33	13.41	13.61

Table 4.4 Comparison of R_{est}, R'_{exact} and R_{exact_p} for the case of two-layered earth using the approach of section 4.4 with $\rho_1 = 100$ Ω-m $> \rho_2$, L=10m and r=0.127m.

4.5.2 Applications of Normalized Equivalent Resistivity Curves on a Ring Type Multiple-Rod Electrode in Two-Layered Earth

This section analyses a ring type multiple-rod electrode, as discussed in section 3.5. Due to the prevailing symmetry, the electrode ground resistance can be estimated by simulating only half the physical size of the actual electrode. The FEM solution will be compared to result obtained by ρ_{eqv} and Eq. (2-4).

Example 3

Assume that there are 10 rods connected in a ring formation with radius of ring, R=60m. Each rod has length, L = 45m and radius, r = 0.1778m. Thickness of top layer, D=36m. The top layer resistivity, ρ_1=125 Ω-m and bottom layer resistivity, ρ_2=250 Ω-m. The simplified plan view of the FEM model is shown in Fig. 4.9.

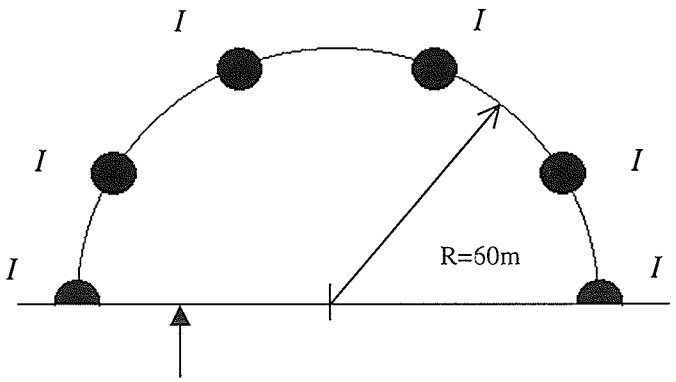

Figure 4.9 Simplified plan view of the FEM model for simulation of the ring type electrode

A known current, I is injected into each rod. Assuming that R_n is the resistance of the individual rod , the estimated electrode ground resistance, R_{est} is:

$$R_{est} = \frac{1}{2} \cdot \left[\sum_{n=1}^{m} \frac{1}{R_n} \right]^{-1} \qquad (4-5)$$

where m is the total number of rods modeled including the half-rods, which lie on the plane of symmetry, in this example m is 6.

Two different FEM simulations produced the following results:

Simulation I : Model the two-layered earth with ρ_1= 125 Ω-m and ρ_2= 250 Ω-m.

$$R'_{exact} = \frac{1}{2} \cdot \left[\frac{1}{11.65} + \frac{1}{11.65} + \frac{1}{5.80} + \frac{1}{5.80} + \frac{1}{5.80} + \frac{1}{5.80} \right]^{-1}$$

$$R'_{exact} \approx \frac{1.16}{2} = 0.58\Omega$$

Simulation II : Model the two-layered earth using ρ_{eqv}.

Step 1:

Assume that there is only a single rod with L=45m and r=0.1778m installed in the same site.

Step 2:

The thickness of the top layer, D=[36/45]L = 0.8 L

Step 3:

The ρ_1/ρ_2 ratio is 1/2, from Appendix C, $\rho_{eqv\_n} = 1.24$.

Step 4:

$$\rho_{eqv} = \rho_{eqv\_n} \times \rho_1$$
$$= 1.24 \times 125$$
$$= 155\ \Omega\text{-m}$$

Step 5:

Using ρ_{eqv}=155 Ω-m to reduce the two-layered earth to a homogeneous earth, the FEM simulation yields,

$$R_{est} \approx \frac{1.1105}{2} \approx 0.56\,\Omega$$

It is evident that Simulations I and II both produce estimations that are close to each other. This shows that the ρ_{eqv} approximation method can be used to deal with multiple-rod grounding problems, provided that the rods are installed vertically and $L >> r$.

Using the value of ρ_{eqv} in Eq. (2-4), one obtains R_{exact} = 0.64 Ω. Comparing this with R_{est}, the error is about 13%. This error falls within the acceptable range since Eq. (2-4) tends to overestimate the resistance anywhere between 5~25%.

4.6 Multi-Layered Earth with Arbitrary ρ_1/ρ_2 Ratio

Thus far, the technique of arriving at an equivalent resistivity, ρ_{eqv} has been confined to the cases of two-layered earth. If the number of layers involved is greater than 2, solving the problem by using FEM can become tedious and sometimes not manageable.

4.6.1 Tackling Multi-Layered Earth Configurations by The Method of Successive Approximations

Fig. 4.10 shows a four-layered earth structure, with layer thicknesses of D_1, D_2 and D_3. The 4th layer extends to infinity and hence D_4 is not shown.

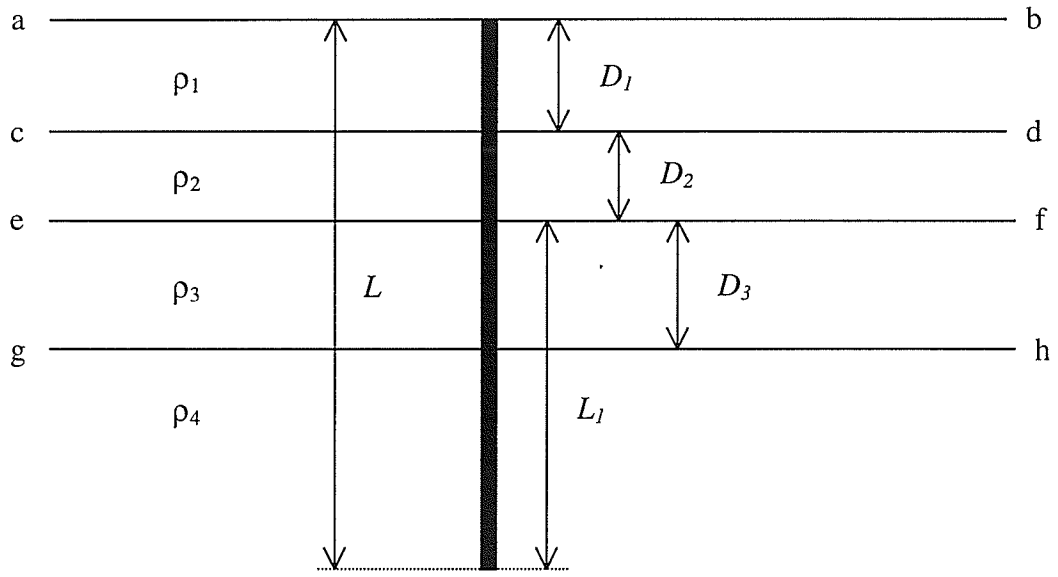

Figure 4.10 A ground rod in four-layered earth

Application of the normalized equivalent resistivity curves in two-layered earth has been discussed in section 4.5. If there are more than 2 layers of soil with different resistivities the following course of action is recommended.

One may start from the bottom-most 2 layers of soil, successively approximate the four-layered earth into a homogeneous earth by using the normalized equivalent resistivity curves. As discussed in section 4.2, if the layer is located at a distance more than $2L$ from the earth surface, its existence can be disregarded i.e., simply extend downward infinitely the layer right on top of it to replace it.

It is extremely important to realize that the notations ρ_1 and ρ_2 used in the discussions involving two-layered earth mean the resistivities of the top and bottom layers. When dealing with multi-layered earth, ρ_1 and ρ_2 denote the resistivities of the 1st and 2nd layers as depicted in Fig. 4.10. In the process of reducing the multi-layered earth to a homogeneous earth, ρ_1 and ρ_2 refer to the resistivities of the top and bottom layers in a relative sense. For instance, if a four-layered earth is to be approximated to a homogeneous earth, the 1st approximation will involve only the 3rd and 4th layers, i.e., ρ_3 and ρ_4. In this case, ρ_3 corresponds to ρ_1 ; ρ_4 corresponds to ρ_2. Although it may sound confusing, the context will make this notion clear.

For the configuration as depicted in Fig. 4.10, the 1st approximation will be to replace the 3rd and 4th layer with an equivalent resistivity, ρ_{eqv_1} . Define the rod length as starting from e-f in Fig. 4.10. The interface between the top and bottom layer is g-h. Hence the thickness of the top layer is D_3, which corresponds to D in the case of a two-layered earth. The effective rod length is not L but $[L-(D_1+D_2)]$, which is denoted as L_1 and shown in Fig. 4.10. The values of L_1, D_3, ρ_3 and ρ_4 completely define a two-layered earth problem and therefore arriving at an equivalent resistivity, ρ_{eqv_1} is possible. Using previously described techniques, after the first approximation, the four-layered earth in Fig. 4.10 is reduced to a three-layered earth as depicted in Fig. 4.11.

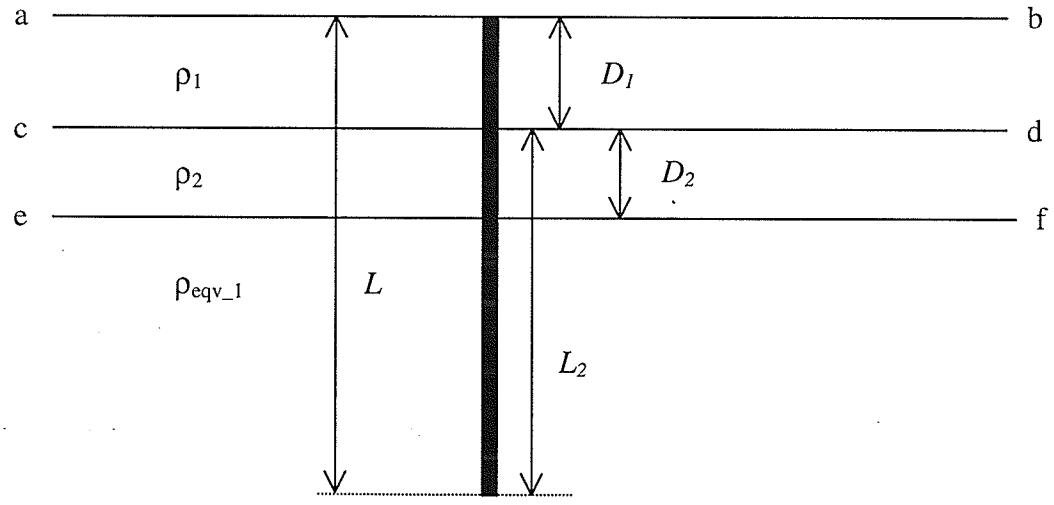

Figure 4.11 Four-layered earth reduced to three-layered earth

The 2nd approximation will involve ρ_2 and ρ_{eqv_1}. Assume that the ground rod starts from c-d in Fig. 4.11. The interface between the top and bottom layer is e-f. Hence the thickness of the top layer is D_2. The effective rod length, L_2 as shown in Fig. 4.11 is $[L\text{-}D_1]$. The values of L_2, D_2, ρ_2 and ρ_{eqv_1} define a two-layered earth problem and an equivalent resistivity, ρ_{eqv_2} is obtainable.

After the 2nd approximation, the three-layered earth in Fig. 4.11 has been reduced to a two-layers earth as depicted in Fig. 4.12. This two-layers earth can be easily reduced to a homogeneous earth with an equivalent resistivity, ρ_{eqv_3} by a 3rd approximation.

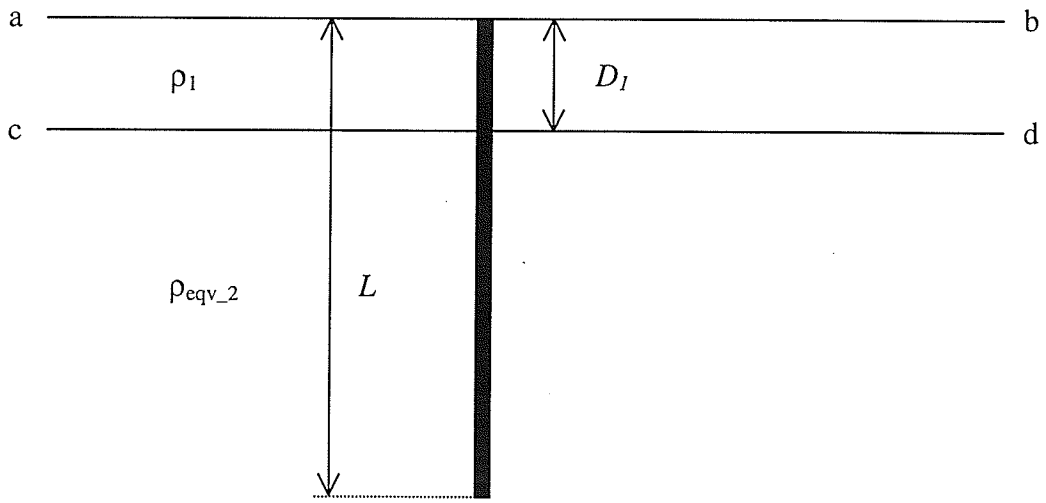

Figure 4.12 Three-layered earth reduced to two-layered earth

In general, a *k*-layer earth requires *(k-1)* approximations to reduced it to a homogeneous earth. The effective length of the rod, L_x is the portion of the rod which is embedded in the earth layer under approximation. Eventually, the effective length of the rod will become the physical length of the rod, L in the $(k\text{-}1)^{th}$ approximation. Once again, it should be clear that the notations ρ_1 and ρ_2 in the normalized equivalent resistivity curves refer to the resistivities of the top and bottom layers soil in a relative sense not the resistivity of the 1st and 2nd layer as depicted in Fig 4.10.

4.6.2 Dealing with Arbitrary ρ_1/ρ_2 Ratio

In a practical case, the ρ_1/ρ_2 ratio may differ from the values used to arrive at the normalized equivalent resistivity curves in Appendix C. One method of dealing with this situation is to round off the ratio to the nearest available ρ_1/ρ_2 ratio for which a normalized equivalent resistivity curve is available. The process of rounding up or rounding down the ρ_1/ρ_2 ratio either adds or diminishes the safety factor in the design. Rounding up will increase the safety factor, which may not be a bad idea. However, rounding down the ratio causes the safety factor to diminish. This is not a very severe problem since it can always be overcome by careful and proper designs.

Another method is to interpolate between two normalized equivalent resistivity curves. For instance, if the required ρ_1/ρ_2 ratio is 11, this normalized equivalent resistivity curve can be obtained by interpolating the normalized equivalent resistivity curves corresponding to ρ_1/ρ_2 ratios of 10 and 12.

Since the trend of variations does not show a linear dependence on the ρ_1/ρ_2 ratios, interpolation does introduce error but this error is insignificant. However, extrapolating should never be considered. If a normalized equivalent resistivity curve corresponding to a ρ_1/ρ_2 ratio that is beyond the range of the curves in Appendix C is required, this curve will have to be generated as outlined in section 4.3.

Consider the case when $\rho_1>\rho_2$. In this case the normalized equivalent resistivity curve shows an increasing trend as shown in Fig. 4.13, reproduced from Appendix C. Consider any arbitrary values for D, ρ_1 and ρ_2 say, $D = 0.5L$; $\rho_1 = 140\ \Omega$-m; $\rho_2 = 20\ \Omega$-m. In this case the ρ_1/ρ_2 ratio is 7, corresponding to which a normalized equivalent resistivity curve is not readily available from Appendix C. This situation can be overcome by performing interpolation between the normalized equivalent resistivity curves corresponding to ρ_1/ρ_2 ratios of 6 and 8.

From the normalized equivalent resistivity curve of $\rho_1/\rho_2 = 6$ and D=0.5L,

The corresponding normalized equivalent resistivity, $\rho_{eqv\_n} = 0.26$

From the normalized equivalent resistivity curve of $\rho_1/\rho_2 = 8$ and D=0.5L,

The corresponding normalized equivalent resistivity, $\rho_{eqv\_n} = 0.20$

To obtain the normalized equivalent resistivity for $\rho_1/\rho_2 = 7$ and D=0.5L,

Performing interpolation, the required ρ_{eqv_n} is:

$$\rho_{eqv\_n} = \frac{(0.20-0.26)}{(8-6)} \cdot (7-6) + 0.26 = 0.23$$

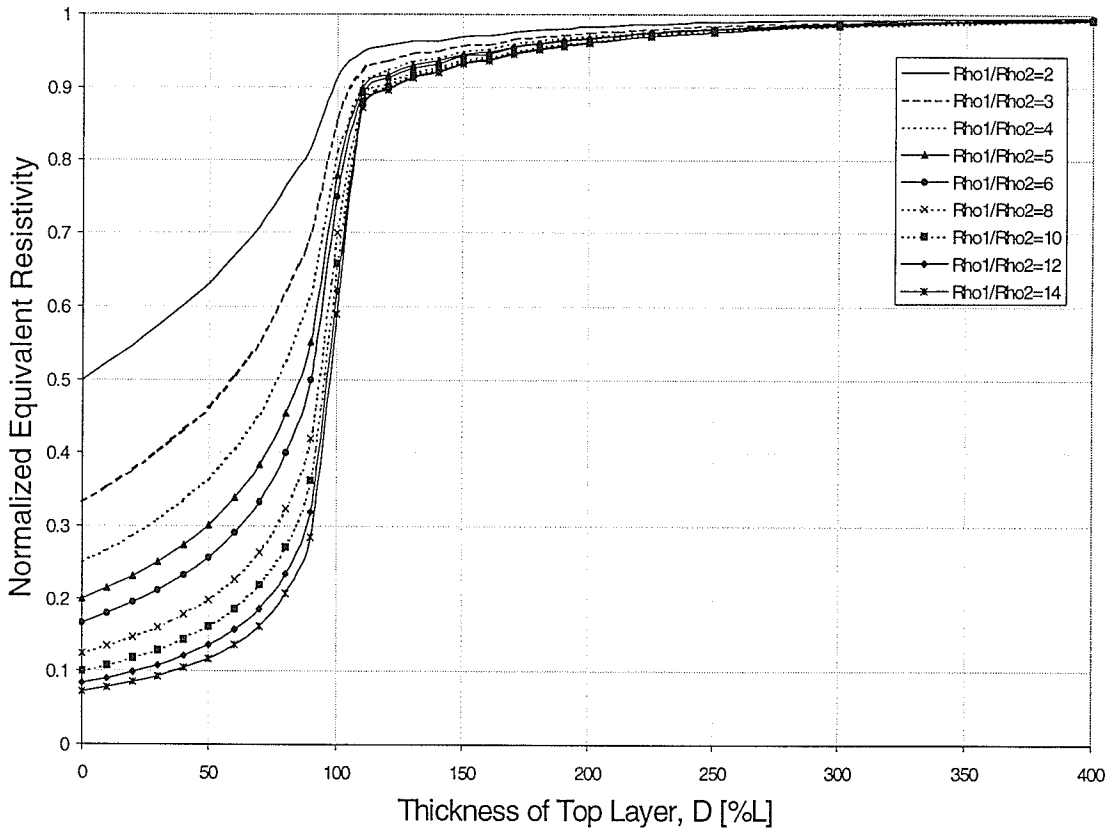

Figure 4.13 Normalized equivalent resistivity curves for $\rho_1 > \rho_2$

Examples of cases involving multi-layered earth grounding i.e., more than two layers, will now be discussed. Example 4 involves a single rod grounding whereas example 5 deals with a ring type multiple-rod grounding.

Example 4

A vertical ground rod with L =100m and r =0.127m is embedded in a four-layered earth as depicted in Fig. 4.10. D_1=D_2=D_3=20m, ρ_1=70 Ω-m, ρ_2=100 Ω-m, ρ_3=30 Ω-m and ρ_4=20 Ω-m .

1st Approximation:

Starting from the two bottom-most layers, the effective rod length, L_1=60m, which is the sum of the lengths of the portion of the rod in these 2 layers. The thickness of the top layer, D =20m, therefore is 33% of L_1. Keep in mind that the notations ρ_1 and ρ_2 mean the top layer resistivity and bottom layer resistivity, not the resistivity of the top most and second layers. Hence, ρ_1/ρ_2 =1.5.

From Appendix C,

If ρ_1/ρ_2 =1; D=33%; ρ_{eqv_n} = 1.00

If ρ_1/ρ_2 =2; D=33%; ρ_{eqv_n} = 0.58

Perform interpolation for ρ_1/ρ_2 =1.5; D=33%

$$\rho_{eqv\_n1} = 0.79$$

$$\therefore \rho_{eqv\_1} = 0.79 \times 30$$

$$\approx 24.0\ \Omega\text{-m}$$

2nd Approximation:

With the lowest 2 layers replaced by a single layer with ρ_{eqv_1} of 24Ω-m, the four-layered earth is reduced to a three-layered earth. Proceed with the 2nd approximation to reduce this three-layered earth to a two-layered one.

The effective rod length, L_2=80m, D=2/8=25%, the ρ_1/ρ_2=100/24 ≈ 4.00

From Appendix C, $\rho_{eqv\_n2} = 0.30$

$$\therefore \rho_{eqv\_2} = 0.30 \times 100$$
$$= 30\ \Omega\text{-m}$$

3rd Approximation:

After the 2nd approximation, the four-layered earth has been reduced to two-layered earth with resistivity ρ_1=70 Ω-m and ρ_2=30 Ω-m. The effective rod length, L_3 = 100m, D=20%, $\rho_1/\rho_2 = 70/30 \approx 2.33$.

From Appendix C,

If ρ_1/ρ_2=2; D=20%; $\rho_{eqv\_n} = 0.545$

If ρ_1/ρ_2=3; D=20%; $\rho_{eqv\_n} = 0.375$

Perform interpolation for ρ_1/ρ_2=2.33; D=20%

$$\rho_{eqv\_n3} \approx 0.48$$
$$\therefore \rho_{eqv\_3} = 0.48 \times 70$$
$$\approx 34.6\ \Omega\text{-m}$$

After 3 approximations, the four-layered earth is reduced to a homogeneous earth with an equivalent resistivity, ρ_{eqv_3} of 34.6 Ω-m. Using ρ_{eqv_3} in Eq. (2-1) yields a R_{est} of 0.3773 Ω. From FEM, R'_{exact} is 0.3181 Ω with about 8% of error, therefore, the projected exact ground resistance, R_{exact_p} is around 0.3458 Ω . The error between R_{est} and R_{exact_p} is about 9%.

Example 5

This example involves a HVDC ground electrode installed at Coyote, California, USA [88 Prabhakara]. The bipolar HVDC scheme is rated at ± 500kV and 1600MW with 2.6kA of continuous current in monopolar ground return operation, and 16A of continuous unbalance current in bipolar operation. This is a large electrode with 60 wells arranged in a circle of radius equal to 457m and the individual wells are 53m in length and 0.175m in radius, see Appendix D. The authors [88 Prabhakara] used Eq. (2-5) and numerical methods to predict the electrode ground resistance. A very conservative value of 20 Ω-m was used for the electrode design. It turns out that with this value, the electrode has been over designed because the measured resistance is less than 10% of the predicted value.

From Eq. (2-6), it is obvious that the ground resistance depends directly on the resistivity. If predicting a less conservative resistivity with reasonable reliability is possible, a more optimum design would have been achieved.

Geophysical surveys at the electrode site have produced a wide range of information, including the readings and predictions of the resistivities and earth layers. These predictions vary quite significantly depending on the method used and the prevailing conditions at the moment of conducting the survey.

Table 4.5 shows a set of selected geophysical test result at Coyote electrode site [88 Prabhakara], which will be used later together with the method of successive approximation in section 4.6.1 to produce a prediction for the equivalent resistivity.

Earth Layer [m]	Resistivity [Ω-m]
0 ~ 3.05	35
3.05 ~ 8.23	140
8.23 ~ 41.15	45
> 41.15	4

Table 4.5 Selected geophysical test result at Coyote, California, USA [88 Prabhakara]

Fig. 4.14 shows the model of four-layered earth at the Coyote site under the assumption that only 1 well is installed. The four-layered earth will now be successively approximated to a homogeneous earth using the technique suggested in this thesis.

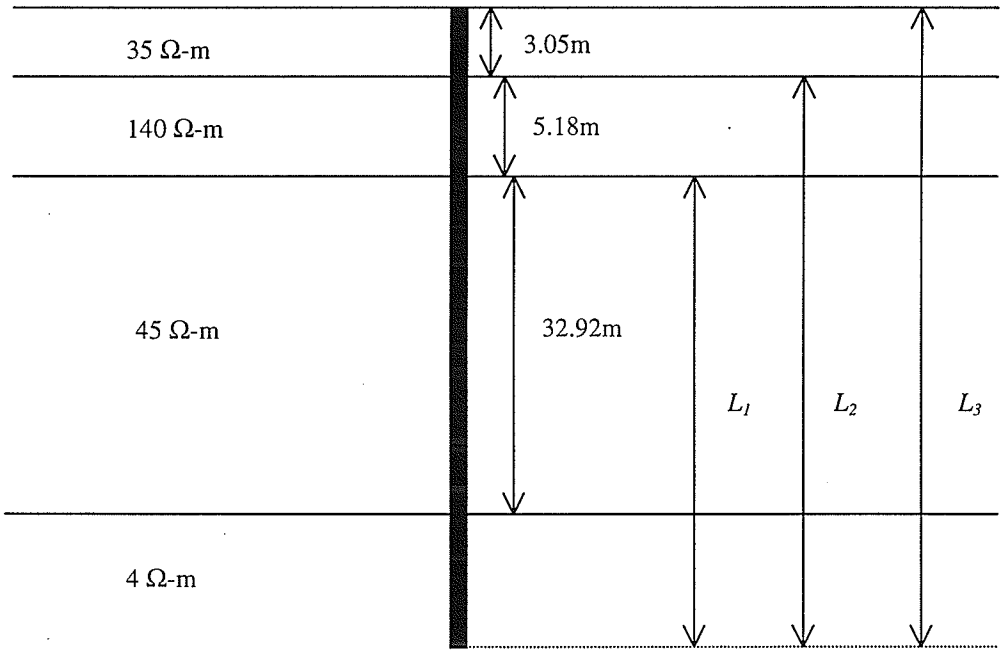

Figure 4.14 Coyote electrode site, four-layered earth model based on Table 4.5

1st Approximation:

The effective rod length embedded in the bottom-most two layers, L_1 = 44.77m. The top layer resistivities, ρ_1 = 45 Ω-m and bottom layer resistivity, ρ_2 = 4 Ω-m. The thickness of the top layer is 32.92m and therefore D=32.92/44.77, which yields 73.53%. The ρ_1/ρ_2 ratio ≈11.25.

From Appendix C,

If ρ_1/ρ_2=10; D=73.5%; ρ_{eqv_n} = 0.24

If ρ_1/ρ_2=12; D=73.5%; ρ_{eqv_n} = 0.20

Perform interpolation for ρ_1/ρ_2=11.25; D=73.5%

$$\rho_{eqv\_n1} \approx 0.22$$

$$\therefore \rho_{eqv\_1} = 0.22 \times 45$$

$$\approx 10.0\ \Omega\text{-m}$$

2nd Approximation:

L_2 =49.95m and ρ_1 = 140 Ω-m and ρ_2 = 10.0 Ω-m, $D \approx 10\%$, ρ_1/ρ_2 = 14. From Appendix C, the normalized equivalent resistivity curve corresponding to ρ_1/ρ_2 ratio of 14,

$$\rho_{eqv\_n2} = 0.08$$

$$\therefore \rho_{eqv\_2} = 0.08 \times 140$$

$$\approx 11.0\ \Omega\text{-m}$$

3rd Approximation:

L_3=53m and ρ_1 = 35 Ω-m and ρ_2 = 11.0 Ω-m, $D \approx 6\%$, $\rho_1/\rho_2 \approx 3.18 \approx 3.00$. From Appendix C, the normalized equivalent resistivity curve corresponding to ρ_1/ρ_2 ratio of 3,

$$\rho_{eqv\_n3} = 0.34$$

$$\therefore \quad \rho_{eqv\_3} = 0.34 \times 35$$

$$\approx 12.0\ \Omega\text{-m}$$

Notice that the prediction of the equivalent resistivity is 40% smaller than the conservative value of 20 Ω-m used throughout the design. This shows that given the geophysical information, the methodology of predicting an equivalent resistivity, presented in this chapter is applicable and reliable in practical engineering designs.

4.7 Chapter Summary

This chapter suggests techniques for efficient handling of multi-layered earth grounding problems, which involve single rod or multiple rods arranged in a ring configuration. Key aspects of the suggested techniques are outlined below:

(1). Locations of earth layers:

It has been shown that if the layers are located at a distance of more than 2L from the earth's surface, their influence is insignificant and can be replaced by using the technique discussed in section 4.2.

(2). Normalized equivalent resistivity curve:

These are general curves that can be used to reduce a two-layered earth to a homogeneous earth, regardless of the rod length, L and radius r provided $L >> r$. The trend of variation is governed by two ratios i.e, the D/L ratio and the ratio of the top layer resistivity, ρ_1 to the bottom layer resistivity, ρ_2, that is the ρ_1/ρ_2 ratio. The ratio ρ_1/ρ_2 is important rather than the absolute values of ρ_1 and ρ_2 .

(3). Successive approximations:

If there exist more than 2 layers of earth, starting from the bottom-most two influential layers, one can employ the method of successive approximations to reduce the multi-layered earth to a homogeneous earth as discussed in section 4.6.1. For *k*-layer earth, *(k-1)* approximations are necessary to reduce it to a homogeneous earth.

(4). Arbitrary ρ_1/ρ_2 ratio:

If a normalized equivalent resistivity curve (Appendix C) is not available for a particular value of ρ_1/ρ_2 ratio, one can either choose to round it up or down, so that the existing curves in Appendix C can be used. Alternatively, if the ρ_1/ρ_2 ratio of interest lies within the range of the existing curves in Appendix C, interpolation can be performed to arrive at an equivalent resistivity, which corresponds to the D and the ρ_1/ρ_2 ratio of interest.

However, extrapolation should never be performed! If the ρ_1/ρ_2 ratio of interest is beyond the range of the existing curves in Appendix C, the required normalized resistivity curve will have to be derived as outlined in section 4.3.

(5). Multiple-rod electrode:

Although the normalized equivalent resistivity curves were generated by using a single vertical ground rod arrangement, they can be employed to tackle grounding scheme involving multiple rods, provided that the rods are installed vertically into the ground and their length, L is much greater than the radius, r.

Assume that only one rod is installed in the selected site. Then, apply the appropriate techniques discussed in this chapter to arrive at an equivalent resistivity, ρ_{eqv}. This ρ_{eqv} is a reliable parameter that can be used for the design of the multiple-rod electrode.

Chapter 5

Non Horizontal Two-Layered Earth

Thus far, all the discussions have been focussed on homogeneous and multi-layered earth composed of parallel layers. In practice, the earth layers may not be parallel to each other.

This type of non-homogeneity presents a new set of challenges, not only from an engineering design perspective but also from the point of view of the geophysical information collection process. Tremendous efforts and exhausting surveying are required in order to obtain detailed information on the nature of the layers. This is both a time consuming and financially burdening process.

In this chapter, an investigation into the influence of inclined-earth layers is carried out; only two layers are considered. The effects on the overall ground resistance due to inclined layers are studied and suggestions are made for handling this type of non-homogeneity. It is necessary to point out that the interfaces between the layers are modeled as flat planes, which is undoubtedly an approximation.

5.1 General Types of Inclinations

There are actually numerous possible cases of inclined layers. For simplicity, a vertical ground rod embedded in a two-layered earth model will be used throughout the discussion. The are in general two types of inclinations, which are labelled Type-I and Type-II in this thesis and are shown in Figs. 5.1 and 5.2.

5.2 Type-I Inclined Earth Layer

The layer is inclined at a particular angle, θ. It is obvious that the increase in the volume of soil with resistivity ρ_1, to the left of the ground rod is compensated by the decrease in the volume of the same soil to the right of the rod. The same applies to the lower layer of soil with resistivity ρ_2. The decrease in volume of the lower layer soil to the left of the rod is compensated by the increase of volume to the right of the rod.

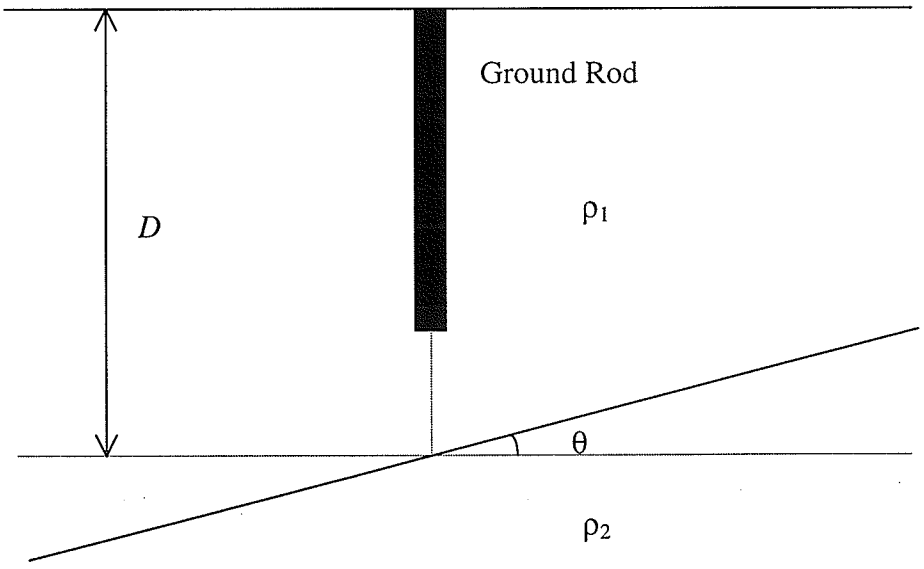

Figure 5.1 Type-I inclined earth layer

Suppose there exists such a location with the geophysical structure as shown as Fig. 5.1. The best way to obtain an optimum design will be to move the entire ground rod to the area, which contains soil with lower resistivity. There is no doubt that the lower the soil resistivity, the smaller the ground resistance. If ρ_1 is smaller than ρ_2, the ground rod should then be moved to the left. On the other hand, if ρ_1 is larger than ρ_2, the ground rod should then be moved to the right.

If θ is large, moving the location of the electrode laterally towards the soil with lower resistivity will be a good way to obtain the optimum design. However, if θ is small, moving the location of the electrode may not be practical. The situation will have to be dealt with as it is.

Suppose that the inclination is small, one can approximate the interface of the inclined layers by a flat plan, running parallel to the earth surface, i.e., the dotted line in Fig. 5.1 with ρ_1 on top and ρ_2 on bottom. This reduces the problem to a two-layered earth problem which can be handled as discussed in previous chapters. The effect of the magnitude of the angle θ on this approximation is discussed in section 5.4.

5.3 Type-II Inclined Earth Layer

This situation is depicted in Figure 5.2. For simplicity, the geometry is assumed to be symmetrical. This is actually the worst case scenario. An increase in θ means a decrease in the volume of the upper layer soil and vice versa. This nonetheless directly affects the ground resistance of the electrode.

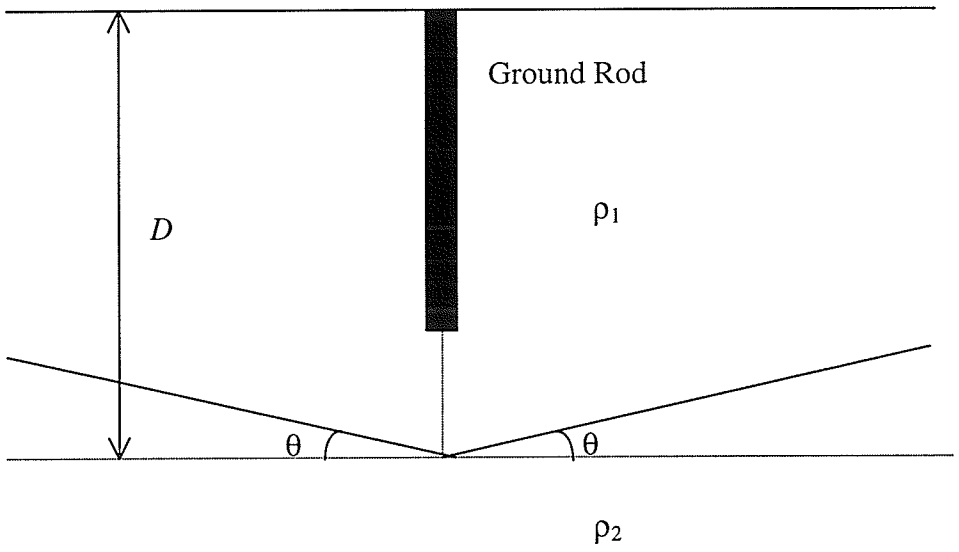

Figure 5.2 Type-II inclined earth layer, V-shaped

The angle θ measures the inclination of the layer interface. In Fig. 5.2, this angle is considered to be positive and the layer's interface is V-shaped. Clearly the other equivalent worst case scenario occurs when the layers are inclined as shown in Fig 5.3.

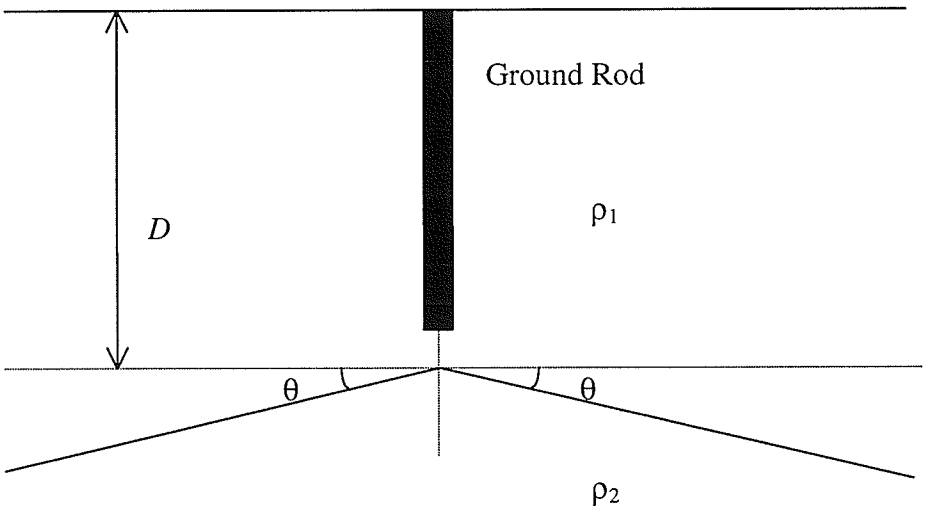

Figure 5.3 Type-II inclined earth layer, inverted V-shaped

In Fig. 5.2, the angle, θ is considered to be negative and the layer interface is in the form of an inverted V-shape.

5.4 FEM Model and Simulation Results

Suppose there is a single vertical ground rod with length, L and radius, r of 20 and 0.127m embedded in an inclined two-layered earth as described in section 5.3, with the top and bottom layers resistivities, ρ_1 and ρ_2 of 100 and 200 Ω-m. The model used for performing the FEM simulation is depicted as Fig. 5.4. The angle of inclination, θ in Fig. 5.4 can have either positive or negative value. If θ is positive, Fig. 5.4 represents the axisymmetric version of Fig. 5.2, otherwise Fig. 5.3. The boundary conditions imposed on the planes of truncation are the same as dicussed in sections 3.2 and 3.3, which are "J-Parallel" on the top plane and "0-Potential" on the edge plane and the bottom plane.

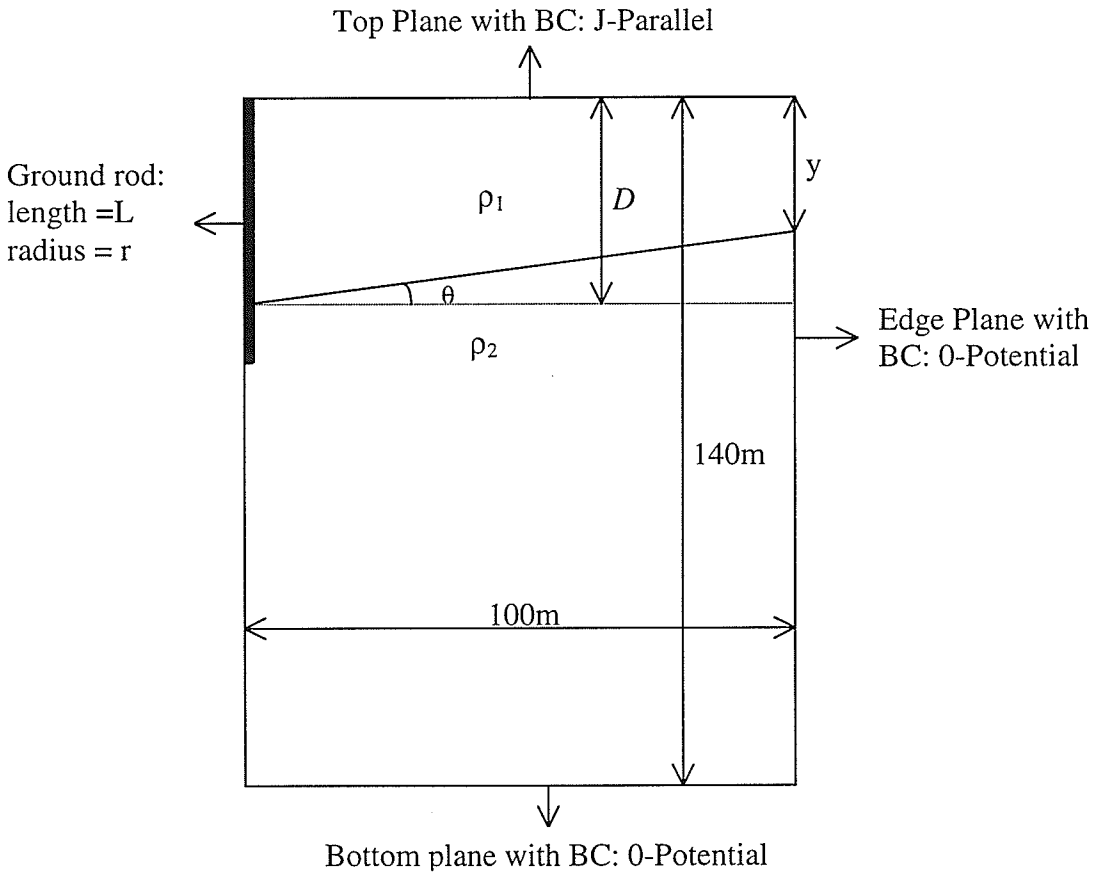

Figure 5.4 FEM axisymmetric model of single vertical rod grounding in an inclined two-layered earth

Tables 5.1, 5.2 and 5.3 show results obtained from FEM simulations for values of D equal to 18, 30 and 40m, which correspond to 90, 150 and 200% of L. The variation of θ considered is from -10 degrees to 10 degrees in 2 degree increments. Notice that when θ is 0 degrees, it implies a parallel running, non-inclined two-layered earth.

The values in the "differences" column listed in Tables 5.1, 5.2 and 5.3 are the percent differences between the R_{est}'s with respect to the R_{est} evaluated when θ is at 0 degrees. This demonstrates the effect of inclination of the layers on the ground resistance of the electrode. Once again, it is worth mentioning here that all the FEM models and meshes used for the simualtion have been checked and errors no worse than 10% can be guaranteed.

Theta, θ [Degrees]	y [m]	R_{est} [Ω]	Difference [%]
10	0.3673	5.609	11.60
8	3.9459	5.442	8.28
6	7.4896	5.360	6.65
4	11.0073	5.251	4.48
2	14.5079	5.092	1.31
0	18.0000	5.026	0.00
-2	21.4921	4.946	1.60
-4	24.9927	4.888	2.75
-6	28.5104	4.819	4.12
-8	32.0541	4.749	5.51
-10	35.6327	4.695	6.58

Table 5.1 D is at 18m (90% of L), ρ_1 and ρ_2 are 100 and 200 Ω-m

Theta, θ [Degrees]	y [m]	R_{est} [Ω]	Difference [%]
10	12.3673	4.383	5.00
8	15.9459	4.336	4.23
6	19.4896	4.300	3.37
4	23.0073	4.260	2.40
2	26.5079	4.230	1.68
0	30.0000	4.160	0.00
-2	33.4921	4.181	0.50
-4	36.9927	4.162	0.05
-6	40.5104	4.125	0.84
-8	44.0541	4.129	0.75
-10	47.6327	4.101	1.42

Table 5.2 D is at 30m (150% of L), ρ_1 and ρ_2 are 100 and 200 Ω-m

Theta, θ [Degrees]	y [m]	R_{est} [Ω]	Difference [%]
10	22.3673	4.178	2.28
8	25.9459	4.158	1.79
6	29.4896	4.140	1.34
4	33.0073	4.116	0.80
2	36.5079	4.097	0.30
0	40.0000	4.085	0.00
-2	43.4921	4.076	0.20
-4	46.9927	4.067	0.40
-6	50.5104	4.056	0.80
-8	54.0541	4.038	1.15
-10	57.6327	4.021	1.57

Table 5.3 D is at 40m (200% of L), ρ_1 and ρ_2 are 100 and 200 Ω-m

5.4.1 Discussion of Results

Tables 5.1, 5.2 and 5.3 present 3 sets of data associated with different values for D. As θ decreases from 10 degrees to -10 degrees, one observes a decrease in R_{est}. This trend of variation agrees with engineering intuition. As θ decreases from 10 degrees to -10 degrees, the volume of the upper layer soil with the lower resistivity, ρ_1 of 100 Ω-m actually increases. This increase in the volume of the upper layer soil causes the equivalent resistivity of the entire earth and ground electrode system to decrease, resulting in a drop in the ground resistance since the ground resistance is proportional to the earth's equivalent resistivity.

The largest difference occurs when θ is at 10 degrees. Based on the results in Table 5.1, this difference can be as high as 11.60% if D is at 90% of L. One can expect the percent difference to be around this magnitude if D is within 130% of L. An inclination angle of 10 degrees, which represents a 18% slope is fairly abrupt for this ground rod.

The difference that occurs when θ is at -10 degrees is always smaller than the difference that occurs when θ is at 10 degrees. This supports one of the important findings in chapter 4, where it was found that the influence of the lower layer soil on the ground resistance diminishes as the interface between the 2 layers moves downward from the electrode. As θ is changing from 10 degrees to -10 degrees, one can think of it as a situation such that an equivalent interface between the 2 layers of soil is shifting downward from the electrode.

Comparing the results in Tables 5.1, 5.2 and 5.3, it is seen that if the interface is located far enough from the electrode, the inclined-layers may be replaced by a two-layered earth model. The two conditions that encourage the replacement of the inclined-layers by a two-layered earth model are that (refer to Fig. 5.4) y must be larger than L and D must be greater than $2L$, i.e, $y > L$ and $D > 2L$.

5.5 Chapter Summary

In general, the earth may be multi-layered with either horizontal or non horizontal layers. Even if information regarding inclinations is obtainable, the accuracy and reliability are questionable. From an electrical engineering point of view, a parallel running multi-layered earth model is likely sufficient.

If there exist strong geophysical evidence that support the existence of inclined-layers, one should make use of this information to select the best electrode site, such as by moving the electrode to the area with lower soil resistivity. The problems associated with the earth electrode design can be greatly reduced simply by an appropriate site selection.

Suppose that geophysical data does support consideration of inclined-layers in the estimation of ground resistance for the selected electrode site, a design engineer can always approximate the inclined-layers earth model with a parallel running multi-layered earth model. This is allowable because of the uncertainty nature of the geophysical data which mandate a rather large design safety factor. This safety factor will likely take care of the error incurred by replacing the inclined-layers earth model with a parallel running multi-layered earth model.

Based on Table 5.1, when the inclination angle, θ is 10 degrees, the error resulting from replacement for this worst case scenario (V-shaped inclination with a two-layered earth) is about 11%. Practical earth electrode design definitely uses a design safety factor higher than 1.1. On top of that, a V-shaped inclination implies a rough terrain, which is quite unlikely to be a good electrode site selection.

The two favorable conditions for the replacement of the inclined-layered earth model with a parallel running multi-layered earth model are, (refer to Fig. 5.4) that y must be larger than L and D must be greater than $2L$, i.e, $y > L$ and $D > 2L$.

Chapter 6

Thesis Summary and Main Contributions

This chapter summarizes the entire thesis and concludes some of the important findings in this research project. It is known for a fact that the most important parameter in the design of a HVDC earth electrode is the soil resistivity because it governs the performance and dictates the physical arrangement and size of the earth electrode.

In this thesis, a technique has been proposed for the simple and efficient calculation of ground resistance due to vertically embedded electrodes in a two-layered earth with parallel running layers. This technique can be extended to cater for multi-layered earth with parallel running layers.

The approach employed throughout the research project is largely numerical. For multi-layered earth, an equivalent resistivity, ρ_{eqv} is derived thereby simplifying the exact physical system and enabling a design engineer to deal with the problem more efficiently. It produces a more realistic design parameter, which is the equivalent resistivity as compared to the conservative apparent resistivity or bulk resistivity that are commonly used in the design of an earth electrodes.

6.1 Thesis Summary

Chapters 1 and 2 contain background information required for this thesis. These includes the role of an earth electrode in HVDC schemes, discussion on soil resistivity and its measurement, tools and methods employed and classical analytical solutions.

Chapters 3, 4 and 5 constitute the main core of this research work. Chapter 3 discusses the FEM simulation and assesses the accuracy and reliability of the simulation results by comparing them to the available analytical solutions. All the calculations involving 3D simulations were achieved by employing an advanced FEM analysis technique called *'substructuring'*. It is shown that all the results presented in this work contain errors no more than 10% with only a few exceptions, which are associated with Eq. (2-4). Chapter 4 tackles parallel running, multi-layered earth problems whereas chapter 5 focuses on the discussions involving earth with inclined layers.

6.2 Main Contributions

(1) The derived normalized equivalent resistivity curves can be used to simplify the evaluation of the ground resistance due to a single vertical rod buried in ground provided that the length of the rod is much larger than its radius i.e, $L >> r$.

(2) In a two-layered earth problem, it has been shown that if the lower layer is situated at a distance of more than twice the length of the ground rod i.e., $D > 2L$, its existence can be safely disregarded. One may extend the top layer to replace it thereby reducing the two-layered earth to a homogeneous earth.

(3) The above finding can be extended to the multi-layered case as explained in section 4.2.

(4) A simple technique which relies on the ratios of D/L and ρ_1/ρ_2 for reducing a two-layered earth to a homogeneous earth by using the normalized equivalent resistivity curves has been proposed.

(5) An extension of the above technique has led to the method of successive approximation, which allows a multi-layered earth to be approximated to a homogeneous one.

(6) The proposed techniques are also applicable to various arrangements of vertically embedded ground rods provided the condition of $L >> r$ is satisfied, regardless of the formation used i.e, ring, star, hollow square etc.

(7) In all of the above cases, once a problem has been reduced to one with homogeneous earth with some equivalent resistivity, ρ_{eqv}, the ground resistance may be found by using numerical analysis or by resort to use of classical solutions in [36 Dwight], [48 Sunde] and [64 Tagg].

References

[97 Ian] Ian Ferguson, H.d. Odwar, H.D. Boteler, "Review and Synthesis of Large-Scale Electrical Conductivity Soundings in Canada", Report submitted to the Geological Survey of Canada, March 1997.

[90 Ward] Stanley H. Ward, "Resistivity and Induced Polarization Methods", In Geotechnical and Environmental Geophysics, Vol. I Review & Tutorial, Edited by Ward,S.H., Society of Exploration Geophysicists, Tulsa, Okla., pp 147- 189.

[90 McNeill] J.D. McNeill, "Use of Electromagnetic Methods for Groundwater Studies", In Geotechnical and Environmental Geophysics, Vol. I Review & Tutorial, Edited by Ward, S.H., Society of Exploration Geophysicists, Tulsa, Okla., pp 191-218.

[36 Dwight] H.W. Dwight, "Calculation of Resistances to Ground", Electrical Engineering, Vol. 55, Dec. 1936, pp 1319-1328.

[48 Sunde] Erling Sunde, "Earth Conduction Effects in Transmission Systems", D. Van Nostrand Company, Inc, 1949.

[64 Tagg] G.F. Tagg, "Earth Resistances", Pitman Publishing Corporation, 1964.

[82 Ciric] I.M.Ciric, O. Aboul-Atta, S. Bilgen, B.W. Klimpke, A. Wexler, Y.B. Yildir, "Ontario Hydro-GPU HVDC Interconnection Ground Electrode Study", technical report, TR82-1, the University of Manitoba, 1982.

[71 Kimbark] Edward W. Kimbark, "Direct Current Transmission", Volume I, A Wiley-Interscience Publication, John Wiley & Son, Inc, 1971.

[90 Rao] S. Rao, "EHV-AC & HVDC Transmission Engineering & Practice",Chapter 9, Khanna Publishers, 1990.

[88 Prabhakara] F.S. Prabhakara, J.F. Torri, D.F. DeCosta, D.M. Steger, T.W. Williams, "Design, Commissioning and Testing of IPP Ground Electrodes", IEEE Trans. Power Delivery, Vol. 3, No. 4, Oct 1988, pp 2037-2047.

[92 Kraus] John D. Kraus, "Electromagnetics", 4th edition, Electrical Engineering Series, McGraw-Hill, Inc, 1992.

[71 Trinh] Trinh N. Giao, Maruvada P.Sarma, "On The Potential and Field Distribution Around a Ground Electrode for HVDC Transmission", IEEE Trans. Power App. & Syst., Vol. PAS 90, No. 6, Nov.-Dec. 1971, pp 2793-2801.

[91 Szabo] Barna Szabo, Ivo Babuska, "Finite Element Analysis", A Wiley-Interscience Publication, John Wiley & Son, Inc, 1991.

[96 Silvester] Peter P. Silvester, Ronald L. Ferrari, " Finite Elements for Electrical Engineers", 3rd edition, Cambridge University Press, 1996.

[99 ANSYS] ANSYS User's Guides: Analysis Guides; Commands Manual; Elements Manual; Theory Manual; Operations Guides; ASYS, Inc, 1998

Type of Soil	Resitivity (Ω-m)
Loams, garden soil, etc	5~50
Clays	8~50
Clay, Sand and gravel mixture	40~250
Sand and gravel	60~100
Slates, shale, sandstone, etc	10~500
Crystalline rocks	200~10,000

Table A.1 Typical values of resistivity of some soils, reproduced from [64 Tagg].

Material	Resistivity (Ω-m)
Aluminum	2.9×10^{-8}
Amber	10^{14}
Bakelite	10^{14}
Carbon	3.3×10^{-5}
Copper	1.7×10^{-8}
Glass(plate)	10^{13}
Graphite	10^{-5}
Halowax	10^{11}
Mica	10^{15}
Oil(mineral)	10^{14}
Paraffin	10^{15}
Polyethylene	10^{15}
Polystyrene	10^{16}
Polyvinyl	10^{15}
Rubber	10^{13}
Rubber(neoprene)	10^{13}
Quartz	10^{17}
Soil(clay)	2×10^{2}
Soil(sandy)	5×10^{2}
Stone(limestone)	10^{2}
Sulfur	10^{15}
Urban ground	5×10^{3}
Vacuum	∞
Teflon	10^{15}
Water(distilled)	10^{4}
Water(fresh)	10^{2}~10^{3}
Water(sea)	0.2

Table A.2 Typical values of resistivity of some material [92 Kraus].

An Example Illustrating the Technique of Substructuring

Suppose there is a parallel plate capacitor with two different dielectric materials as depicted in Fig. B.1, which is the 2D model of a capacitor (side view). The dielectric materials and the electrodes have an interfacing area of A cm^2. The dimensions are arbitrarily chosen for simplicity.

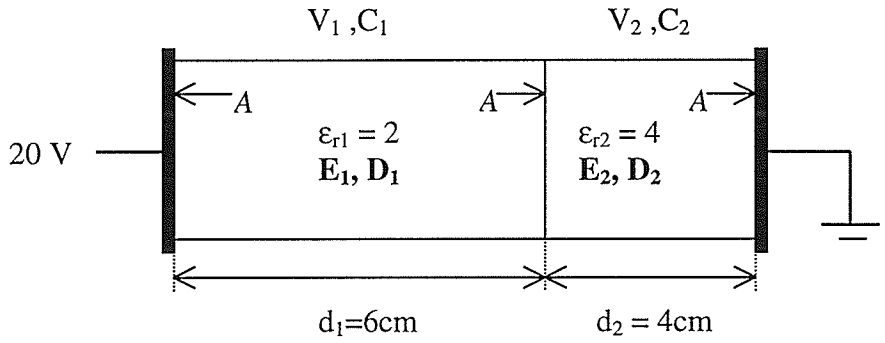

Figure B.1 Parallel plate capacitor

The relative permittivity of materials 1 and 2 are denoted by ε_{r1} and ε_{r2}. V_1 and V_2 are the voltages spanning across the 2 types of material. Similarly, $\mathbf{E_1}$, $\mathbf{D_1}$, $\mathbf{E_2}$, and $\mathbf{D_2}$ are the electric field and electric flux density in the corresponding materials. C_1 is the capacitance due to material 1 whereas C_2 is the capacitance due to material 2.

I. Analytical solution

From electromagnetic theory,

$$C_1 = \frac{\varepsilon_o \varepsilon_{r1} A}{d_1} = \frac{1}{3}\varepsilon_0 A \qquad \text{and} \qquad C_2 = \frac{\varepsilon_o \varepsilon_{r2} A}{d_2} = \varepsilon_0 A$$

The applicable boundary conditions are:

$$\mathbf{D_1} = \mathbf{D_2}$$

$$\varepsilon_1 \mathbf{E_1} = \varepsilon_2 \mathbf{E_2}$$

$$\therefore \mathbf{E_1} = 2\,\mathbf{E_2}$$

Let, $V = V_1 + V_2$

$= \mathbf{E_1}\, d_1 + \mathbf{E_2}\, d_2$

Hence, $V = \mathbf{E_1}\, d_1 + \tfrac{1}{2}\, \mathbf{E_1}\, d_2$

Therefore, $\mathbf{E_1} = V / [d_1 + \tfrac{1}{2}\, d_2]$

$= 20 / [6+2]$

$= 2.5$ V/cm

$\mathbf{E_2} = \mathbf{E_1}/2$

$= 1.25$ V/cm

$\mathbf{D_1} = \mathbf{D_2} = \varepsilon_0 \varepsilon_1 \mathbf{E_1} = \varepsilon_0 \varepsilon_2 \mathbf{E_2}$

$= 4.4271 \times 10^{-9}$ C/cm^2

II. FEM solution

There are 2 ways of modeling this problem:

(A). Conventional meshing technique.

(B). Substructuring technique.

(A) Conventional meshing

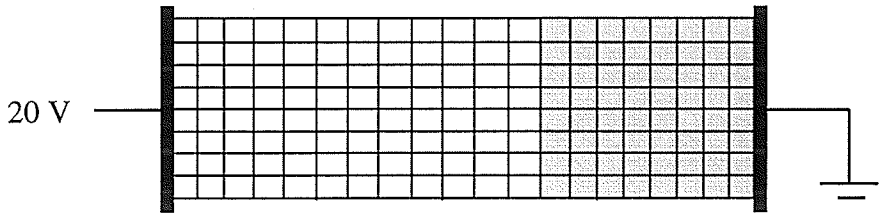

Figure B.2 FEM model for conventional meshing

Material 1 is not shaded whereas material 2 is shaded. This conventional meshing method uses 160 elements and 537 nodes. Material 1 is meshed with 96 elements and material 2 with 64 elements.

By using *ANSYS 5.5*, this model produces the following results:

$$\mathbf{E}_1 = 2.5 \text{ V/cm}$$
$$\mathbf{E}_2 = 1.2 \text{ V/cm}$$
$$\mathbf{D}_1 = \mathbf{D}_2 = 4.427 \times 10^{-9} \text{ C/cm}^2$$

It is evident that these results are a perfect match with the analytical solution.

(B) Substructuring Technique

Essentially, this method condenses a group of nodes to form an element, called the *'superelement'*, which is also known as a *'substructure'*. With regard to *ANSYS 5.5*, this technique involves three passes or stages, which are the *'generation pass'*, *'use pass'* and *'expansion pass'*. For more information, see [99 ANSYS].

(I) Generation Pass

In the *'generation pass'*, the focus is on creating the *'superelement'*. The user has to create the portion to be modeled and mesh it. While creating the *'superelement'*, all the nodes located at the interfaces between this *'superelement'* and other *'superelements'* or other elements must be defined as *'master degree of freedoms'*. The created *'superelement'* can later be used as a conventional element.

(II) Use Pass

This is the stage where the user uses the *'superelement'* in the FEM model. Extra attention is required to ensure proper connectivity of nodes, especially at the interfaces of the *'superelement'* with other *'superelements'* or elements. More specifically, proper connectivity of nodes between the *'master degree of freedoms'* with other *'master degree of freedoms'* or other nodes must be ensured.

(III) Expansion Pass

In the *'use pass'*, the user obtains solution for all the conventional nodes and the *'master degree of freedoms'* within the FEM model. In other words, the solution at the interfaces of the *'superelement'* is already available after the *'use pass'* but not the solution within the *'superelement'*.

In order to obtain the solution within the *'superelement'* , the user needs to perform an *'expansion pass'* on the selected *'superelement'*. Each *'superelement'* or *'substructure'* requires an individual *'expansion pass'* to obtained the solution within it. Before performing any *'expansion pass'*, the information from both the *'generation pass'* and *'use pass'* must become available.

Using the substructuring technique, one arrives at the following FEM model;

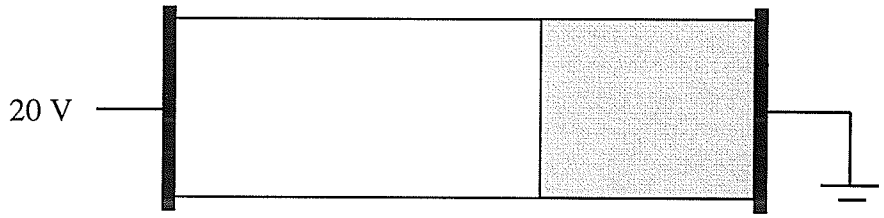

Figure B.3 FEM model for substructure technique

Material 1 is not shaded whereas material 2 is shaded. There are only 2 elements and 154 nodes that are involved in the *'use pass'*. Compared with the conventional meshing method in (A), which uses 160 elements and 537 nodes, the FEM model size here has been greatly reduced.

After the *'use pass'*, the user needs to perform 2 *'expansion passes'* to obtained the total solution. In this model, 94 elements were used in the *'generation pass'* for creating the *'superelement'* corresponding to material 1 and 64 elements were used for creating the *'superelement'* corresponding to material 2.

After the *'expansion pass'*, one obtains the following results:

$$\mathbf{E}_1 = 2.5 \text{ V/cm}$$

$$\mathbf{E}_2 = 1.2 \text{ V/cm}$$

$$\mathbf{D}_1 = \mathbf{D}_2 = 4.427 \times 10^{-9} \text{ C/cm}^2$$

This shows that the technique of *'substructuring'* if used properly can produce very good results. The accuracy of this technique depends on two main factors. The first factor being the validity of the assumption that the elements within the *'superelement'* are linear. If the connectivity of the overall nodes within the entire FEM model which involves *'superelement'* is good, so will the accuracy.

Appendix C:

Normalized Equivalent Resistivity Curves

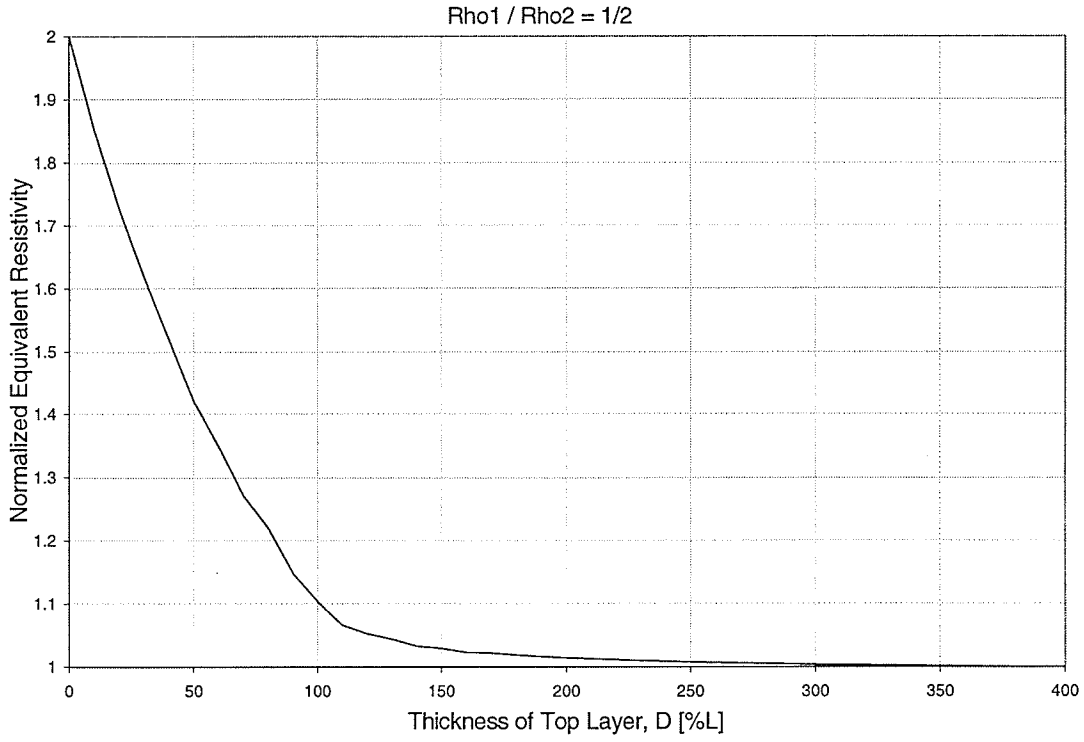
Rho1 / Rho2 = 1/2
Normalized Equivalent Resistivity
2
1.9
1.8
1.7
1.6
1.5
1.4
1.3
1.2
1.1
1
0
50
100
150
200
250
300
350
400
Thickness of Top Layer, D [%L]

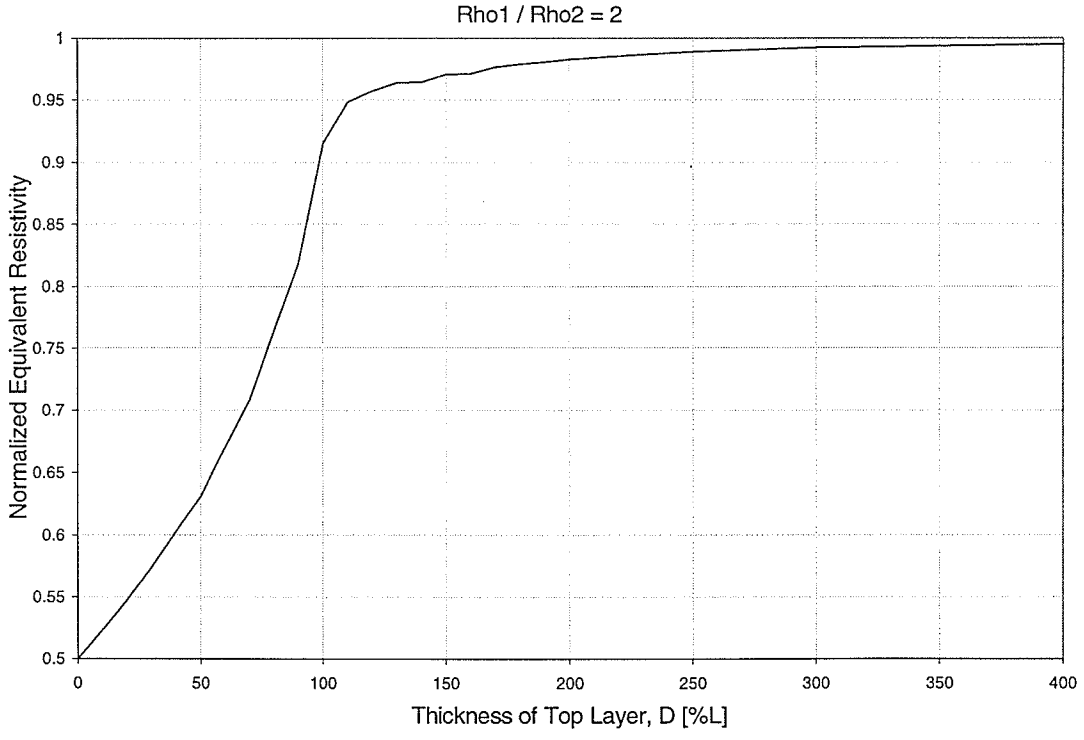
Rho1 / Rho2 = 2
Normalized Equivalent Resistivity
1
0.95
0.9
0.85
0.8
0.75
0.7
0.65
0.6
0.55
0.5
0
50
100
150
200
250
300
350
400
Thickness of Top Layer, D [%L]

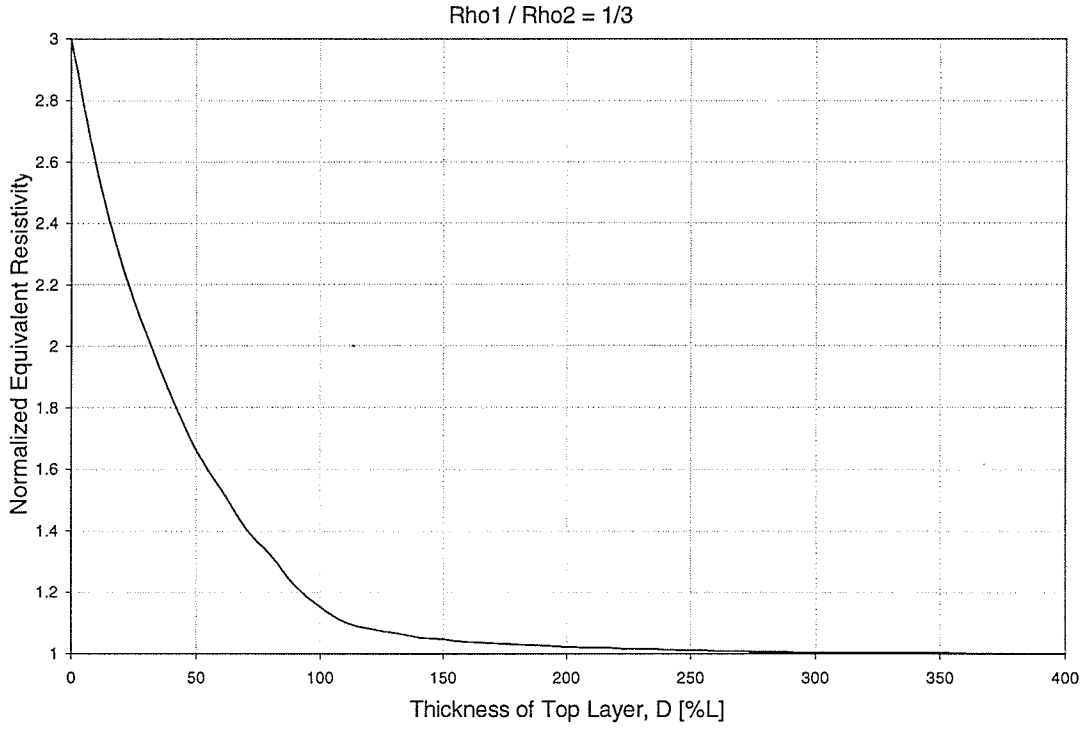
Rho1 / Rho2 = 1/3
Normalized Equivalent Resistivity
3
2.8
2.6
2.4
2.2
2
1.8
1.6
1.4
1.2
1
0
50
100
150
200
250
300
350
400
Thickness of Top Layer, D [%L]

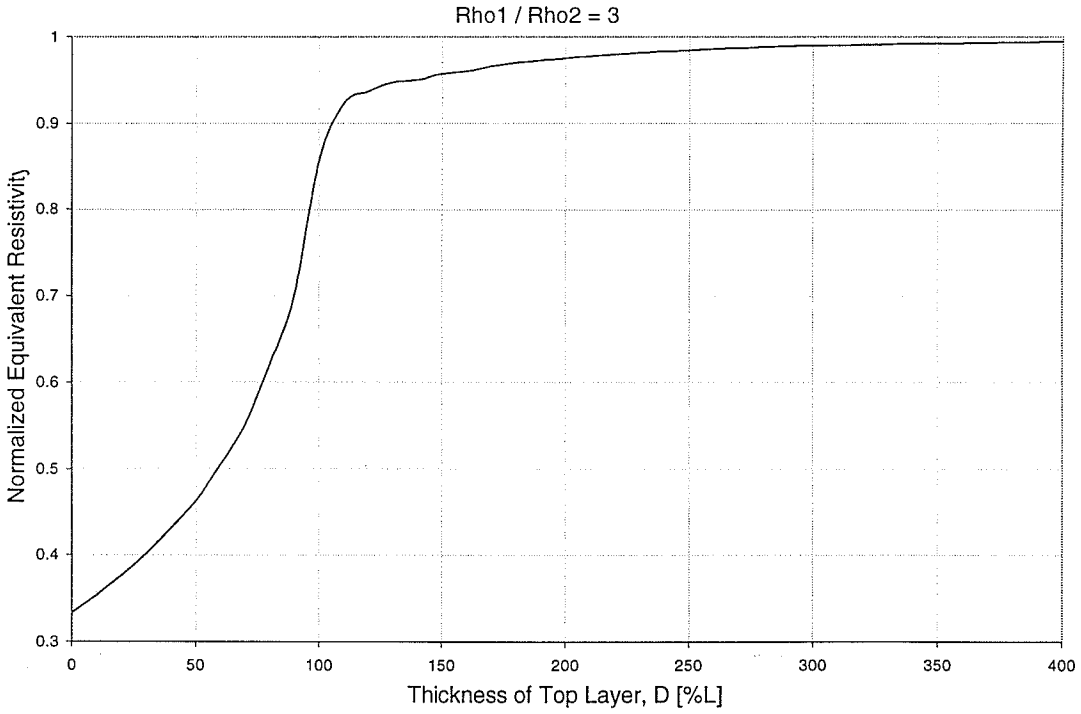
Rho1 / Rho2 = 3
Normalized Equivalent Resistivity
1
0.9
0.8
0.7
0.6
0.5
0.4
0.3
0
50
100
150
200
250
300
350
400
Thickness of Top Layer, D [%L]

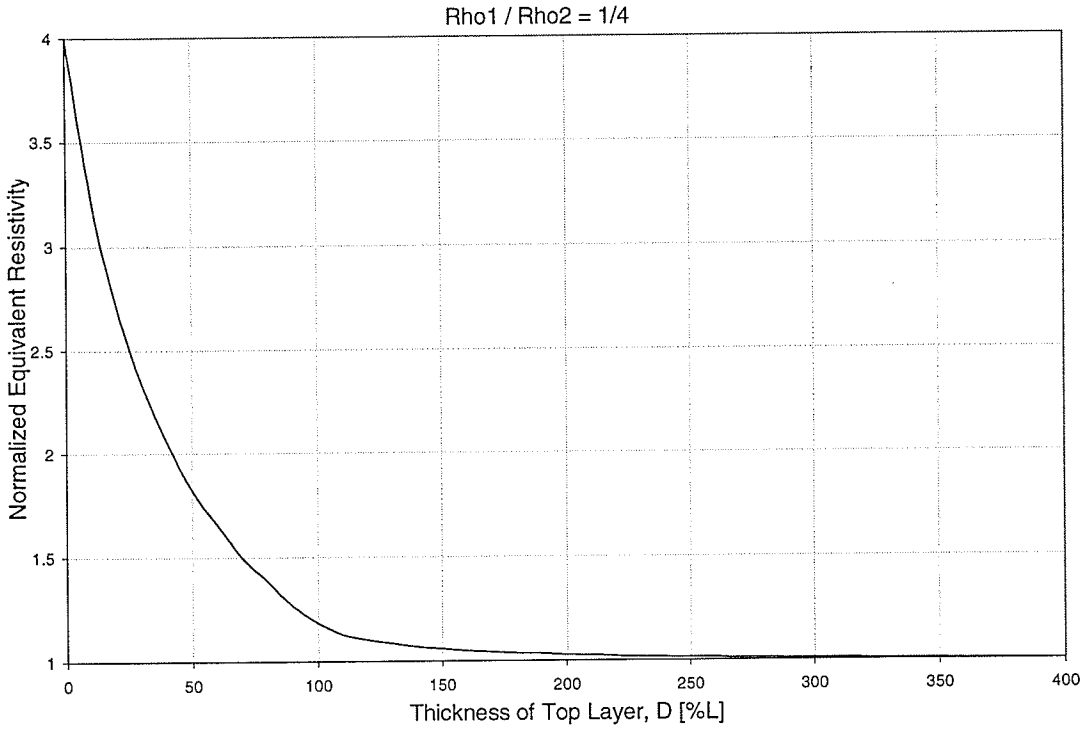
Rho1 / Rho2 = 1/4
Normalized Equivalent Resistivity
4
3.5
3
2.5
2
1.5
1
0
50
100
150
200
250
300
350
400
Thickness of Top Layer, D [%L]

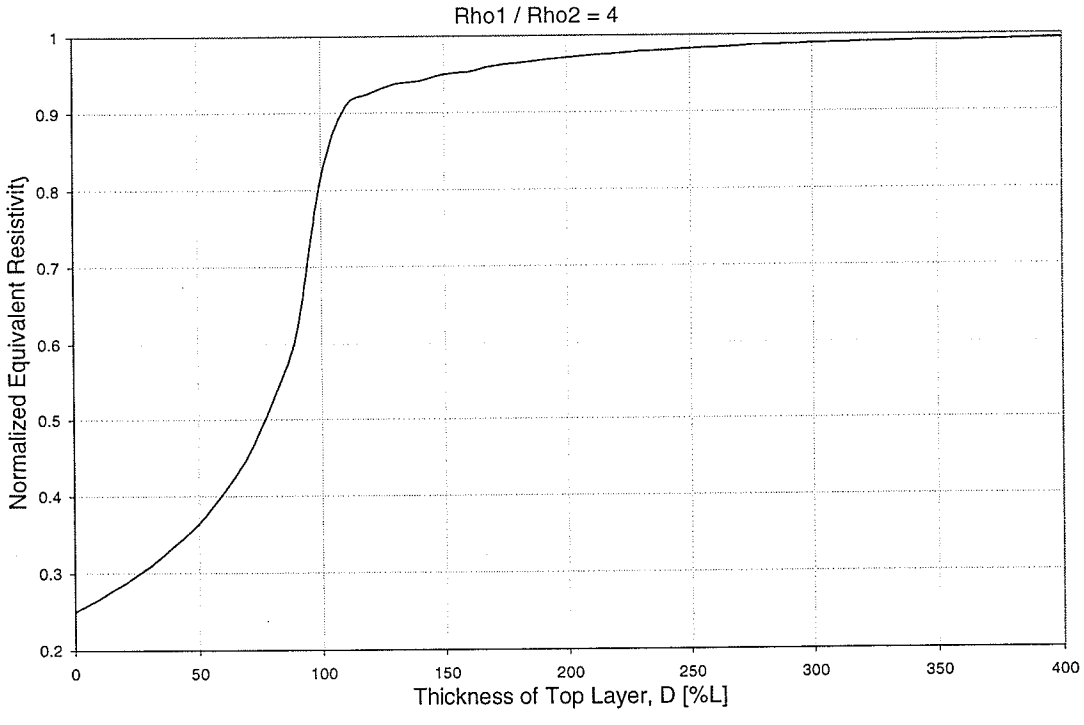
Rho1 / Rho2 = 4
Normalized Equivalent Resistivity
1
0.9
0.8
0.7
0.6
0.5
0.4
0.3
0.2
0
50
100
150
200
250
300
350
400
Thickness of Top Layer, D [%L]

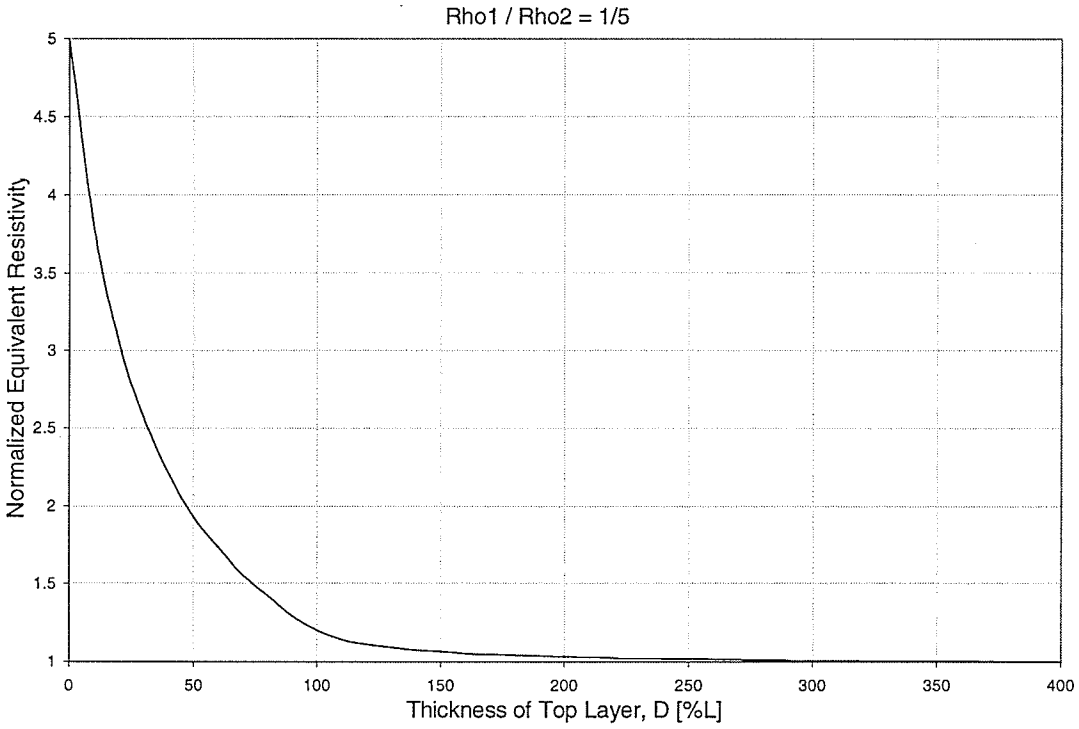
Rho1 / Rho2 = 1/5
Normalized Equivalent Resistivity
5
4.5
4
3.5
3
2.5
2
1.5
1
0
50
100
150
200
250
300
350
400
Thickness of Top Layer, D [%L]

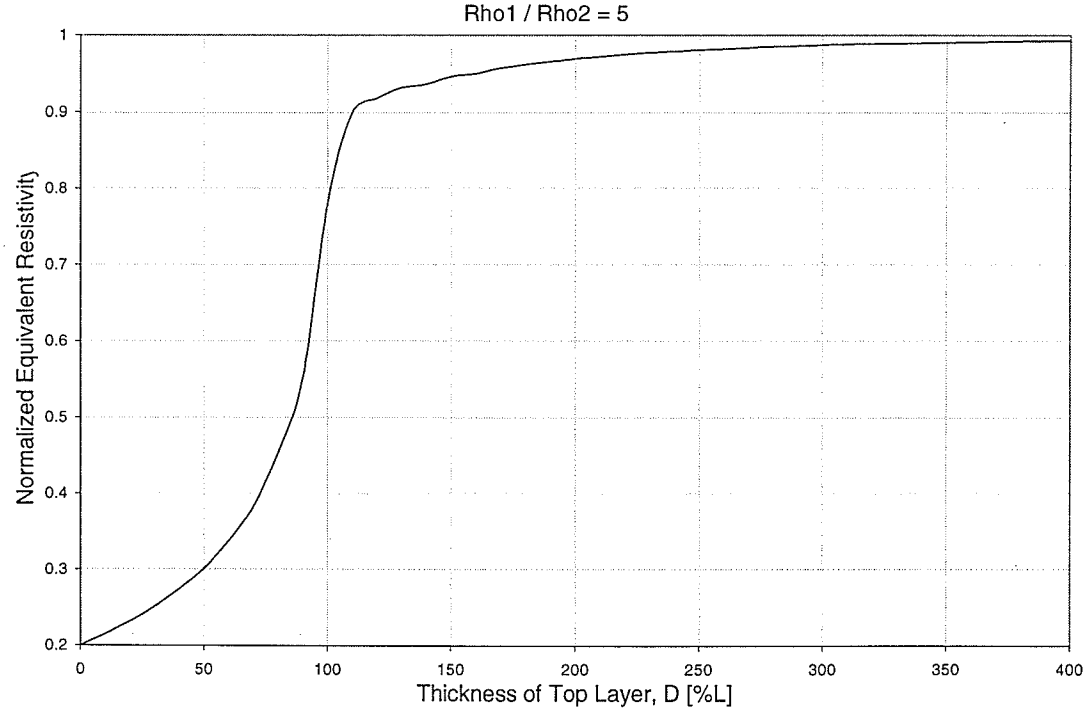
Rho1 / Rho2 = 5
Normalized Equivalent Resistivity
1
0.9
0.8
0.7
0.6
0.5
0.4
0.3
0.2
0
50
100
150
200
250
300
350
400
Thickness of Top Layer, D [%L]

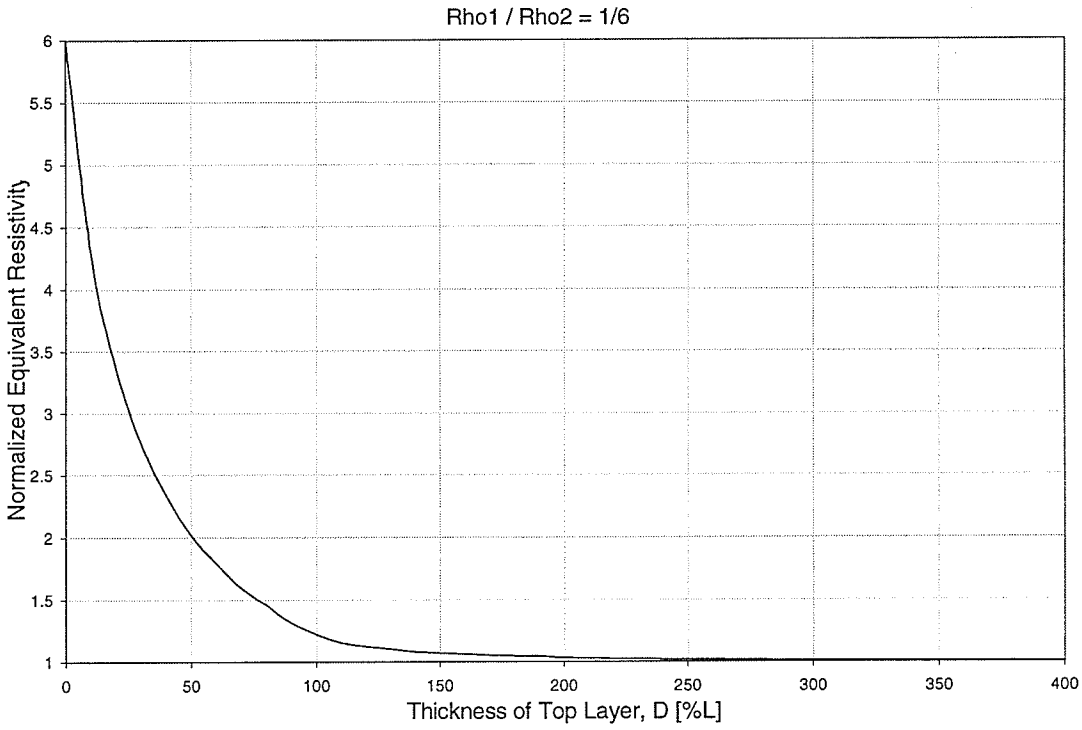
Rho1 / Rho2 = 1/6
Normalized Equivalent Resistivity
6
5.5
5
4.5
4
3.5
3
2.5
2
1.5
1
0
50
100
150
200
250
300
350
400
Thickness of Top Layer, D [%L]

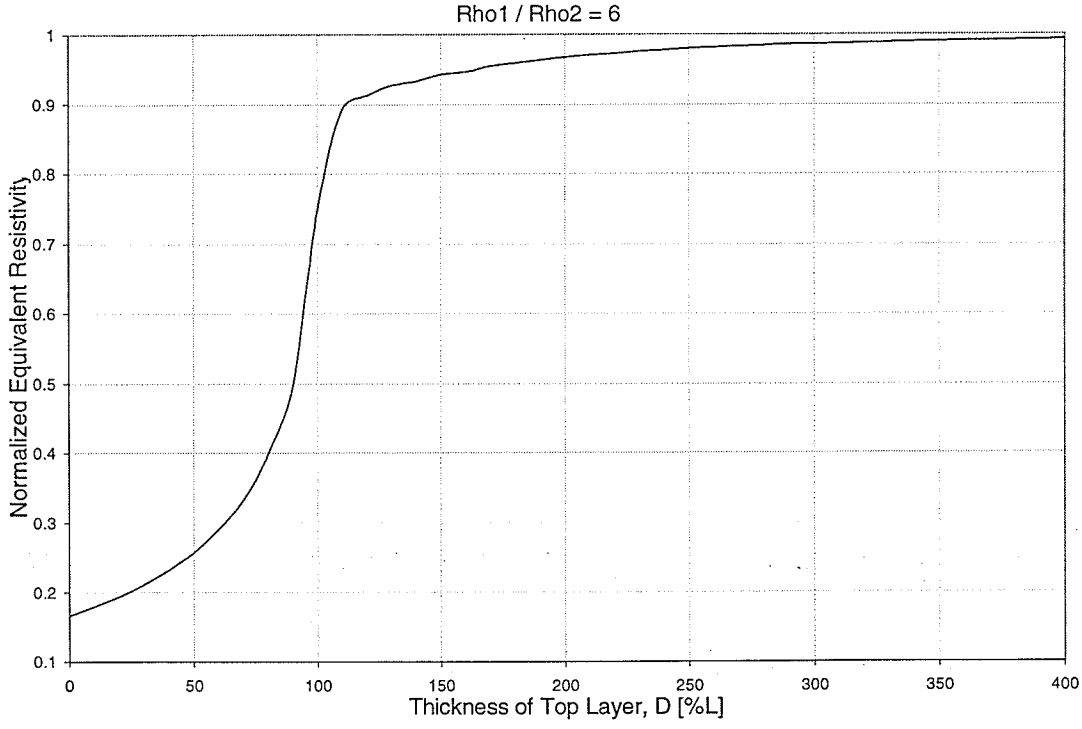
Rho1 / Rho2 = 6
Normalized Equivalent Resistivity
1
0.9
0.8
0.7
0.6
0.5
0.4
0.3
0.2
0.1
0
50
100
150
200
250
300
350
400
Thickness of Top Layer, D [%L]

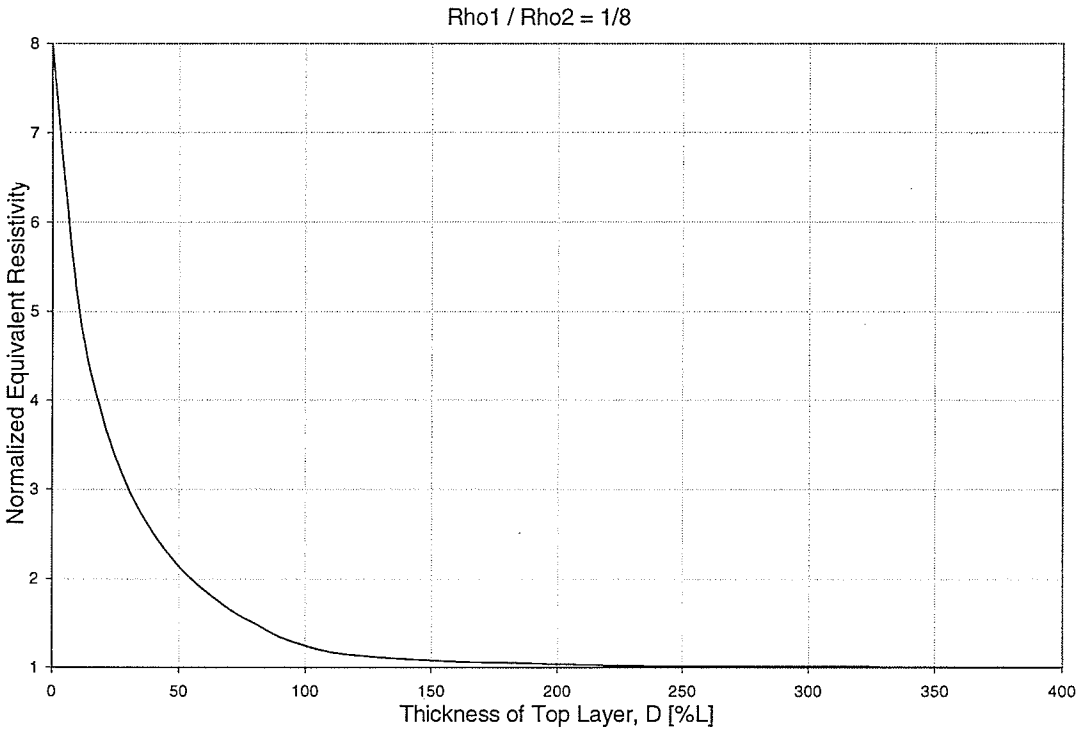
Rho1 / Rho2 = 1/8
Normalized Equivalent Resistivity
Thickness of Top Layer, D [%L]
1
2
3
4
5
6
7
8
0
50
100
150
200
250
300
350
400

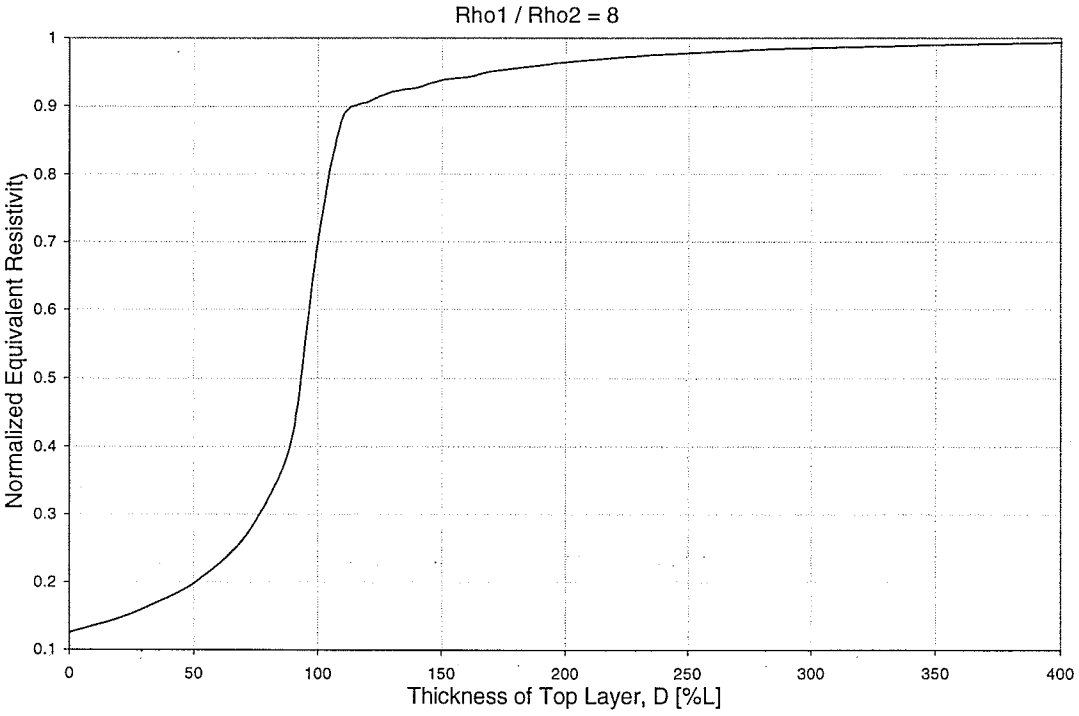
Rho1 / Rho2 = 8
Normalized Equivalent Resistivity
Thickness of Top Layer, D [%L]
0.1
0.2
0.3
0.4
0.5
0.6
0.7
0.8
0.9
1
0
50
100
150
200
250
300
350
400

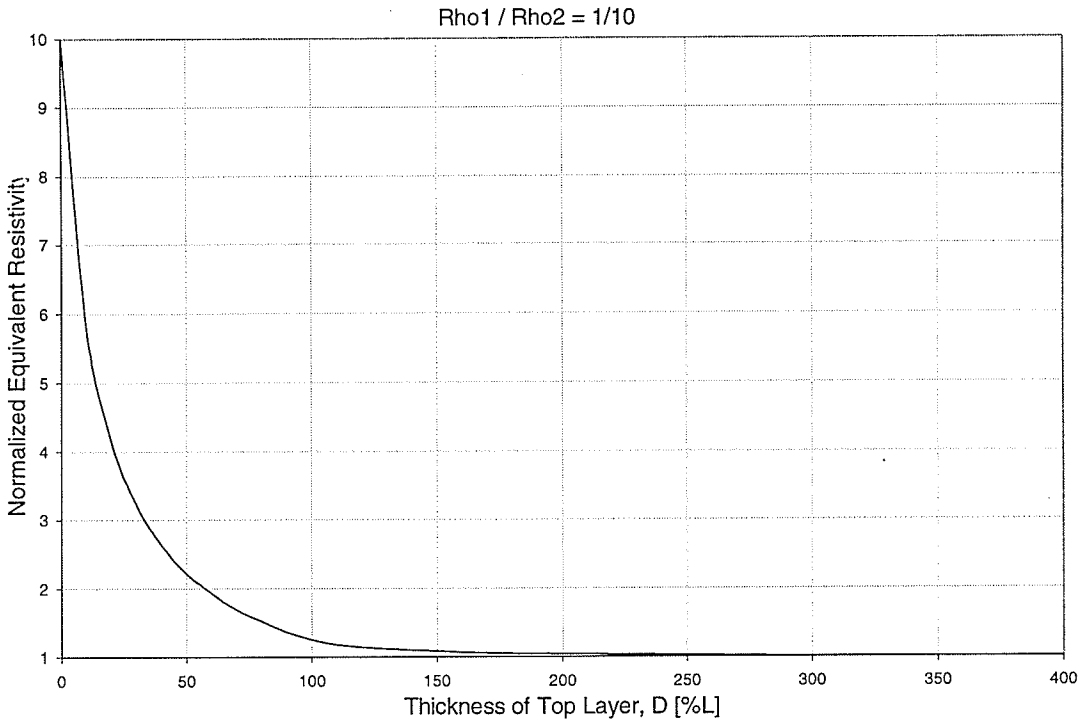
Rho1 / Rho2 = 1/10
Normalized Equivalent Resistivity
Thickness of Top Layer, D [%L]
10
9
8
7
6
5
4
3
2
1
0
50
100
150
200
250
300
350
400

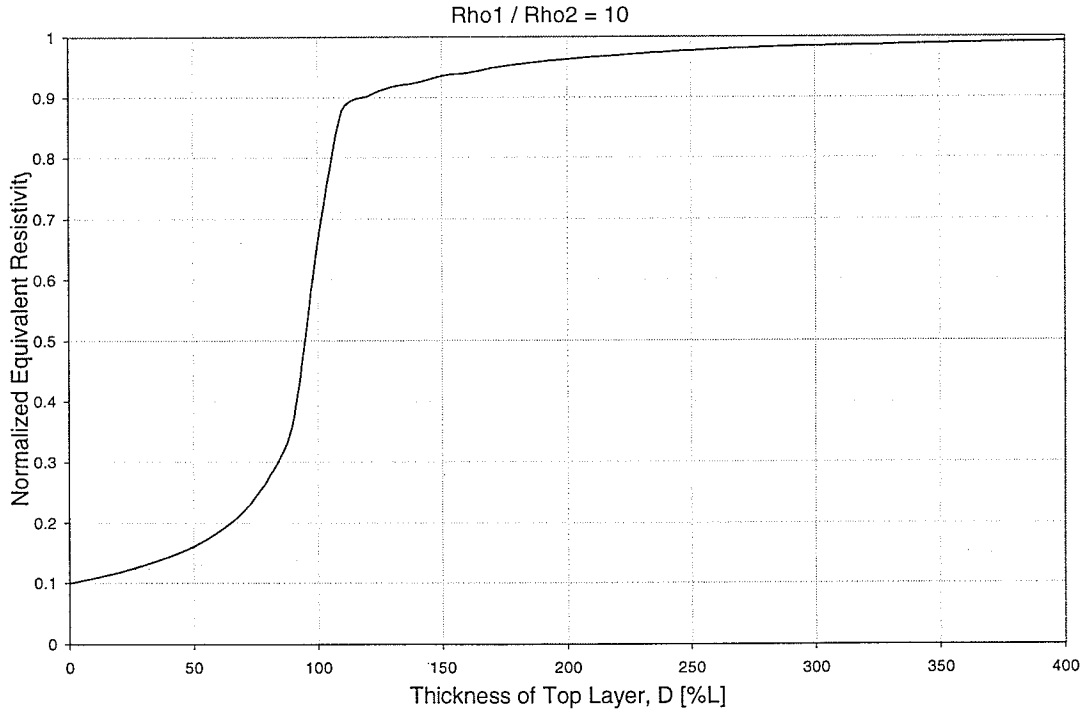
Rho1 / Rho2 = 10
Normalized Equivalent Resistivity
Thickness of Top Layer, D [%L]
1
0.9
0.8
0.7
0.6
0.5
0.4
0.3
0.2
0.1
0
0
50
100
150
200
250
300
350
400

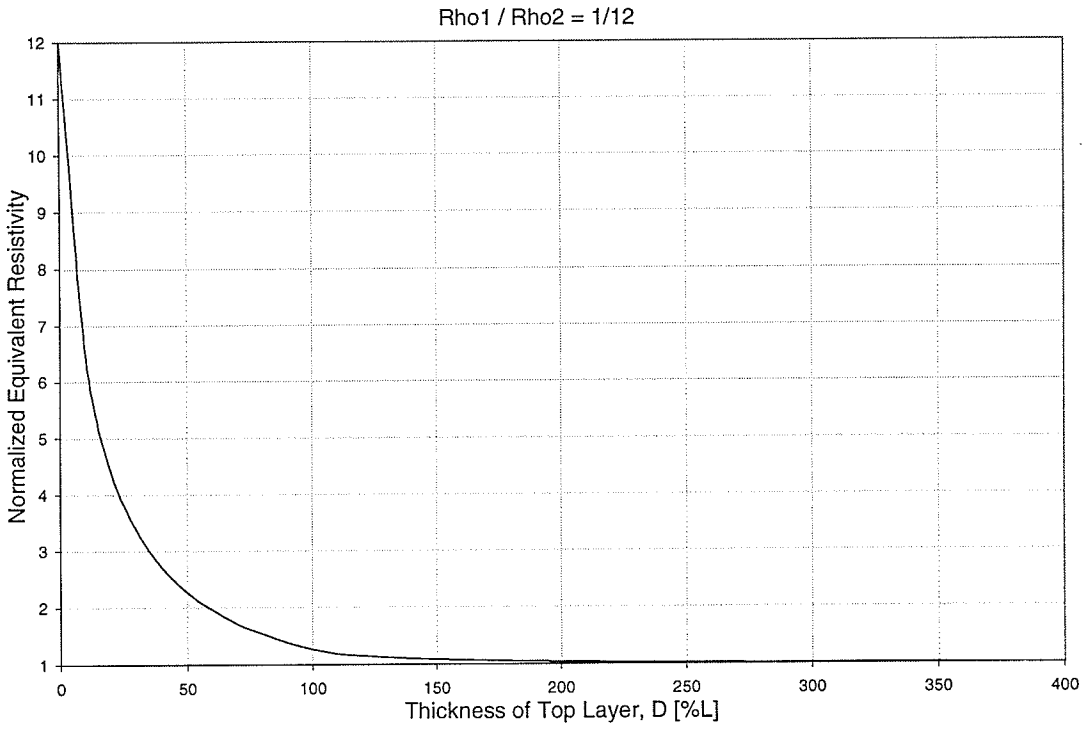
Rho1 / Rho2 = 1/12
Normalized Equivalent Resistivity
Thickness of Top Layer, D [%L]
12
11
10
9
8
7
6
5
4
3
2
1
0
50
100
150
200
250
300
350
400

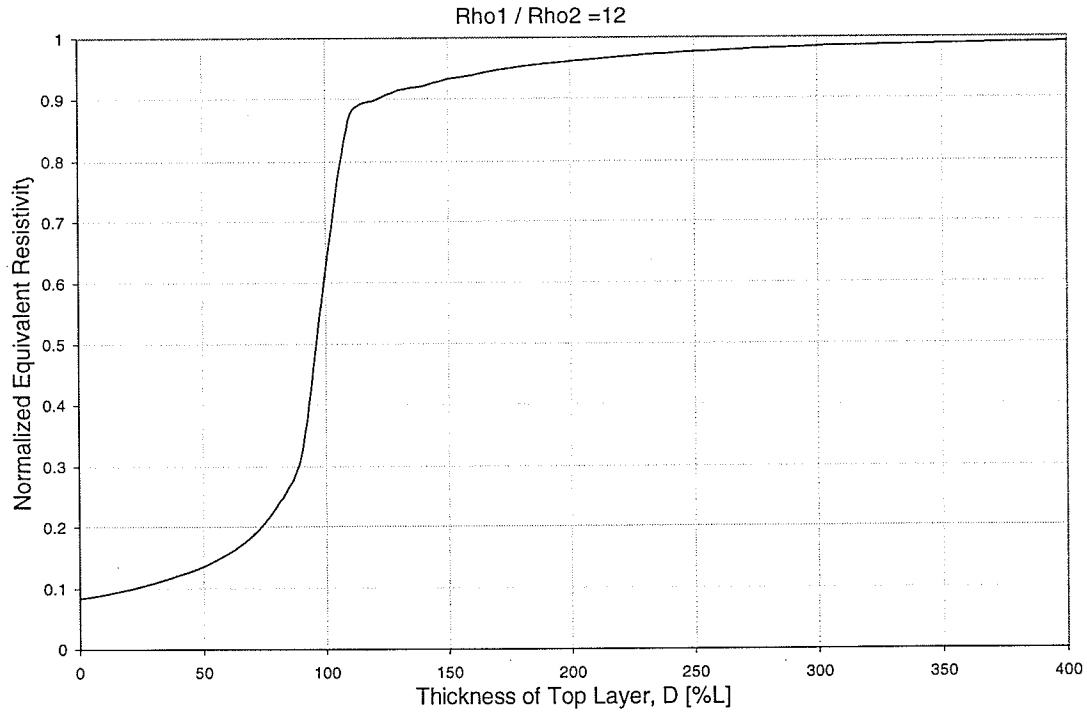
Rho1 / Rho2 =12
Normalized Equivalent Resistivity
Thickness of Top Layer, D [%L]
1
0.9
0.8
0.7
0.6
0.5
0.4
0.3
0.2
0.1
0
0
50
100
150
200
250
300
350
400

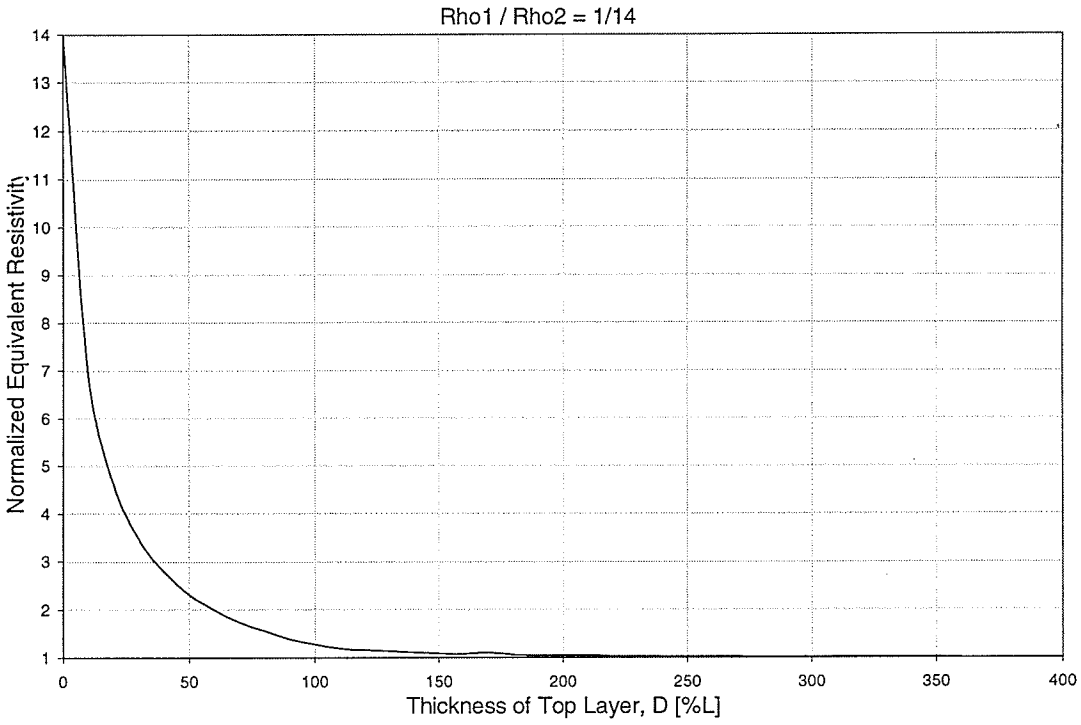
Rho1 / Rho2 = 1/14
Normalized Equivalent Resistivity
Thickness of Top Layer, D [%L]
14
13
12
11
10
9
8
7
6
5
4
3
2
1
0
50
100
150
200
250
300
350
400

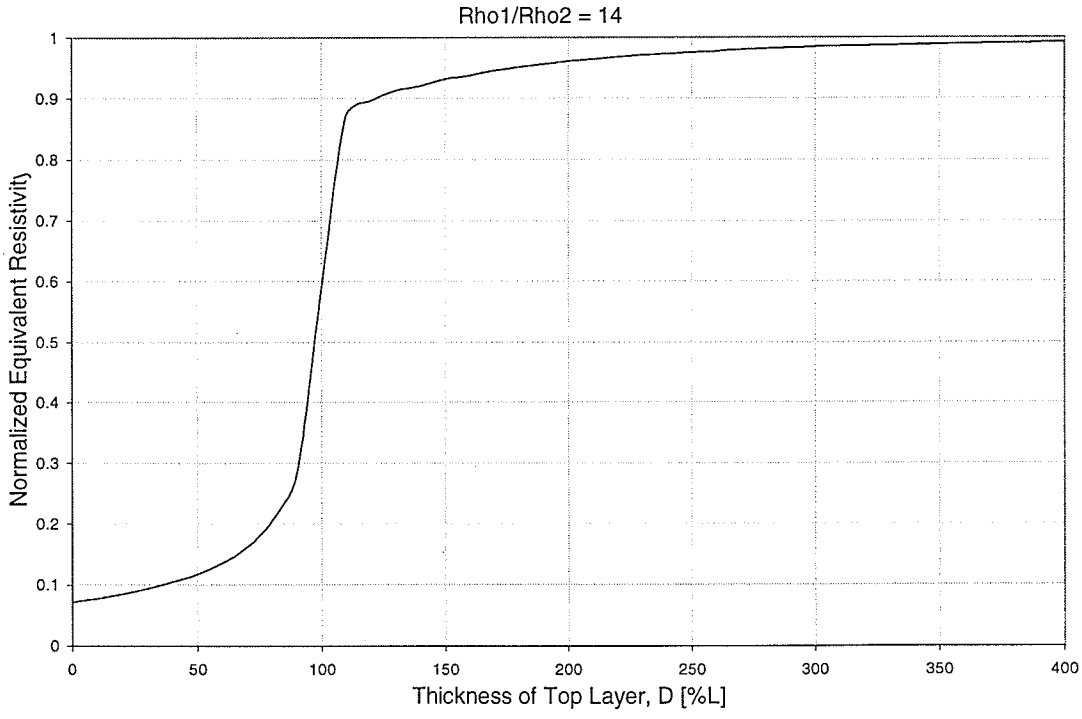
Rho1/Rho2 = 14
Normalized Equivalent Resistivity
Thickness of Top Layer, D [%L]
1
0.9
0.8
0.7
0.6
0.5
0.4
0.3
0.2
0.1
0
0
50
100
150
200
250
300
350
400

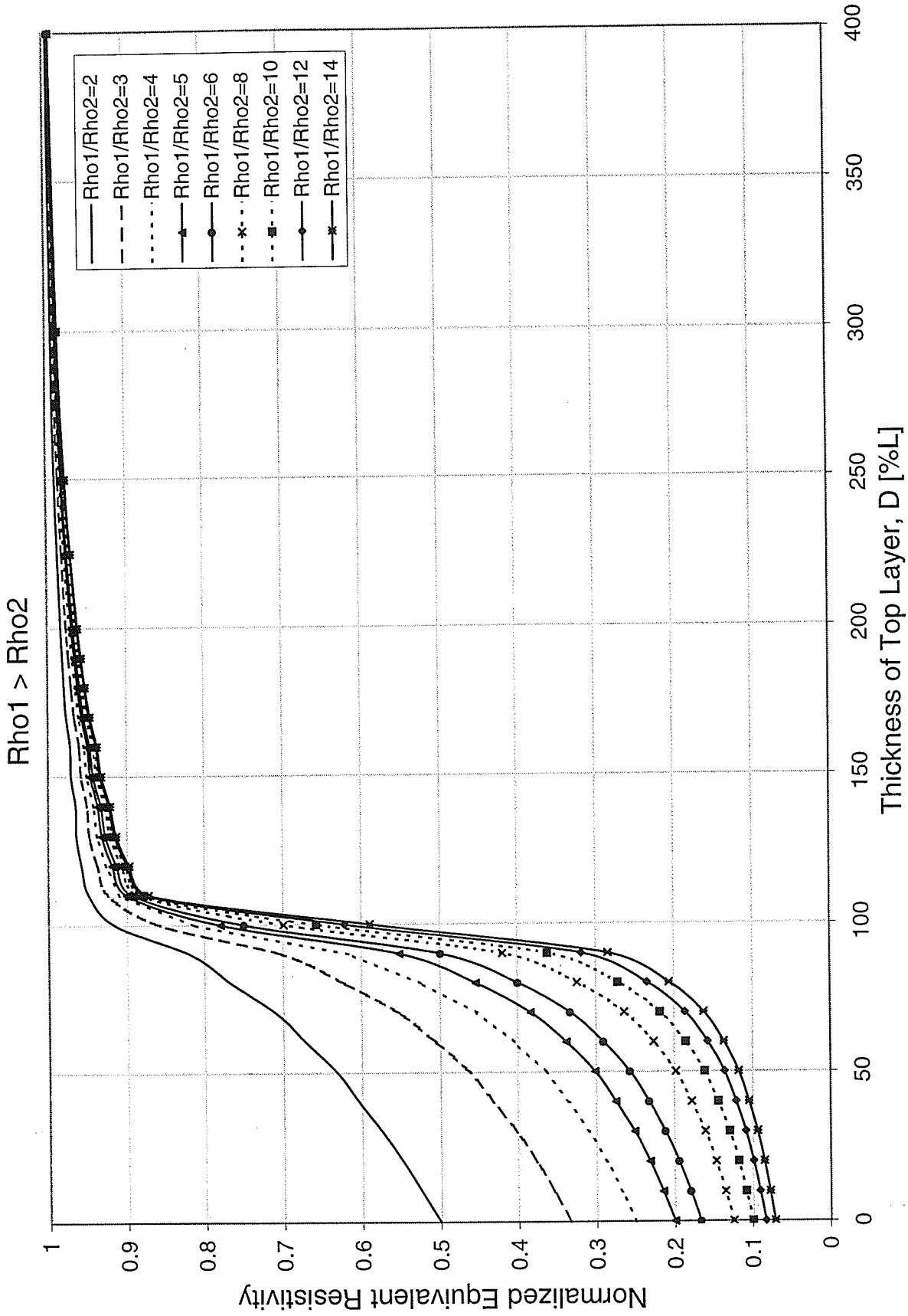
Rho1 > Rho2
Rho1/Rho2=2
Rho1/Rho2=3
Rho1/Rho2=4
Rho1/Rho2=5
Rho1/Rho2=6
Rho1/Rho2=8
Rho1/Rho2=10
Rho1/Rho2=12
Rho1/Rho2=14
Normalized Equivalent Resistivity
1
0.9
0.8
0.7
0.6
0.5
0.4
0.3
0.2
0.1
0
0
50
100
150
200
250
300
350
400
Thickness of Top Layer, D [%L]

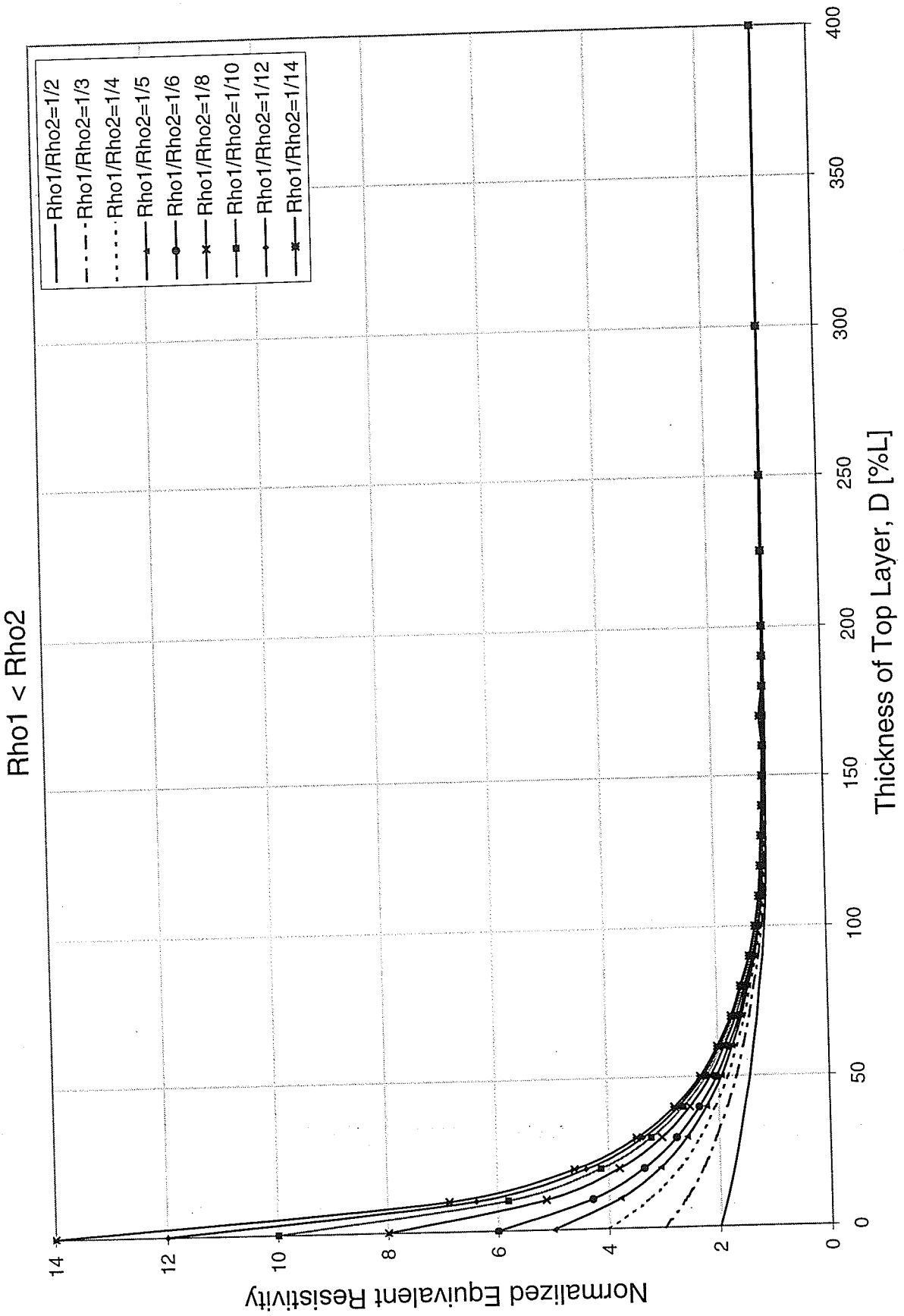
Rho1 < Rho2
Rho1/Rho2=1/2
Rho1/Rho2=1/3
Rho1/Rho2=1/4
Rho1/Rho2=1/5
Rho1/Rho2=1/6
Rho1/Rho2=1/8
Rho1/Rho2=1/10
Rho1/Rho2=1/12
Rho1/Rho2=1/14
Normalized Equivalent Resistivity
0
2
4
6
8
10
12
14
Thickness of Top Layer, D [%L]
0
50
100
150
200
250
300
350
400

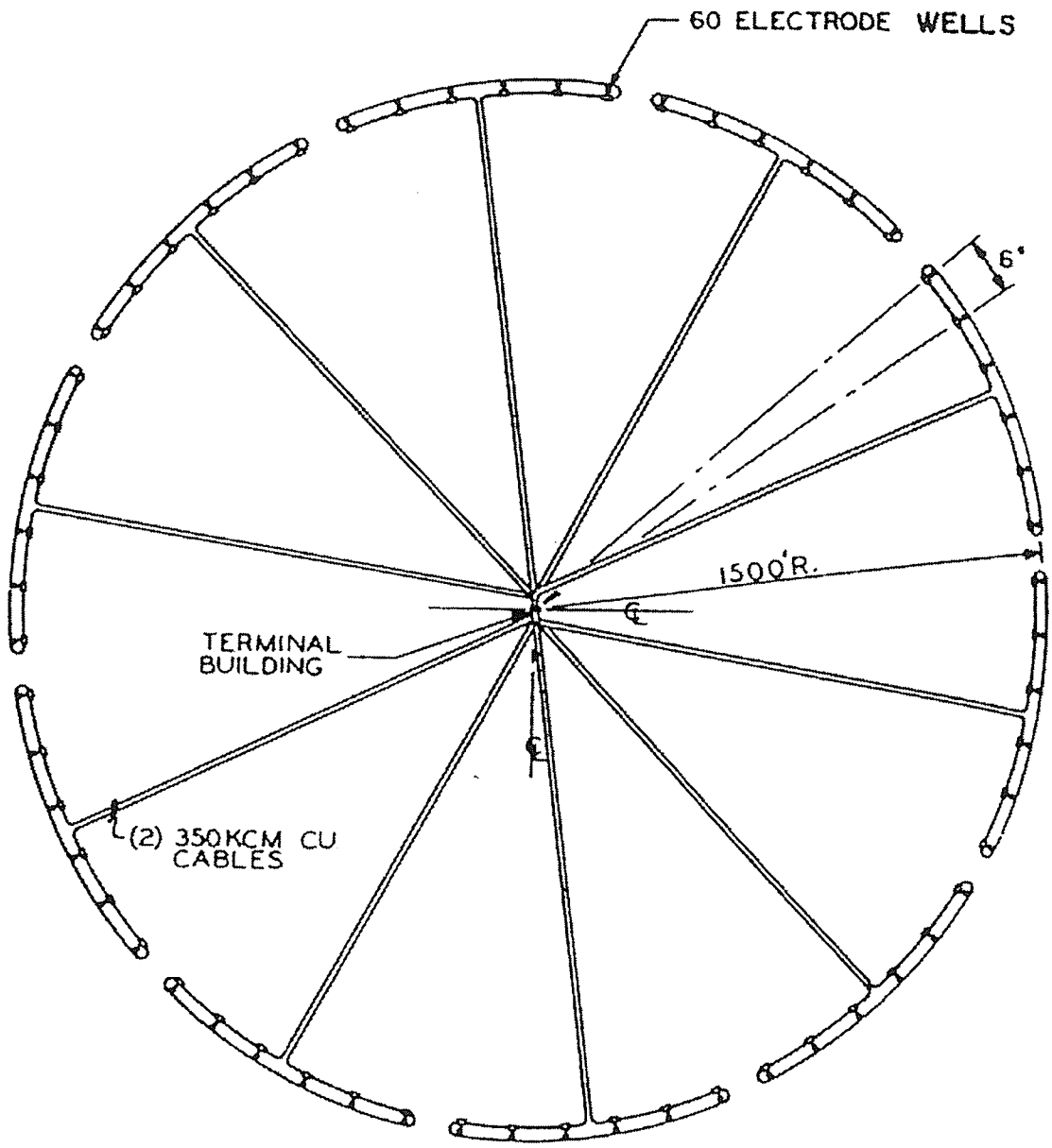

Figure D.1 Plan view of the ring electrode configuration, reproduced from [88 Prabhakara]

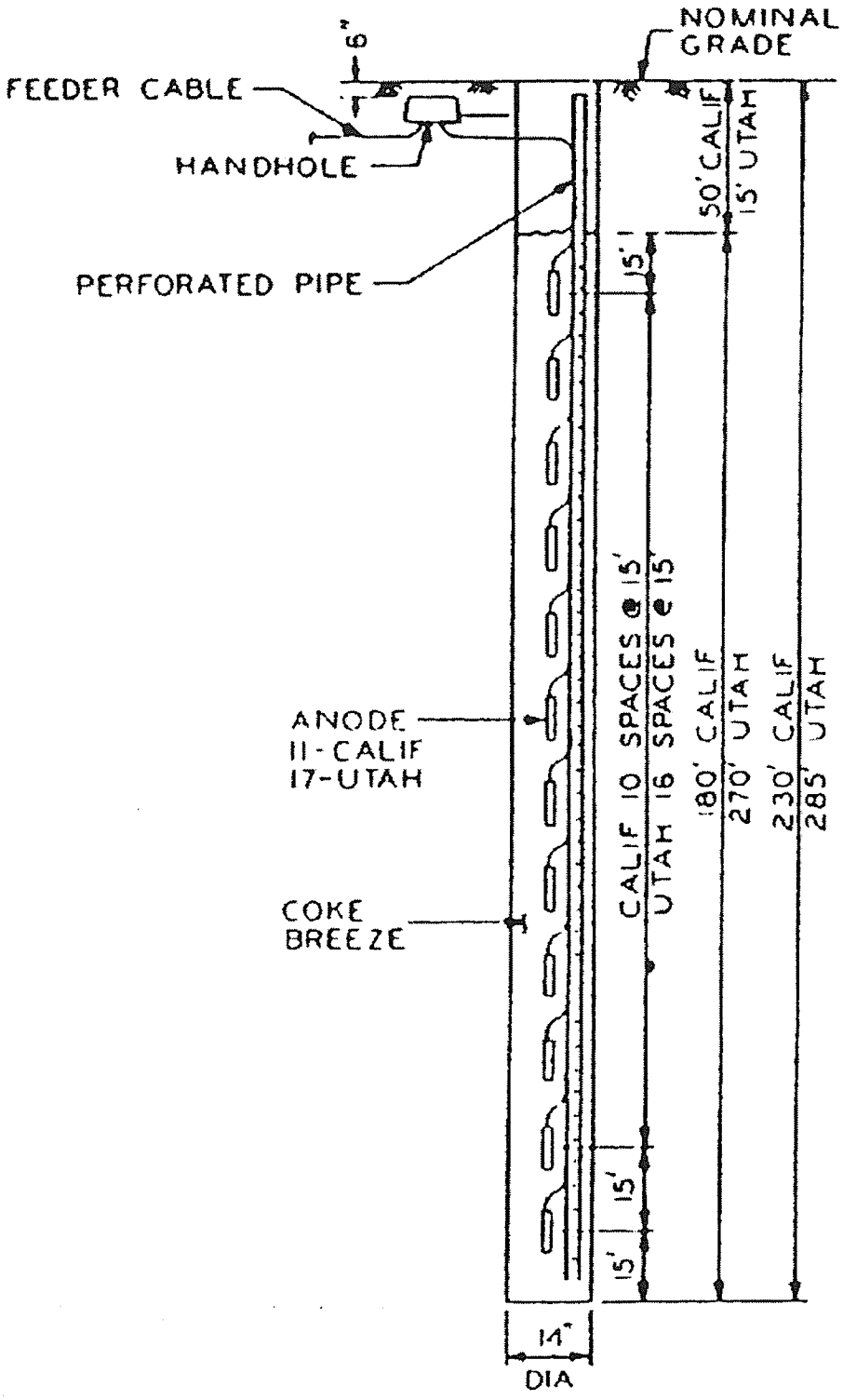

Figure D.2 A typical deep well, reproduced from [88 Prabhakara]